



Simulation of Systems Governed by Non-Quadratic Hamiltonians in Heisenberg Formalism

Taha HAMMADIA

April - June 2024

Supervised by Danijela Marković (CNRS) and Elie Gouzien (Alice & Bob)

Laboratoire Albert Fert, CNRS, Thales, Université Paris-Saclay, Palaiseau, France



ALICE & BOB

Abstract

The development of quantum devices for quantum information and quantum neuromorphic computing leads to the necessity to simulate open bosonic systems. Such systems are characterized by the canonical bosonic commutation relations which have interesting properties that are derived. Solving the dynamics of open systems described by more than quadratic Hamiltonians, by unusual jump operators like two-photon loss or under an external drive is quite challenging. Attempts to simulate these systems *via* the evolution of the density matrix, by imposing a cutoff in the Fock basis, are limited by its memory complexity which grows exponentially with the number of bosonic modes. This report undertakes part of the work by presenting the problem in a rigorous manner and leveraging the Heisenberg representation to propose and compare different methods of resolution that circumvent the memory complexity problem. These methods try to estimate the value of the moments, which describe the full dynamics. A great emphasis is put into writing correctly the Heisenberg representation for an open system. The complexities of the different methods will be evaluated. Furthermore, since the different methods are based on approximations, stability problems arise and need to be studied. We present a framework to study the stability of the numerical system and compare it for different cases between the different methods. Finally, analytical expressions are derived for some particular cases. Doing so allows to deepen the understanding of the resolution of differential equations on operators.

Keywords: open bosonic systems, Heisenberg representation, quantum Langevin equation, mean field, cumulant, bosonic commutation relations, equation of evolution of operators, numerical stability, time evolution approximation

Dedication

To my parents whose sacrifices cannot be enumerated.

To my family who has always supported me.

To my friends who shared the path with me.

To my professors and tutors who guided me.

Acknowledgements

I am deeply indebted to the administration of the International Center for Fundamental Physics, in particular to the coordinators of the Master and to Médina Mahrez who plays a key role in the organization of the Master. I would also like to thank the SOIE of Ecole Polytechnique whose administrative work allowed for the required paperwork to be processed smoothly.

This endeavour would have been impossible without the help of my supervisors Dr. Danijela Marković of the CNRS and Dr. Elie Gouzien of Alice & Bob. Their advice and directions were crucial for developing an understanding of the problem. My internship would not have been a success without their advice and knowledge. I would also like to thank Dr. Yann Beaujeault-Taudiere for suggesting to use the Padé approximant. Thanks should also go to Julien Dudas for their insights on the application side of our project. I am also grateful to the Laboratoire Albert Fert administration, both from the CNRS and Thales side.

I am tremendously grateful to Thales Research and Technology Palaiseau who financed this project and who are a big contributor to the success of the Laboratoire Albert Fert.

Many thanks should go to my parents and family for their unabating support throughout the different stages of my life. Finally, thanks should go to the professors, students and Post-Doctoral Fellows I met during my internship, in particular to Julien Dudas, Théo Malas-Danzé, Julien Berthomier, Baptiste Carles and Clara Zimmermann.

Contents

Résumé / Abstract	ii
Dedication	iii
Acknowledgements	iv
Introduction	1
1 Generalities and Review of the Literature	2
1.1 Bosonic Commutation Relations	2
1.1.1 Motivation	2
1.1.2 Properties	2
1.2 Quantum Dynamics	3
1.2.1 Schrödinger Representation - Density Matrix	3
1.2.2 Heisenberg Representation	4
1.2.3 Mean Field Methods (MF)	7
2 Solving Non-Quadratic Hamiltonians	11
2.1 General Form of Quantum Langevin Equation	11
2.1.1 Sanity Check: Adding Jump Operators	12
2.2 Mean Field (MF) Methods	12
2.2.1 Summary of Other Methods	12
2.2.2 Stability Analysis	15
2.2.3 Numerical Tests	16
2.3 Time Evolution Approximation (TEA)	16
2.4 Complexity of the Methods	18
2.4.1 Density Matrix Method	18
2.4.2 Usual MF	18
2.4.3 Cumulant Method	19
2.4.4 Time Evolution Approximation	19
3 Conclusion	20
3.1 Summary of the Report	20
3.2 Open questions	20
Bibliography	21
A Additional Definitions	25
A.1 Notions of Complexity	25
A.1.1 Presentation of the Problem	25
A.1.2 Notation Conventions	25
A.2 Bell Numbers	26
B Sufficient Condition for Multiplicity of Heisenberg Representation	27

C	Derivation of Quantum Langevin Equation	30
C.1	General Derivation	30
C.2	Two-Cavity Model	31
C.2.1	Model	31
C.2.2	Heisenberg-Langevin Equations	31
D	Expression of Some Quantities as a Function of Moments	33
D.1	Quasi-Probabilities	33
D.1.1	Sanity Check: Coherent State	35
D.2	Probability of Number Occupation	36
D.2.1	Sanity Checks	37
E	Analytical Expressions for Some Hamiltonians	38
E.1	Results and Techniques	38
E.1.1	Time-Ordered Exponential	38
E.1.2	Derivation with Respect to Operators	39
E.2	Examples	39
E.2.1	One-Mode Kerr Hamiltonian	39
E.2.2	Cross-Kerr Hamiltonian	40
E.2.3	Partial Generalization	40
F	Summary of the Methods	42
G	Other Numerical Results	53
G.1	General Considerations	53
G.2	Test of X-gate	53
H	Miscellaneous	60
H.1	Proof of Theorem 1.1.1	60
H.2	Proof of Theorem 1.1.2	60
H.3	Solving Quadratic Hamiltonian with One Photon Loss	61
H.4	Number of Equations - MF Equations	62
H.5	Proofs and Corollaries - Initial States (Theorem 2.2.1)	62
H.6	Proof of Independent Resolution on Projectors	63
H.7	Properties of Stability Matrix	64
H.8	Complexity of TEA - Computation of the Commutators	64
H.9	Proofs for Times of Validity - TEA	65
I	Sum of Gaussian States (UNFINISHED)	66
I.1	One-Mode Gaussian State	66
I.1.1	One-Mode Squeeze Operator	66
I.1.2	Scalar Product of One-Mode Gaussian States	66
I.1.3	Squeeze and Displacement Operators	67
I.1.4	Cumulants of One-Mode Gaussian States	67
I.1.5	Cumulants of One-Mode Gaussian <i>Projectors</i>	68

List of Tables

2.1	Comparison of the complexities of the methods (Part 1). For definition of notations, see section 2.4	19
2.2	Comparison of the complexities of the methods (Part 2). For definition of notations, see section 2.4	19
F.1	Summary of the methods	43
F.2	Stability of the Methods - Verbal description	44
F.3	Stability of the MF Methods - Plots. The red corresponds to positive values while blue corresponds to negative values of the maximum real value of the eigenvalues of the stability matrix for an initial coherent state $ \alpha\rangle$. The same color-bar is used for the same physical system which are separated by a double line.	52

List of Figures

1.1	Cumulants and moments for the state $ 1.5 - 1.25i\rangle$ from dynamics [26] for the dimension 500 in logarithm scale. The index (j, k) corresponds to $\langle a^{\dagger j} a^k \rangle$. $\langle a^{\dagger k} a^j \rangle$ and $\langle a^{\dagger j} a^k \rangle$ are complex-conjugate, thus we limit ourselves to $j \leq k$. The indices are ranked in an increasing order of $j + k$. For each subset of fixed $j + k$, the lexicographic order is imposed.	9
2.1	Cumulants and moments for the state $\propto \frac{ 3\rangle + -3\rangle}{\sqrt{2}}$ from dynamics [26] for the dimension 500 in logarithm scale. The index (j, k) corresponds to $a^{\dagger j} a^k$. The index (j, k) corresponds to $\langle a^{\dagger j} a^k \rangle$. $\langle a^{\dagger k} a^j \rangle$ and $\langle a^{\dagger j} a^k \rangle$ are complex-conjugate, thus we limit ourselves to $j \leq k$. For each subset of fixed $j + k$, the lexicographic order is imposed.	14
2.2	Cumulants and moments for the projector $\frac{ 2\rangle\langle 1.5-3.7i }{\langle 1.5-3.7i 2\rangle}$ using the exact numerical expression. The index (j, k) corresponds to $\langle a^{\dagger j} a^k \rangle$. The indices are ranked in an increasing order of $j + k$. For each subset of fixed $j + k$, the lexicographic order is imposed.	14
2.3	Maximal value for the real part of the eigenvalues of the stability matrix \mathcal{L} for quantum jump $\sqrt{\kappa}a$, coherent state $ \alpha\rangle$ and $p = 1$.	16
2.4	Maximal value for the real part of the eigenvalues of the stability matrix \mathcal{L} for quantum jump $\sqrt{\kappa}a^2$, coherent state $ \alpha\rangle$ and $p = 2$.	16
2.5	Evolution of $\langle a \rangle(t)$ for $H = a^{\dagger 3} + a^3$ comparing different cut-offs p and dimensions for dynamics [26]. Continuous line corresponds to the TEA for some cut-off while dashed line corresponds to dynamics for some dimension which corresponds to the value of p . $q = 0$ corresponds to not using the Padé approximate (cf. section 2.3).	17
2.6	Evolution of $\text{Re}\{\langle a \rangle(t)\}$ using the TEA method improved using the Padé approximant for different values of p and q , for $H = a^{\dagger} b^{\dagger} b a$ and $L = \sqrt{0.1}a$. Continuous line corresponds to the TEA for some cut-off while dashed line corresponds to dynamics [26] for some dimension.	18
A.1	Plot of Bell numbers from the OEIS [50] in \log_{10} scale	26
B.1	Inverse Pascal triangle structure that appears under the regularity condition for the pair of operators (A, B) . Deriving corresponds to creating two upwards branches to the left (derive A) and to the right (derive B). The implication $\mathcal{P}(n+1) \implies \mathcal{P}(n)$ goes downwards.	29
G.1	Plot of $\langle a^{\dagger} a \rangle(t)$ using dynamics [26] in dashed lines. Plot of $\langle a^{\dagger}(t) a(t) \rangle$ using TEA using Padé approximate (cf. section 2.3) in continuous line. The dashed-dotted lines correspond to the limits for $\langle a^{\dagger} a \rangle(t)$ (1) and for $\langle a^{\dagger}(t) a(t) \rangle$ (0).	54
G.2	Cumulants and moments for the projector $S[0.5] 1.5\rangle$ with $S[z] \equiv \exp\{\frac{1}{2}(z^* a^2 - z a^{\dagger 2})\}$ [61] using dynamics [26] for the space dimension 500. The index (j, k) corresponds to $\langle a^{\dagger j} a^k \rangle$. $\langle a^{\dagger k} a^j \rangle$ and $\langle a^{\dagger j} a^k \rangle$ are complex-conjugate, thus we limit ourselves to $j \leq k$. The indices are ranked in an increasing order of $j + k$. For each subset of fixed $j + k$, the lexicographic order is imposed.	54
G.3	Maximal value for the real part of the eigenvalues of the stability matrix \mathcal{L} for quantum jump $\sqrt{\kappa}a^{\dagger}a$, coherent state $ \alpha\rangle$ and $p = 2$.	55
G.4	Maximal value for the real part of the eigenvalues of the stability matrix \mathcal{L} for Hamiltonian $H = a^{\dagger 2} a^2$, quantum jump $\sqrt{\kappa}a$ and coherent state $ \alpha\rangle$ and $p = 3$. khan refers to cumulant method , min-cut refers to the method Minimum cut and smart_divide_in_half refers to the method Divide in half .	55

G.5	Maximal value for the real part of the eigenvalues of the stability matrix \mathcal{L} for Hamiltonian $H = -a^{\dagger 2}a^2$, quantum jump $\sqrt{\kappa}a$ and coherent state $ \alpha\rangle$ and $p = 3$. <code>khan</code> refers to <code>cumulant method</code> , <code>min-cut</code> refers to the method <code>Minimum cut</code> and <code>smart_divide_in_half</code> refers to the method <code>Divide in half</code>	56
G.6	$\text{Im}\{\langle a \rangle(t)\}$ for the Hamiltonian $H = a^{\dagger 2}a^2$, initial state $ \alpha = 1.5\rangle$, and jump operator $\sqrt{0.5}a$. Continuous line corresponds to MF methods for $p = 3$. Dashed lines correspond to <code>dynamics</code> [26].	56
G.7	$\text{Im}\{\langle a \rangle(t)\}$ for the Hamiltonian $H = a^{\dagger 2}a^2$, initial state $ \alpha = 1.5\rangle$, and jump operator $\sqrt{3.25}a$. Continuous line corresponds to MF methods for $p = 3$. Dashed lines correspond to <code>dynamics</code> [26].	57
G.8	$\text{Re}\{\langle ab \rangle(t)\}$ for the Hamiltonian $H = a^{\dagger}b^{\dagger}ba$, initial state $ \alpha = 1.5, \beta = 1.5\rangle$, and jump operator $\sqrt{0.5}a$. Continuous line corresponds to MF methods for $p = 3$. Dashed lines correspond to <code>dynamics</code> [26].	57
G.9	$\text{Re}\{\langle ab \rangle(t)\}$ for the Hamiltonian $H = a^{\dagger}b^{\dagger}ba$, initial state $ \alpha = 1.5, \beta = 1.5\rangle$, and jump operator $\sqrt{3.25}a$. Continuous line corresponds to MF methods for $p = 3$. Dashed lines correspond to <code>dynamics</code> [26].	58
G.10	$\text{Re}\{\langle ab \rangle(t)\}$ for the Hamiltonian $H = a^{\dagger}b^{\dagger}ba$, initial state $ \alpha = 1.5, \beta = 1.5\rangle$, without jump operators (i.e. very instable). Continuous line corresponds to MF methods for $p = 7$. Dashed lines correspond to <code>dynamics</code> [26].	58
G.11	$\text{Im}\{\langle a \rangle(t)\}$ for the non-Hermitian Hamiltonian $H = a^{\dagger}a^4$, initial state $ \alpha = 1.5 + i\rangle$, without jump operator a . Continuous line corresponds to MF methods for $p = 10$. Dashed lines correspond to <code>dynamics</code> [26].	59
G.12	Dynamics of a stabilized X-gate that transfers the state $ 0\rangle$ to the state $ 1\rangle$ during T , [62]. Plot obtained using the <code>cumulant method</code> for different values of p . $\langle x \rangle(t)$ goes from +5 at $t = 0$ to -5 at $t = T$	59

Introduction

Let there be light

Genesis 1:3

The year 2025 marks the 100th birthday of the formulation of the Heisenberg principle and the algebraic structure of quantum physics [1]. 2025 will be celebrated as the International Year of Quantum Science and Technology organized by the UNESCO [2]. This quantum century has allowed humankind to develop technologies based on the understanding of the Universe provided by quantum physics ([classical] computers, telecommunications, medical imaging, nuclear energy, chemistry, metrology...). Nowadays, a new application of quantum physics, which aims to leverage quantum information, is being developed: quantum computing.

Quantum computers aim to exploit the potential advantage provided by quantum information that is absent in classical information. Such an advantage can be formulated as the superposition principle [3], the exponential size of the Hilbert space [4] or entanglement [5]. Many objects have been explored for building quantum computers. Amongst them, we can cite: trapped ions [6–8], cold atoms [9] including Rydberg atoms [10], diamond cavities [11], supra-conducting circuits [12, 13]... This project focuses on light, which can be in the optical range or in the microwave range (bosonic error correction in Alice & Bob and quantum neuromorphic computing in Laboratoire Albert Fert).

The development of quantum computing devices based on light in all its forms, whether they are based on single photon sources [14], on linear optics [15], on the generation of continuous states of light [16] or on manipulating superposition of coherent states [17] has increased the hopes of seeing useful quantum computers in our lifetimes. Nevertheless, engineering such devices requires being able to simulate them beforehand. Since quantum computers are not mature enough to use them for simulation [18], it still needs to be done on classical computers. This becomes challenging as we approach applications where a quantum advantage is hoped for.

This project is part of the effort of simulating quantum devices based on bosons. This is important since many applications, like quantum machine learning and quantum neuromorphic computing [19–21], require to run the quantum device a considerable amount of times (for example once for each set of parameters to be tried). In particular, machine learning and neuromorphic tasks require using non-linearities to engineer, amongst others, powerful classification tools. Previously, this non-linearity was achieved *via* measurements. However, current devices at Laboratoire Albert Fert can produce a Kerr effect. Even though analytical expressions can be found for self-Kerr and cross-Kerr (cf. [Appendix E](#)), adding non-diagonal terms makes the problem very challenging, thus the interest of this work.

In this report, we study the evolution in the Heisenberg picture of bosonic modes evolving under some unitary evolution with some quantum jumps that simulate the interaction with a Markovian environment, or include the environment modes. We shall present some methods that aim at solving such systems. We start by presenting a overview of the problem and of the literature (cf. [chapter 1](#)). Afterwards, we present our personal contribution (cf. [chapter 2](#)). A great care will be taken to quantitatively compare the different methods (cf. [subsection 2.2.3](#) and [section 2.4](#)). Additionally, we try to provide proofs for the different claims we make. In order not to hamper the reading of the report, the results and the proofs are demarcated clearly, allowing the hastened reader to skip them if needed. The report contains many appendices that clarify it and provide additional details.

Chapter 1

Generalities and Review of the Literature

[The universe] cannot be read until we have learnt the language and become familiar with the characters in which it is written. It is written in mathematical language...

Galileo Galilei

1.1 Bosonic Commutation Relations

1.1.1 Motivation

Let us consider a system made of N bosonic modes that are described using the annihilators a_1, \dots, a_N which follow the commutation relations

$$[a_i, a_j^\dagger] = \delta_{ij}, \quad (1.1)$$

$$[a_i, a_j] = 0. \quad (1.2)$$

As we shall see afterwards, in order to study the time evolution of a_i , we need to evaluate, among other things, $[a_i, H]$, where H is the Hamiltonian of the system. In general, H can be written as a polynomial of the operators a_1, \dots, a_N and of $a_1^\dagger, \dots, a_N^\dagger$. We introduce the notation

$$H = \text{poly}_m(a_1, \dots, a_N; a_1^\dagger, \dots, a_N^\dagger), \quad (1.3)$$

meaning that the degree of H is less or equal to m (in the sense that, for each term of H , the **sum** of the powers of different operators is **less or equal** to m). Therefore, we need to know the properties of commutation relations between polynomials of bosonic annihilators and creators.

1.1.2 Properties

Commutator Algebra

In this part, we recall some usual properties of the commutator [22]. The proofs are given in [section H.1](#).

Theorem 1.1.1. *The commutator $[\cdot, \cdot]$ satisfies the following properties*

1. $[\cdot, \cdot]$ is anti-symmetric under exchange of the arguments.
2. $[\cdot, \cdot]$ is bilinear (i.e. linear in each variable).

3. $\forall A, B, C, [A, BC] = [A, B]C + B[A, C]$ and $[BC, A] = [B, A]C + B[C, A]$.

The last result has an interesting corollary if we consider a bosonic annihilator a .

Corollary 1.1.1.1. *Let a be a bosonic annihilator, for each $n \in \mathbb{N}$, $[a, a^{\dagger n}] = na^{\dagger(n-1)}$ and $[a^n, a^{\dagger}] = na^{(n-1)}$*

Degree of Commutator of Polynomials

The goal of this part is to state the result [Theorem 1.1.2](#). This result will be very important in analysing the differential systems to solve and will allow us to distinguish between linear and non-linear systems. Even though this result is mentioned in the literature [\[23\]](#), the proof could not be found in the literature we read. The proof in [section H.2](#) is, at the best of our knowledge, original.

Theorem 1.1.2. *Let $p, m \in \mathbb{N}$, we have*

$$\left[\text{poly}_p \left(a_1, \dots, a_N; a_1^{\dagger}, \dots, a_N^{\dagger} \right), \text{poly}_m \left(a_1, \dots, a_N; a_1^{\dagger}, \dots, a_N^{\dagger} \right) \right] = \text{poly}_{p+m-2} \left(a_1, \dots, a_N; a_1^{\dagger}, \dots, a_N^{\dagger} \right) \quad (1.4)$$

where $\text{poly}_q \left(a_1, \dots, a_N; a_1^{\dagger}, \dots, a_N^{\dagger} \right)$ designates any polynomial of degree q .

1.2 Quantum Dynamics

Let us consider a quantum system driven by the Hamiltonian H and by the jump operators L_n [\[8\]](#) which represent the interaction of the system with its environment. Before considering the Heisenberg representation, it is useful to remind the results of the Schrodinger representation.

1.2.1 Schrödinger Representation - Density Matrix

Presentation of the Method

In the Schrödinger picture, the dynamics of the system is described by the state of the system, the operators being time-independent. For a closed system, the axioms of quantum mechanics indicate that the system can be described by a time-dependent ket $|\psi\rangle$ [\[24\]](#). For an open system interacting with the environment, the description needs to be modified. Indeed, the state is now described by a density operator $\rho_S(t)$ that allows for statistical mixtures of quantum states (the subscript S stands for Schrödinger). The density operator is Hermitian, semi-positive and of trace equal to one. Its time evolution, under a Hamiltonian $H_S(t)$ and quantum jumps $L_n(t)$ is given by the master equation [\[8\]](#).

$$\frac{d\rho_S(t)}{dt} = \frac{1}{i\hbar} [H_S(t), \rho_S(t)] + \frac{1}{2} \sum_n \left(2L_n(t)\rho_S(t)L_n^{\dagger}(t) - \left\{ L_n^{\dagger}(t)L_n(t), \rho \right\} \right). \quad (1.5)$$

In practice, solving the master equation [Equation 1.5](#) is done by truncating the Fock space, turning the operators into finite dimension matrices represented in the Fock basis. The obtained system is thus solved numerically. This method is implemented by the Python module `QuTip` [\[25\]](#) or `dynamiqs` [\[26\]](#).

Performance

The required dimension for each mode goes linearly with the **maximum** number of photons expected for the mode. In particular, the method fails to describe Hamiltonians that lead to an increase of the number of photons in time. More rigorously, let us denote $M_{\max, i}$ the maximal number of photons per mode. The memory complexity (cf. [section A.1](#) for the convention on the notation for complexity) is $\Theta \left(\prod_{i=1}^N M_{\max, i} \right)$. In particular, we see that the space dimension grows **exponentially** with the number of modes (for each additional mode, the dimension of the Hilbert space is multiplied by the maximum number of photons considered in this mode). Therefore, this approach is inefficient for describing a large number of modes.

1.2.2 Heisenberg Representation

We have seen in [subsection 1.2.1](#) that solving the dynamics of the system in the Schrödinger picture requires a large memory. This can be very limiting since matrix operations need to be done on this representation, leading to a large time complexity. In this part, we change the representation of the dynamics in the hope that these problems will be solved.

In the Heisenberg representation, the dynamics are described by the evolution of the operators and a time-independent density matrix. This transformation is defined carefully in this section.

Reminders Concerning the Heisenberg Picture

In this part, the subscript or superscript S refers to the Schrödinger picture, while H refers to the Heisenberg picture. The evolution of a quantum state is given by the Kraus operators K_k [\[8, 27\]](#)

$$\rho_S(t) = \sum_k K_k^{(S)}(t) \rho(0) K_k^{(S)\dagger}(t), \quad (1.6)$$

with the normalization condition $\sum_k K_k^{(S)\dagger}(t) K_k^{(S)}(t) = \mathbb{1}$ and the sum \sum_k being potentially uncountable. This condition ensures that the trace of $\rho_S(t)$ is preserved. The Heisenberg representation is defined as [\[28\]](#)

Definition 1.2.1 (Heisenberg Representation). *The Heisenberg representation of an operator $O_S(t)$ (with explicit time-dependence) is given by:*

$$O_H(t) \equiv \sum_k K_k^{(S)\dagger}(t) O_S(t) K_k^{(S)}(t). \quad (1.7)$$

The Heisenberg representation of a density matrix is given by $\rho_H(t) \equiv \rho_S(0)$ (time-independent).

The definition of the Heisenberg picture comes from the fact that **the averages of observables should not depend on the representation**. This can be generalized to any operator O by taking linear combinations of $\frac{O+O^\dagger}{2}$ and $\frac{O-O^\dagger}{2i}$ which are observable. The average of the operator $O_S(t)$ (i.e. with explicit time-dependence) is given by

$$\begin{aligned} \langle O_S \rangle(t) &= \text{Tr}\{\rho_S(t) O_S(t)\} = \sum_k \text{Tr}\{K_k^{(S)}(t) \rho_S(0) K_k^{(S)\dagger}(t) O_S(t)\} \\ &= \sum_k \text{Tr}\{\rho_S(0) K_k^{(S)\dagger}(t) O_S(t) K_k^{(S)}(t)\} \\ &= \text{Tr}\left\{\rho_S(0) \sum_k K_k^{(S)\dagger}(t) O_S(t) K_k^{(S)}(t)\right\}. \end{aligned} \quad (1.8)$$

We observe that $(A + \lambda B)_H = A_H + \lambda B_H$ and $(O^\dagger)_H = (O_H)^\dagger$. However, it is quite important to observe that in general $(AB)_H \neq A_H B_H$ unless the sum over k is on one element (i.e. closed system). In fact,

$$A_H(t) B_H(t) = \sum_k \sum_l K_k^{(S)\dagger}(t) A_S K_k^{(S)}(t) K_l^{(S)\dagger}(t) B_S K_l^{(S)}(t) \quad (1.9)$$

$$(AB)_H(t) = \sum_k K_k^{(S)\dagger}(t) A_S B_S K_k^{(S)}(t). \quad (1.10)$$

Furthermore, the average $\langle AB \rangle(t)$ is associated to $(AB)_H(t)$.

The interest of the Heisenberg picture is to study the evolution of average of operators, allowing us to follow a smaller number of quantities than required for solving the master equation [Equation 1.5](#). For this purpose, we need to write the equation of evolution of the operators.

Theorem 1.2.1 (Evolution equation in the Heisenberg Picture). *Under the Hamiltonian $H_S(t)$ and jump operators $L_n(t)$, the time evolution of $O_H(t)$, with O_S time-independent, is given by*

$$\frac{dO_H}{dt} = \left(\frac{1}{i\hbar} [O_S, H_S(t)] + \frac{1}{2} \sum_n \left(L_n^\dagger(t) [O_S, L_n(t)] - [O_S, L_n^\dagger(t)] L_n(t) \right) \right)_H. \quad (1.11)$$

Proof. The master equation is given by:

$$\frac{d\rho_S(t)}{dt} = \frac{1}{i\hbar} [H_S(t), \rho_S(t)] + \frac{1}{2} \sum_n \left(2L_n(t)\rho_S(t)L_n^\dagger(t) - \{L_n^\dagger(t)L_n(t), \rho_S(t)\} \right). \quad (1.12)$$

Taking the average for the time-independent operator O_S , we find:

$$\begin{aligned} \frac{d \text{Tr}\{\rho_S(t)O_S\}}{dt} &= \frac{1}{i\hbar} \text{Tr}\{[H_S(t), \rho_S(t)]O_S\} + \frac{1}{2} \sum_n \left(2 \text{Tr}\{L_n(t)\rho(t)L_n^\dagger(t)O_S\} - \text{Tr}\{\{L_n^\dagger(t)L_n(t), \rho(t)\}O_S\} \right) \\ &= \frac{1}{i\hbar} \text{Tr}\{H_S(t)\rho(t)O_S\} - \frac{1}{i\hbar} \text{Tr}\{\rho(t)H_S(t)O_S\} \\ &+ \frac{1}{2} \sum_n \left(2 \text{Tr}\{\rho(t)L_n^\dagger(t)O_S L_n(t)\} - \text{Tr}\{L_n^\dagger(t)L_n(t)\rho(t)O_S\} - \text{Tr}\{\rho(t)L_n^\dagger(t)L_n(t)O_S\} \right) \\ &= \frac{1}{i\hbar} \langle [O_S, H_S(t)] \rangle + \frac{1}{2} \sum_n \left(2 \langle L_n^\dagger(t)O_S L_n(t) \rangle - \langle O_S L_n^\dagger(t)L_n(t) \rangle - \langle L_n^\dagger(t)L_n(t)O_S \rangle \right) \end{aligned}$$

We observe that: $2L_n^\dagger O_S L_n - O_S L_n^\dagger L_n - L_n^\dagger L_n O_S = L_n^\dagger (O_S L_n - L_n O_S) + (L_n^\dagger O_S - O_S L_n^\dagger) L_n = L_n^\dagger [O_S, L_n] - [O_S, L_n^\dagger] L_n$. Furthermore, since our computation does not depend on the initial state $\rho(0)$, we deduce that:

$$\frac{dO_H}{dt} = \left(\frac{1}{i\hbar} [O_S, H_S(t)] + \frac{1}{2} \sum_n \left(L_n^\dagger [O_S, L_n] - [O_S, L_n^\dagger] L_n \right) \right)_H \quad (1.13)$$

□

Remark 1.2.1.1. *Theorem 1.2.1 implies that the evolution of an operator in Heisenberg picture can be computed using the standard bosonic commutation relations, since O_S is a constant in Theorem 1.2.1. This is important since commutation relations are not conserved for $t > 0$ (to see this consider $H = \hbar\omega a^\dagger a$ with the jump operator $L = \sqrt{\kappa}a$ where $[a(t), a^\dagger(t)] = e^{-\kappa t}$, see section H.3 for a proof).*

Remark 1.2.1.2. *Equation 1.11 does not need to have a closed form in O_H . It can depend on the Heisenberg representation of other operators. This is the crux of the problem of solving non-quadratic Hamiltonians (cf. subsection 1.2.3).*

Example where $(AB)_H \neq A_H B_H$: This example is from [28]. Consider $H = \hbar\omega a^\dagger a$ with jump operators $L_1 = \sqrt{\kappa}a$ (spontaneous emission) and $L_2 = \sqrt{\kappa}e^{-\frac{\beta\hbar\omega}{2}}a^\dagger$ (thermal excitation). We can show that $a(t) = e^{-i\omega t - \frac{\gamma t}{2}}a(0)$ with $\gamma \equiv \kappa(1 - e^{-\beta\hbar\omega})$. Thus: $a^\dagger(t)a(t) = e^{-\gamma t}a^\dagger(0)a(0)$. However, by writing and solving the differential equation on $n(t) \equiv (a^\dagger a)(t)$, we find: $n(t) = e^{-\gamma t}(n(0) - n_\infty) + n_\infty$, with n_∞ corresponding to the Bose-Einstein distribution $n_\infty \equiv \frac{1}{e^{\beta\hbar\omega} - 1}$. Indeed, $n(t)$ represents the population which can go to a nonzero value while $a^\dagger(t)a(t)$ is a correlation that decays towards zero. Appendix B presents a sufficient condition that ensures that $(AB)_H = A_H B_H$. Even though the result is in itself not very practical, proving it gives a better understanding of the Heisenberg representation for an open system that can be seen by writing the equations of evolution for $(AB)_H$ and $A_H B_H$.

Comment on Bosonic Commutation Relations: Even though $a(t)$ does not satisfy bosonic commutation relations for an open system and thus does not describe a boson in general, we show in this part that bosonic commutation relations are preserved. More specifically:

Theorem 1.2.2 (Preservation of Bosonic Commutation Relations). *We have for any open or closed bosonic system:*

$$([a_i, a_j])(t) = 0 \quad (1.14)$$

$$\left([a_i, a_j^\dagger]\right)(t) = \delta_{ij} \quad (1.15)$$

Proof. We show more generally that the Heisenberg representation of a scalar λ is constant. This proves the desired result since canonical bosonic commutators are scalar. We have

$$\lambda_H(t) = \sum_k K_k^{(S)\dagger}(t) \lambda K_k^{(S)}(t) = \lambda \sum_k K_k^{(S)\dagger}(t) K_k^{(S)}(t) = \lambda, \quad (1.16)$$

where we used the normalization condition $\sum_k K_k^{(S)\dagger}(t) K_k^{(S)}(t) = \mathbb{1}$. \square

Corollary 1.2.2.1. *In the case of a **closed** system, we can write:*

$$[a_i(t), a_j(t)] = 0 \quad (1.17)$$

$$[a_i(t), a_j^\dagger(t)] = \delta_{ij} \quad (1.18)$$

This shows that $a_i(t)$ describes a boson for a closed system.

Remark 1.2.2.1. *We expect that adding the external input $a_{in}(t)$ and keeping the output $a_{out}(t)$, as done in a quantum Langevin equation, leads to a closed system where $(AB)_H = A_H B_H$. So far, this was not proven formally.*

Case of Time-Independent Hamiltonian without Jump Operators

In the case of a time-independent Hamiltonian without jump operators (i.e. closed system), the Schrödinger and Heisenberg pictures of the aforementioned Hamiltonian are the same.

Theorem 1.2.3 (Time-Independent Hamiltonian for a Closed System). *For time-independent H_S : $H_S = H_H$.*

Proof. For H_S time-independent: $U_S(t) = e^{-i\frac{H_S t}{\hbar}}$, which commutes with H_S . \square

Corollary 1.2.3.1. *If H_S is time-independent for a closed system, then H_H is time-independent.*

In the following, we will be interested in the operators that are not explicitly time-dependant, such as polynomials of ladder operators.

Theorem 1.2.4. *For H_S and O_S time-independent for a closed system, the time-evolution of O_H is given by*

$$O_H(t) = e^{i\frac{H_H t}{\hbar}} O_H(0) e^{-i\frac{H_H t}{\hbar}} \quad (1.19)$$

Proof. For H_S and O_S time-independent, the equation of evolution of O_H is given by

$$\frac{dO_H(t)}{dt} = \frac{1}{i\hbar} [O_H(t), H_H] \quad (1.20)$$

Since H_H is time-independent, the solution of the differential equation is $O_H(t) = e^{i\frac{H_H t}{\hbar}} O_H(0) e^{-i\frac{H_H t}{\hbar}}$. This can be proven by showing that the right hand side *satisfies the same differential equation and has the same initial condition.* \square

For the following, we will consider that all the operators are in the Heisenberg picture and drop the subscript H . In order to compute $O(t)$ explicitly, we introduce the following quantity.

Definition 1.2.2 (Composition of Commutators). We define the sequence of operators $\text{Comm}_n(H|O)$ by

$$\text{Comm}_0(H|O) = O \quad (1.21)$$

$$\forall n \in \mathbb{N}, \text{Comm}_{n+1}(H|O) = [H, \text{Comm}_n(H|O)] \quad (1.22)$$

which formally defines $[H, [H, \dots [H, O]]]$.

Using this definition, we can write the time evolution of $O(t)$:

Theorem 1.2.5. For H time-independent, we have

$$O(t) = \sum_{n=0}^{\infty} \frac{1}{n!} \left(\frac{it}{\hbar} \right)^n \text{Comm}_n(H|O(0)) \quad (1.23)$$

Proof. We introduce the linear operator: $\Lambda : X \mapsto \frac{1}{i\hbar}[X, H]$ (right hand side of Equation 1.20). Let us consider the linear differential equation: $\frac{dX}{dt} = \Lambda(X(t))$. The solution of this differential equation is $X(t) = \exp\{t\Lambda\}(X(0)) \equiv \sum_{n=0}^{\infty} \frac{t^n}{n!} \Lambda^{(n)}(X(0))$, where $\Lambda^{(n)}$ designates the composition n times. This is just a re-writing of Equation 1.23. \square

Remark 1.2.5.1. In Equation 1.23, we can take H both in the Heisenberg and the Schrödinger representations. Since we are computing its commutators with $O(0)$, H should be considered in the Schrödinger picture. In particular, since all the operators are in the Schrödinger picture, **we can use the canonical commutation relations**.

1.2.3 Mean Field Methods (MF)

Equations on Moments / Cumulants

We recall that the advantage of the Heisenberg picture is that it allows to follow a small number of interesting quantities, which does not have to scale in an exponential fashion with the number of modes. These quantities can be followed by writing differential equations on moments (i.e. averages on monomials of annihilators and creators) or on cumulants (defined in section 1.2.3).

Let N denote the number of bosonic modes. It will turn out that we will find the differential equations (on moments or cumulants) by taking the average of the Heisenberg equations for the monomials of a_i and a_i^\dagger , which can be written as $\text{poly}_p(a_1, \dots, a_N; a_1^\dagger, \dots, a_N^\dagger)$. Let us consider the Hamiltonian $H = \text{poly}_m(a_1, \dots, a_N; a_1^\dagger, \dots, a_N^\dagger)$. If we limit ourselves to unitary evolution, we find

$$\begin{aligned} \frac{d \left\langle \text{poly}_p(a_1, \dots, a_N; a_1^\dagger, \dots, a_N^\dagger) \right\rangle}{dt} &= \frac{1}{i\hbar} \left\langle \left[\text{poly}_p(a_1, \dots, a_N; a_1^\dagger, \dots, a_N^\dagger), H \right] \right\rangle \\ &= \left\langle \text{poly}_{p+m-2}(a_1, \dots, a_N; a_1^\dagger, \dots, a_N^\dagger) \right\rangle. \end{aligned} \quad (1.24)$$

Therefore, writing a closed differential system with monomials of degree less or equal to p is possible if and only if $m \leq 2$, i.e. in the case of a quadratic Hamiltonian [21, 29]. States produced by quadratic Hamiltonians (i.e. Gaussian evolution) from vacuum are called Gaussian states [29, 30]. They are characterized by a Gaussian Wigner distribution [8, 30, 31]. Knowing exactly the moments for a non-quadratic Hamiltonian requires solving *an infinite number of Heisenberg equations*. Such an evolution is called non-Gaussian. Therefore, closing the system of equation on moments requires using an approximation that allows to express higher order moments as a function of lower order moments.

In general, there are $(2N+1)^p$ monomials containing at most p annihilators and creators. However, using bosonic commutation relations, we can limit ourselves to normal order (i.e. we limit ourselves to polynomials having creators at the left and annihilators to the right). The moments of degree less or equal to p can be put in the form $\left\langle \left(\prod_{i=1}^N a_i^{\dagger j_i} \right) \left(\prod_{i=1}^N a_i^{k_i} \right) \right\rangle$ with $\sum_{i=1}^N j_i + k_i \leq p$. We might be interested in knowing the number of independent Heisenberg equations for moments of order p . Let $1 \leq q \leq p$

denote the total degree of a monomial. To count the number of monomials of degree q , we can consider a_i and a_i^\dagger as boxes where we can put q balls. The corresponding combinatorics problem corresponds to choosing q balls amongst q balls and $2N - 1$ separators (that separate between the boxes), i.e. $\binom{2N+q-1}{q}$ choices. Summing over the different q 's, we get in total $\sum_{q=1}^p \binom{2N+q-1}{q}$ monomials to follow. We can further reduce the number of moments to follow by imposing $\sum_{i=1}^N j_i \leq \sum_{i=1}^N k_i$, roughly by half (in the sense that the number of moments is $\sim \frac{1}{2} \sum_{q=1}^p \binom{2N+q-1}{q} = O(p^{2N})$ for $p \rightarrow \infty$, N constant and $\sim \frac{(2N)^p}{2p!}$ for $N \rightarrow \infty$, p constant; see [section H.4](#) for a proof of these statements). In conclusion, fixing the order of the operators in the moments reduces significantly the number of moments to follow.

For the remaining, we define: $\tau_H \equiv m - 2$, the ‘‘Hamiltonian non-linearity’’. This number measures the degree of non-linearity of the Hamiltonian.

Interesting Corollary: Let us consider the value of [Equation 1.23](#) for $O = a_i$. Since each commutation with H adds τ_H to the degree of the polynomial, we have:

$$\text{Comm}_n(H|a_i) = \text{poly}_{1+n\tau_H}(a_1, \dots, a_N; a_1^\dagger, \dots, a_N^\dagger) \quad (1.25)$$

In particular, for $\tau_H \geq 1$ (or H non-quadratic), the annihilator $a_i(t)$ cannot be expressed in terms of a polynomial of a finite degree of the initial ladder operators. This should be contrasted with the quadratic case where $a_i(t)$ is linear in the ladder operators (i.e. $a_i(t) = \sum_{j=1}^N (F_{ij}(t)a_j(t) + G_{ij}(t)a_j^\dagger(t))$ as in [\[29\]](#)). Thus, there is a **fundamental** physical difference between quadratic and non-quadratic Hamiltonians. Quadratic Hamiltonians lead to new bosonic quasi-particles [\[32\]](#) while non-quadratic Hamiltonians lead to excitations of any arbitrary number of the initial particles (i.e. $a_i(t)$ can contain for example a_i, a_i^2, \dots).

Cumulant Method

This part is largely inspired by [\[33\]](#) that introduces cumulants in normal order for a given state. In order to follow the evolution of initial cat states and other non-Gaussian states, we give a more general definition of cumulants. The problem of writing equations in terms of moments is that they increase exponentially as a function of the degree (at least for coherent states with $|\alpha| > 1$, see [Figure 1.1](#)). The idea is to introduce a quantity that decreases as a function of the degree. For many cases, cumulants can play such a role.

Moment Generating Function (MGF) The **normal** characteristic function for the multi-mode case for the operator X is defined as [\[8, 33\]](#)

$$M^{[X]}(\vec{z}, \vec{z}^*) \equiv \text{Tr} \left\{ X \left(\prod_{k=1}^N e^{iz_k^* a_k^\dagger} \right) \left(\prod_{k=1}^N e^{iz_k a_k} \right) \right\}. \quad (1.26)$$

In [\[33\]](#), X is a density operator. In our case, we only impose the normalization condition $\text{Tr}\{X\} = 1$, ensuring that $M^{[X]}(\vec{0}, \vec{0}) = \text{Tr}\{X\} = 1$. In particular, we can deduce directly the values of moments in normal order from the derivatives of $M^{[X]}(\vec{z}, \vec{z}^*)$

$$\text{Tr} \left\{ X \left(\prod_{k=1}^N a_k^{\dagger j_k} \right) \left(\prod_{k=1}^N a_k^{l_k} \right) \right\} = \left[\prod_{k=1}^N \frac{\partial^{j_k+l_k}}{\partial (iz_k^*)^{j_k} \partial (iz_k)^{l_k}} \right] M^{[X]}(\vec{0}, \vec{0}). \quad (1.27)$$

This makes $M^{[X]}(\vec{z}, \vec{z}^*)$ the normal order moment generating function. While the symmetric characteristic function is associated with the Wigner function, $M^{[X]}(\vec{z}, \vec{z}^*)$ is associated with the Glauber–Sudarshan P –distribution defined as the complex Fourier transform of $M^{[X]}(\vec{z}, \vec{z}^*)$ [\[31, 33–35\]](#),

$$P^{[X]}(\vec{\beta}, \vec{\beta}^*) \equiv \frac{1}{\pi^{2N}} \int dz_1 dz_1^* \dots dz_N dz_N^* M^{[X]}(\vec{z}, \vec{z}^*) e^{-i\vec{\beta} \cdot \vec{z}} e^{-i\vec{\beta}^* \cdot \vec{z}^*}. \quad (1.28)$$

The P –distribution [\[31, 33\]](#) allows to represent a state ρ on the coherent state basis:

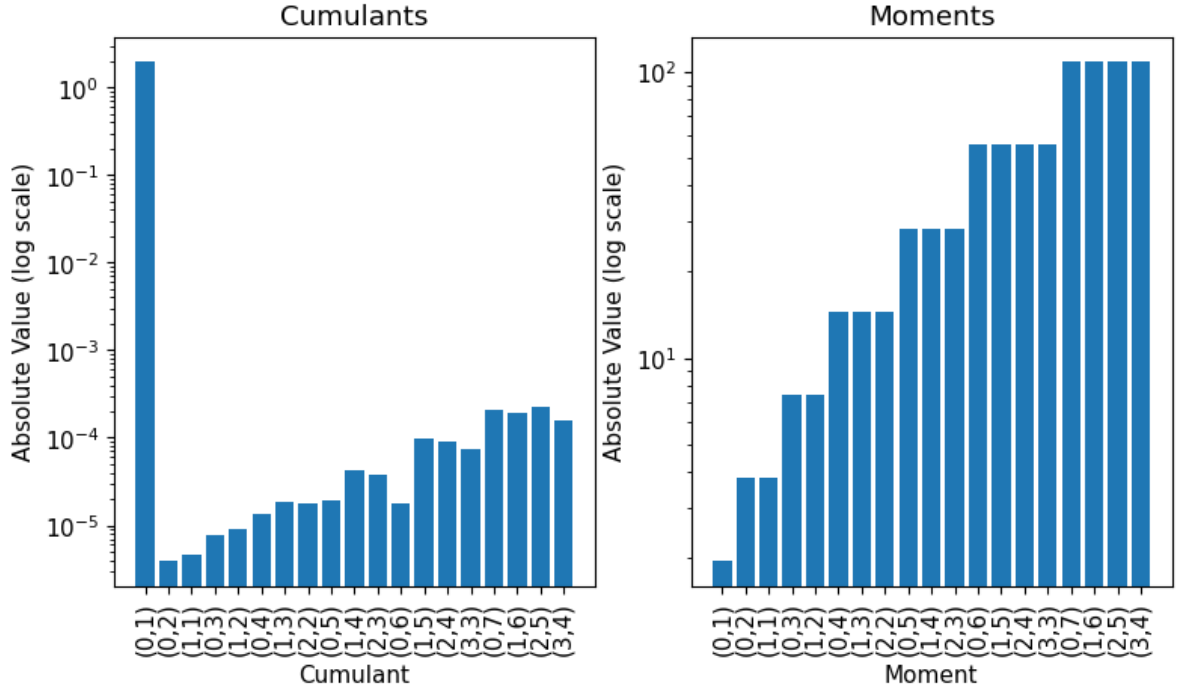


Figure 1.1: Cumulants and moments for the state $|1.5 - 1.25i\rangle$ from **dynamics** [26] for the dimension 500 in logarithm scale. The index (j, k) corresponds to $\langle a^{\dagger j} a^k \rangle$. $\langle a^{\dagger k} a^j \rangle$ and $\langle a^{\dagger j} a^k \rangle$ are complex-conjugate, thus we limit ourselves to $j \leq k$. The indices are ranked in an increasing order of $j + k$. For each subset of fixed $j + k$, the lexicographic order is imposed.

$$X = \int d\beta_1 d\beta_1^* \dots d\beta_N d\beta_N^* P^{[X]}(\vec{\beta}, \vec{\beta}^*) \left| \vec{\beta} \right\rangle \left\langle \vec{\beta} \right| \quad (1.29)$$

where $\left| \vec{\beta} \right\rangle \equiv |\beta_1\rangle \otimes \dots \otimes |\beta_N\rangle$.

Cumulant Generating Function (CGF) The CGF is defined as: $K^{[X]}(\vec{z}, \vec{z}^*) \equiv \ln M^{[X]}(\vec{z}, \vec{z}^*)$. $K^{[X]}(\vec{0}, \vec{0}) = \ln \text{Tr}\{X\} = 0$. $K^{[X]}(\vec{z}, \vec{z}^*)$ defines the cumulants as its derivatives at $(\vec{0}, \vec{0})$.

$$C_{\left(\prod_{k=1}^N a_k^{\dagger j_k}\right) \left(\prod_{k=1}^N a_k^{l_k}\right)}^{[X]} \equiv \left[\prod_{k=1}^N \frac{\partial^{j_k+l_k}}{\partial (iz^*)^{j_k} \partial (iz)^{l_k}} \right] K^{[X]}(\vec{0}, \vec{0}). \quad (1.30)$$

It is possible to link moments and cumulants using the Faà di Bruno formula [36, 37]. The lemma uses the notion of **partitions**. For a finite set I , $\mathcal{P}(I)$ denotes the **set** of **sets** of disjoint **subsets** of I whose union is I . We denote $\mathcal{P}(n)$ as a short hand for $\mathcal{P}(\{1, \dots, n\})$. For example, $\{\{1, 2\}, \{3\}\}$ and $\{\{1, 2, 3\}\}$ are partitions of $I = \{1, 2, 3\}$. More accurately,

$$\mathcal{P}(3) = \left\{ \left\{ \{1\}, \{2\}, \{3\} \right\}, \left\{ \{1, 2\}, \{3\} \right\}, \left\{ \{1, 3\}, \{2\} \right\}, \left\{ \{2, 3\}, \{1\} \right\}, \left\{ \{1, 2, 3\} \right\} \right\}.$$

The number of elements of $\mathcal{P}(n)$ is given by the Bell number B_n (cf. [section A.2](#)), i.e. $B_3 = 5$.

Lemma 1.2.5.1 (Faà di Bruno formula). *Let f and g be differentiable n -times. We have:*

$$\frac{\partial^n}{\partial x_1 \dots \partial x_n} f(g) = \sum_{\pi \in \mathcal{P}(n)} f^{(|\pi|)}(g) \prod_{B \in \pi} \frac{\partial^{|B|} g}{\prod_{i \in B} \partial x_i} \quad (1.31)$$

where x_i can be any set of variables, with some potentially equal.

From this formula, we can deduce identities allowing us to express moments as a function of cumulants and cumulants as a function of moments:

Theorem 1.2.6 (Passage from moments to cumulants and vice-versa in normal order). *Let O_k be operators such that $\prod_{k=1}^n O_k \equiv O_1 \dots O_N$ is written in the **normal** order. The following relations are true even if $\text{Tr}\{X\} \neq 1$.*

$$C_{\prod_{k=1}^n O_k}^{[X]} = \sum_{\pi \in \mathcal{P}(n)} \frac{(-1)^{|\pi|-1} (|\pi| - 1)!}{M^{[X]}(\vec{0}, \vec{0})^{|\pi|}} \prod_{B \in \pi} \text{Tr} \left\{ X \prod_{i \in B} O_i \right\} \quad (1.32)$$

$$\text{Tr} \left\{ X \prod_{k=1}^n O_k \right\} = \sum_{\pi \in \mathcal{P}(n)} e^{K^{[X]}(\vec{0}, \vec{0})} \prod_{B \in \pi} C_{\prod_{i \in B} O_i}^{[X]} \quad (1.33)$$

where $\prod_{i \in B} O_i$ is written in increasing order of i

Proof. In this proof, we do **not** suppose that $\text{Tr}\{X\} = 1$.

For Equation 1.32, we use the relation $K^{[X]}(\vec{z}, \vec{z}^*) = \ln M^{[X]}(\vec{z}, \vec{z}^*)$. We use the Faà di Bruno formula Equation 1.31 evaluated at $(\vec{0}, \vec{0})$. Further, we can show by induction that $\ln^{(n)} x = \frac{(-1)^{n-1} (n-1)!}{x^n}$, $n \geq 1$.

For Equation 1.33, we use the relation $M^{[X]}(\vec{z}, \vec{z}^*) = \exp\{K^{[X]}(\vec{z}, \vec{z}^*)\}$. We use the Faà di Bruno formula Equation 1.31 evaluated at $(\vec{0}, \vec{0})$. Further, $\exp^{(n)} x = \exp\{x\}$. \square

Corollary 1.2.6.1. *Since we always impose that $\text{Tr}\{X\} = 1$, the passage relations become:*

$$C_{\prod_{k=1}^n O_k}^{[X]} = \sum_{\pi \in \mathcal{P}(n)} (-1)^{|\pi|-1} (|\pi| - 1) \prod_{B \in \pi} \text{Tr} \left\{ X \prod_{i \in B} O_i \right\} \quad (1.34)$$

$$\text{Tr} \left\{ X \prod_{k=1}^n O_k \right\} = \sum_{\pi \in \mathcal{P}(n)} \prod_{B \in \pi} C_{\prod_{i \in B} O_i}^{[X]} \quad (1.35)$$

where $\prod_{i \in B} O_i$ is written in increasing order of i

Method (truncated cumulants) The method proposed in [33] is to write differential equations on the *cumulants*, which we will follow. However, it is possible to use cumulants to write differential equations on moments [30, 38]. It is also possible to envision writing a closure relation using moments while writing differential equations on cumulants. This can be done by linking the higher degree moments to lower degree moments by setting the left hand side of Equation 1.34 to zero. The intuition behind writing the differential equations on cumulants is that for coherent states, cumulants are 0 beyond the order 1 and for Gaussian states cumulants are 0 beyond the order 2. Thus, at least for short times, we can suppose that cumulants beyond some order p are 0 as “it takes time for them to be occupied”. This can be done by following the steps.

1. Express the cumulants up to order p in terms of moments using Equation 1.34.
2. Write the quantum Langevin equations for the moments which relate the time derivative of a moment to other moments.
3. Write the time derivative of the cumulants in terms of moments by combining the two previous steps.
4. Express the moments in terms of cumulants by replacing moments by cumulants using Equation 1.35. Impose that cumulants of order larger than p are equal to 0.

One important limitation of the **truncated cumulants** is that the computation time is exponential in the cutoff p . The exponential time comes from summing on partitions in Equation 1.34 and Equation 1.35, whose number (the Bell numbers) grows quasi-exponentially (see Figure A.1). Writing the differential system on the cumulants becomes therefore cumbersome quite rapidly. See section A.2 for more information about Bell numbers.

Chapter 2

Solving Non-Quadratic Hamiltonians

We must be clear that when it comes to atoms, language can be used only as in poetry.

Niels Bohr

Unless stated otherwise, the results of this chapter are original to the best of our knowledge.

2.1 General Form of Quantum Langevin Equation

In [Appendix C](#), we present two derivations of the quantum Langevin equation which includes many photon loss, while including other jump operators that are represented by L_n . Many photon loss is described by the loss rate κ_ν . The incoming field, denoted by $a_{\text{in}}(t)$, corresponds to an incoming propagating field. The first considers incoming propagating modes while the second considers a two cavity model.

$$\frac{da}{dt} = \frac{1}{i\hbar}[a, H] + \frac{1}{2} \sum_n \left(L_n^\dagger[a, L_n] - [a, L_n^\dagger] L_n \right) - \sum_{\nu=1}^{\infty} \nu a^{\dagger(\nu-1)} \left(\sqrt{\kappa_\nu} a_{\text{in}}(t) + \frac{\kappa_\nu}{2} a^\nu \right) \quad (2.1)$$

We observe that having higher than one photon loss is enough to lead to a nonlinear system (i.e. non-Gaussian dynamics). Furthermore, the term $-\nu \sqrt{\kappa_\nu} a^{\dagger(\nu-1)} a_{\text{in}}(t)$ couples the cavity field and the input field in a multiplicative manner.

Examples

Let us consider two examples:

One Photon Loss: $\kappa_1 = \kappa$ and $\forall \nu \geq 2, \kappa_\nu = 0$. We get:

$$\frac{da}{dt} = \frac{1}{i\hbar}[a, H] + \frac{1}{2} \sum_n \left(L_n^\dagger[a, L_n] - [a, L_n^\dagger] L_n \right) - \frac{\kappa}{2} a - \sqrt{\kappa} a_{\text{in}}(t) \quad (2.2)$$

which is the standard quantum Langevin equation.

Two Photon Loss: $\kappa_2 = \kappa$ and $\forall \nu \neq 2, \kappa_\nu = 0$. We get:

$$\frac{da}{dt} = \frac{1}{i\hbar}[a, H] + \frac{1}{2} \sum_n \left(L_n^\dagger[a, L_n] - [a, L_n^\dagger] L_n \right) - \kappa a^\dagger a^2 - 2\sqrt{\kappa} a^\dagger a_{\text{in}}(t) \quad (2.3)$$

2.1.1 Sanity Check: Adding Jump Operators

Alternatively, we could have obtained the quantum jump term of 2.1 due to photon loss by adding the jump operators $\tilde{L}_\nu \equiv \sqrt{\kappa_\nu} a^\nu$ to the Hamiltonian with the jump operators L_n . The additional term is indeed

$$\frac{1}{2} \left(\tilde{L}_\nu^\dagger [a, \tilde{L}_\nu] - [a, \tilde{L}_\nu^\dagger] \tilde{L}_\nu \right) = -\frac{\kappa_\nu}{2} [a, a^{\dagger\nu}] a^\nu = -\frac{\nu\kappa_\nu}{2} a^{\dagger(\nu-1)} a^\nu. \quad (2.4)$$

However, we cannot recover the term proportional to the input. This is because the input term $a_{\text{in}}(t)$ comes from considering the quantum state of the input field. This is not taken into account by the Heisenberg-Langevin equation, because it makes the density matrix of the Universe written as: $\rho_{\text{sys}} \otimes \rho_{\text{env}}$, and the environment is assumed to be Markovian.

Remark 2.1.0.1. *In the rest of this report, we do not consider the $a_{\text{in}}(t)$ term. If $a_{\text{in}}(t)$ describes a macroscopic coherent state, it can be simulated by adding a linear term to the Hamiltonian (for one-photon loss, we need to add the term $-i\hbar\sqrt{\kappa_1} (a^\dagger a_{\text{in}} - a_{\text{in}}^\dagger a)$, with a_{in} a complex number). Otherwise, we do not know how to deal with time-dependent $a_{\text{in}}(t)$ in general [39, 40].*

2.2 Mean Field (MF) Methods

As stated in the introduction, the goal of the MF method is to follow the moments that allow to rebuild all the desired quantities. The number of quantities to follow is expected to be much smaller than the number of variables of the density matrix. In this part, we present our contributions to the MF methods. As shown in Appendix D, many quantities can be found by knowing the moments. Additionally, MF methods can tackle time-dependent Hamiltonians and quantum jumps (cf. section G.2).

2.2.1 Summary of Other Methods

Writing the Differential System

The goal of this part is to follow the evolution of the moments of degree less or equal to p . We recall that the MF methods are based on approximating the equation of evolution of the moments. In particular, the equations of evolution for moments of degrees greater or equal to $p - \tau_H$ are approximated since the moments of degree larger than p appear in them. Such a term can be for example $\langle a^{p+1} \rangle$. Since we do not follow such a quantity, we need to be able to write it (in an approximate manner) in terms of moments of order less or equal to p .

We have studied the following ways of approximating the moments of order larger than p .

1. **Truncated cumulants:** this method is presented in section 1.2.3.
2. **Divide in half:** this method is presented in section 2.2.1.
3. **Minimum Cut:** this method is presented in section 2.2.1.

Explicitly, we are interested in writing the moment $\left\langle \left(\prod_{l=1}^N a_l^{\dagger j_l} \right) \left(\prod_{l=1}^N a_l^{k_l} \right) \right\rangle$ with $\sum_{l=1}^N j_l + k_l > p$.

Divide in Half The intuition behind this approach is that, if we take $p \geq \tau_H$, cutting the moment in two parts gives terms of degrees less or equal to p . For example, $\langle a^{p+1} \rangle \mapsto \left\langle a^{\lfloor \frac{p+1}{2} \rfloor} \right\rangle \left\langle a^{\lceil \frac{p+1}{2} \rceil} \right\rangle$.

More rigorously, this is done by representing the moment $\left\langle \left(\prod_{l=1}^N a_l^{\dagger j_l} \right) \left(\prod_{l=1}^N a_l^{k_l} \right) \right\rangle$ by the tuple $T \equiv (j_1, \dots, j_N, k_1, \dots, k_N)$. The tuple can be manipulated by following Algorithm 1. This algorithm is actually a heuristic as there are some cases that fail (for example (3, 4, 4, 9) for $p = 10$). Nevertheless, the method works for all the applications of interest.

The reason behind trying to divide the ladder operator at position i between the two resulting moments is to keep some correlation between them *via* the aforementioned ladder operator. Furthermore, **divide in half** is intuitively *expected* to be very accurate because the replacement is done by moments whose equation of evolution is correct. Thus the error is *expected* to propagate to the second order.

Algorithm 1 Divide in Half Algorithm

Require: T a tuple of length $2N$, $p \in \mathbb{N}^*$ with $p \geq \tau_H$

if $\text{sum}(T) \leq p$ **then**

$L \leftarrow [T]$

else

$i \leftarrow \text{find_idx}(T, p)$

$\triangleright \text{find_idx}$ gives the smallest i s.t. $\text{sum}(T[:i+1]) > p$

$v \leftarrow \min\left(p - \text{sum}(T[:i]), \left\lceil \frac{T[i]}{2} \right\rceil\right)$

\triangleright Divide in half here

$L \leftarrow [T[:i] + (v) + (0,) \times (2N - i - 1), (0) \times i + (T[i] - v) + T[i+1:]]$

end if

return L

Minimum Cut The intuition behind this method is to divide the moment into the smallest possible number of chunks. This is done by taking chunks of size p from $\left\langle \left(\prod_{l=1}^N a_l^{\dagger j_l} \right) \left(\prod_{l=1}^N a_l^{k_l} \right) \right\rangle$ going from the left to the right. For example, $\langle a^{p+1} \rangle \mapsto \langle a^p \rangle \langle a \rangle$.

More rigorously, like in [section 2.2.1](#), this is done by representing the moment $\left\langle \left(\prod_{l=1}^N a_l^{\dagger j_l} \right) \left(\prod_{l=1}^N a_l^{k_l} \right) \right\rangle$ by the tuple $T \equiv (j_1, \dots, j_N, k_1, \dots, k_N)$. The tuple is divided into chunks whose sum is equal to p . Usually, there will remain a last chunk whose sum is strictly less than p . The tuple can be manipulated by following [Algorithm 2](#). This algorithm is correct since each chunk has a sum less or equal to p .

Algorithm 2 Minimum Cut Algorithm

Require: T a tuple of length $2N$, $p \in \mathbb{N}^*$

$c \leftarrow 0, i \leftarrow 0, j \leftarrow 0, L \leftarrow []$

while $j < 2N$ **do**

if $c + T[j] < p$ **then**

\triangleright Python convention

$c \leftarrow c + T[j], j \leftarrow j + 1$

\triangleright Accumulate ladder operators

else

\triangleright We have a chunk of degree p

$L \leftarrow L + [(0) \times i + T[i:j] + (0) \times (2N - j - 1)]$

$\triangleright (0) \times i = (0, 0, \dots, 0)$ i times

$T[j] \leftarrow T[j] - p + \text{sum}(T[i:j])$

\triangleright Subtract the part already in a chunk

$c \leftarrow 0, i \leftarrow j, T[:j] \leftarrow (0) \times j$

end if

end while

$L \leftarrow L + (0) \times i + T[i:]$

\triangleright The rest goes into a last chunk

return L

Initial States

For all the three methods, finding the initial condition can be done by finding the *initial values of the moments*. We can show that this can be done for a large class of states. Indeed, we prove [Theorem 2.2.1](#) in [section H.5](#) and give corollaries for a sum of coherent and of Fock states.

Theorem 2.2.1 (Initial Value of Moments). *Let us consider the states $\{|\phi[\xi]\rangle\}_\xi$. We denote $a|\phi[\xi]\rangle = \lambda[\xi]|\phi^{(1)}[\xi]\rangle$, with $|\phi^{(1)}[\xi]\rangle$ is another state obtained after applying a once on $|\phi[\xi]\rangle$. Let $|\psi\rangle = \sum_{\xi=1}^X c_\xi \bigotimes_{i=1}^N |\phi_i[\xi]\rangle$. We have*

$$\langle \psi | \left(\prod_{l=1}^N a_l^{\dagger j_l} \right) \left(\prod_{l=1}^N a_l^{k_l} \right) | \psi \rangle = \sum_{\xi=1}^X \sum_{\zeta=1}^X c_\xi^* c_\zeta \prod_{l=1}^N \left(\prod_{\gamma=0}^{j_l-1} \lambda_l^{(\gamma)*}[\xi] \right) \left(\prod_{\kappa=0}^{k_l-1} \lambda_l^{(\kappa)}[\zeta] \right) \langle \phi_l^{(j_l)}[\xi] | \phi_l^{(k_l)}[\zeta] \rangle \quad (2.5)$$

where $|\phi^{(k)}[\xi]\rangle$ is the resulting state after applying k times a on $|\phi[\xi]\rangle$.

Numerical Implementation: Even though [Theorem 2.2.1](#) gives the expressions of the moments for states that are linear superpositions of states that we can handle, the resulting approximated differential system is very wrong since the state is very far from being Gaussian (see for example [Figure 2.1](#)).

Nevertheless, we have: $\rho = \sum_{\xi=1}^{\chi} \sum_{\zeta=1}^{\chi} c_{\xi}^* c_{\zeta} \bigotimes_{i=1}^N |\phi_i[\zeta]\rangle\langle\phi_i[\xi]|$. By linearity, the linear system can be solved by solving each projector $\bigotimes_{i=1}^N \frac{|\phi_i[\zeta]\rangle\langle\phi_i[\xi]|}{\langle\phi_i[\xi]|\phi_i[\zeta]\rangle}$ (of trace one if $\langle\phi_i[\xi]|\phi_i[\zeta]\rangle \neq 0$) independently (a similar idea is presented in [30] for Gaussian evolution). A proof is given in section H.6. This requires knowing the dot products $\langle\phi_i[\xi]|\phi_i[\zeta]\rangle$. Indeed, if we consider a sum over coherent states, the projectors have zero cumulants for degrees larger or equal to 2 (see fig. 2.2).

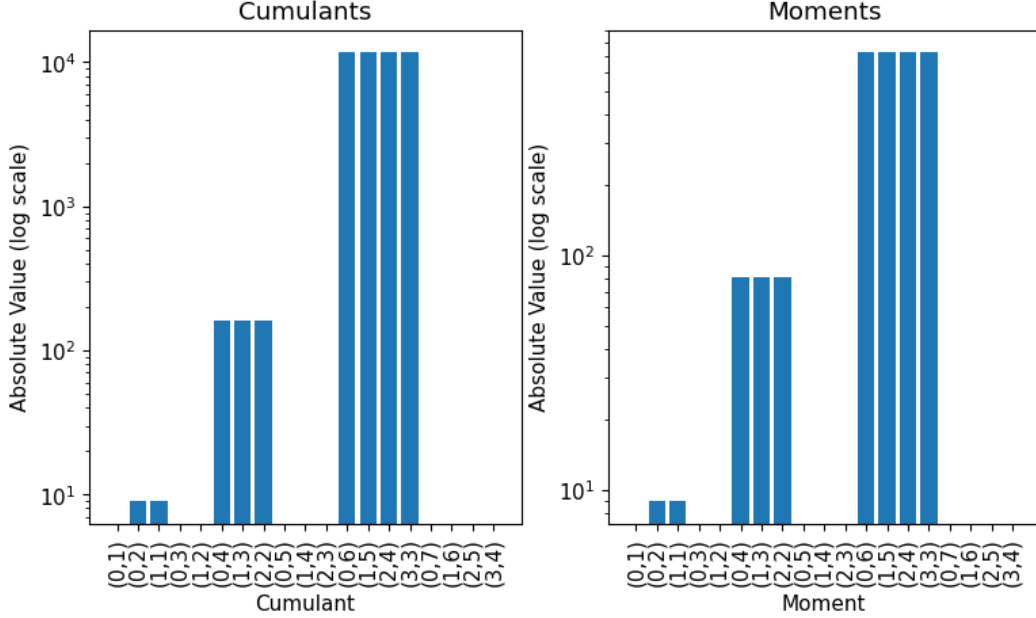


Figure 2.1: Cumulants and moments for the state $\propto \frac{|3\rangle+|-3\rangle}{\sqrt{2}}$ from dynamiqs [26] for the dimension 500 in logarithm scale. The index (j, k) corresponds to $a^{\dagger j} a^k$. The index (j, k) corresponds to $\langle a^{\dagger j} a^k \rangle$. $\langle a^{\dagger k} a^j \rangle$ and $\langle a^{\dagger j} a^k \rangle$ are complex-conjugate, thus we limit ourselves to $j \leq k$. For each subset of fixed $j + k$, the lexicographic order is imposed.

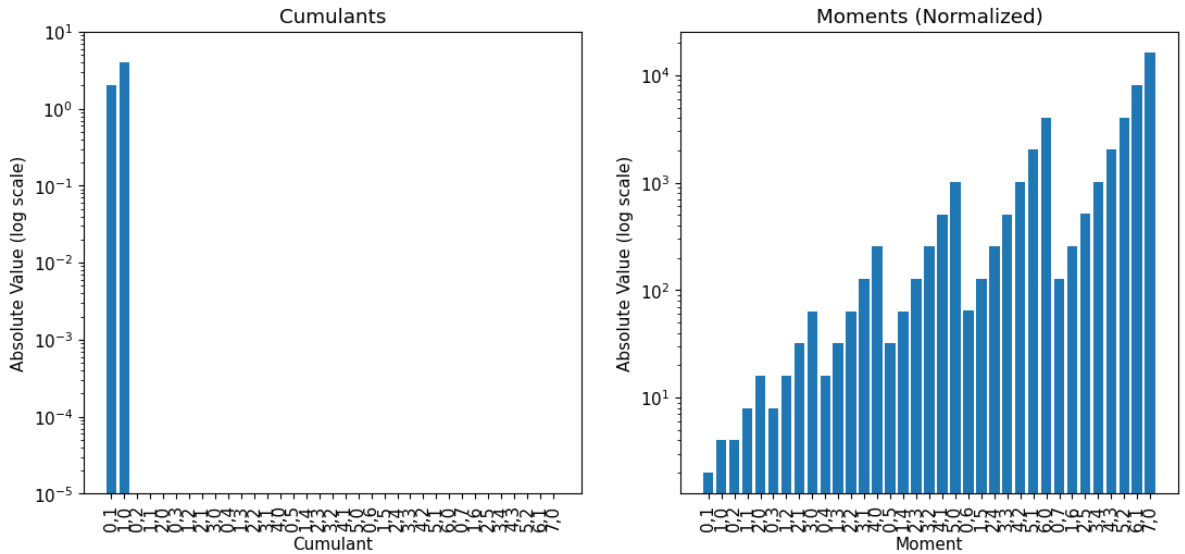


Figure 2.2: Cumulants and moments for the projector $\frac{|2\rangle\langle 1.5-3.7i|}{\langle 1.5-3.7i|2\rangle}$ using the exact numerical expression. The index (j, k) corresponds to $\langle a^{\dagger j} a^k \rangle$. The indices are ranked in an increasing order of $j + k$. For each subset of fixed $j + k$, the lexicographic order is imposed.

To see this, let us consider the projector $\frac{|\alpha\rangle\langle\beta|}{\langle\beta|\alpha\rangle}$. We have $M(z, z^*) = \text{Tr} \left\{ \frac{|\alpha\rangle\langle\beta|}{\langle\beta|\alpha\rangle} e^{iz^*a^\dagger} e^{iza} \right\} = \frac{\langle\beta|e^{iz^*a^\dagger} e^{iza}|\alpha\rangle}{\langle\beta|\alpha\rangle} = e^{iz^*\beta^*} e^{iz\alpha}$ (the expression is in normal order). Thus $\langle a^{\dagger j} a^k \rangle = \beta^{*j} \alpha^k$. And $K(z, z^*) = iz^*\beta^* + iz\alpha$. Thus: $C_a = \alpha$, $C_{a^\dagger} = \beta^*$ and $C_{a^{\dagger j} a^k} = 0$ for $j+k \geq 2$.

2.2.2 Stability Analysis

Closing the system of differential equations requires applying an approximation to estimate the moments of order larger than p . On one hand, the approximation needs to be physically justified, which guarantees its correctness. On the other hand, it has to lead to a stable differential system under numerical errors. Indeed, since we treat the moments as independent variables, stability problems appear. This justifies studying the stability of the differential system under numerical errors. We start by introducing the following notions of local stability. The following notion is abstract and will be clarified afterwards.

Definition 2.2.1 (General Notions of Local Stability). *A system of differential equations can be linearized around any given point of the multi-dimensional space defined by the moments at a given time t . Depending on the real part of the eigenvalues $\{\lambda_i\}_i$ of the linearized differential system, we can classify the stability of the system at that specific point into three classes:*

1. *Stable:* $\forall i, \text{Re}\{\lambda_i\} < 0$
2. *Neutral:* $\forall i, \text{Re}\{\lambda_i\} \leq 0$ and $\exists i, \text{Re}\{\lambda_i\} = 0$
3. *Unstable:* $\exists i, \text{Re}\{\lambda_i\} > 0$

The goal of this notion is to study whether the system amplifies numerical errors or not.

Introduction of \mathcal{L}

We introduce the notation $f[j_1, \dots, j_N, k_1, \dots, k_N] \equiv \left\langle \left(\prod_{l=1}^N a_l^{\dagger j_l} \right) \left(\prod_{l=1}^N a_l^{k_l} \right) \right\rangle$. We shall denote \vec{f} the vector containing $f[j_1, \dots, j_N, k_1, \dots, k_N]$'s. The order of the elements in the vector shall be fixed in the following manner. First, we put the elements such that $0 \leq \sum_{l=1}^N j_l \leq \sum_{l=1}^N k_l$ and $\sum_{l=1}^N j_l + k_l \leq p$ in a **lexicographic order**. Afterwards, we place in the same order the complex conjugate values (i.e. $f[k_1, \dots, k_N, j_1, \dots, j_N] = f[j_1, \dots, j_N, k_1, \dots, k_N]^*$ will come in the same place in the second half than $f[j_1, \dots, j_N, k_1, \dots, k_N]$ in the first half). This ensures that $\vec{f} = \begin{pmatrix} x \\ x^* \end{pmatrix}$. Further, the equation of evolution of \vec{f} that we obtain after applying the approximation can be written in all generality

$$\frac{d\vec{f}}{dt} = \vec{\mathcal{E}}(\vec{f}). \quad (2.6)$$

In order to study the stability, we consider a small deviation $\vec{\epsilon}$ from a solution \vec{f}_0 . To linear order, $\vec{\epsilon}$ satisfies the differential equation:

$$\frac{d\vec{\epsilon}}{dt} = \nabla_{\vec{f}} \vec{\mathcal{E}}(\vec{f}_0) \vec{\epsilon}. \quad (2.7)$$

For the following, we introduce the notation: $\mathcal{L} \equiv \nabla_{\vec{f}} \vec{\mathcal{E}}(\vec{f}_0)$, such that:

$$\mathcal{L}_{j_1, \dots, j_N, k_1, \dots, k_N; r_1, \dots, r_N, s_1, \dots, s_N} \equiv \frac{\partial \mathcal{E}_{j_1, \dots, j_N, k_1, \dots, k_N}}{\partial f[r_1, \dots, r_N, s_1, \dots, s_N]}(\vec{f}_0) \quad (2.8)$$

By construction, the matrix \mathcal{L} can be put in the form

$$\mathcal{L} = \begin{pmatrix} A & B \\ B^* & A^* \end{pmatrix}, \quad (2.9)$$

with A corresponding to $\sum_{l=1}^N j_l \leq \sum_{l=1}^N k_l$ and $\sum_{l=1}^N r_l \leq \sum_{l=1}^N s_l$ and B corresponding to $\sum_{l=1}^N j_l \leq \sum_{l=1}^N k_l$ and $\sum_{l=1}^N r_l \geq \sum_{l=1}^N s_l$. One remarks that some lines and columns are repeated (corresponding to $\sum_{l=1}^N j_l = \sum_{l=1}^N k_l$ and $\sum_{l=1}^N r_l = \sum_{l=1}^N s_l$). This is done to ensure that \mathcal{L} has the form 2.9. Some additional properties of \mathcal{L} are shown in [section H.7](#).

2.2.3 Numerical Tests

We compare the results for some quantum jumps: one-photon loss (cf. Figure 2.3), two-photon loss (cf. Figure 2.4) and dephasing (cf. Figure G.3). We see that one-photon loss stabilizes all the methods. This is corroborated by Figure G.8, Figure G.9, Figure G.6 and Figure G.7 in section G.1. Additionally, two-photon loss stabilizes `cumulant` method only, allowing us to conclude that the `cumulant` method is much more stable than the two others. Dephasing jump has no effect on the stability for all the methods.

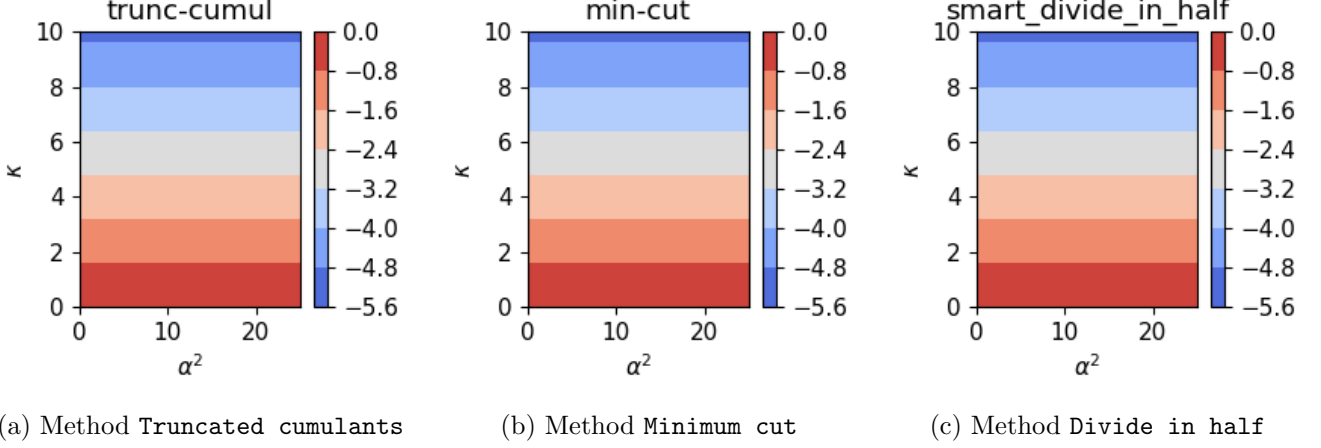


Figure 2.3: Maximal value for the real part of the eigenvalues of the stability matrix \mathcal{L} for quantum jump $\sqrt{\kappa}a$, coherent state $|\alpha\rangle$ and $p = 1$.

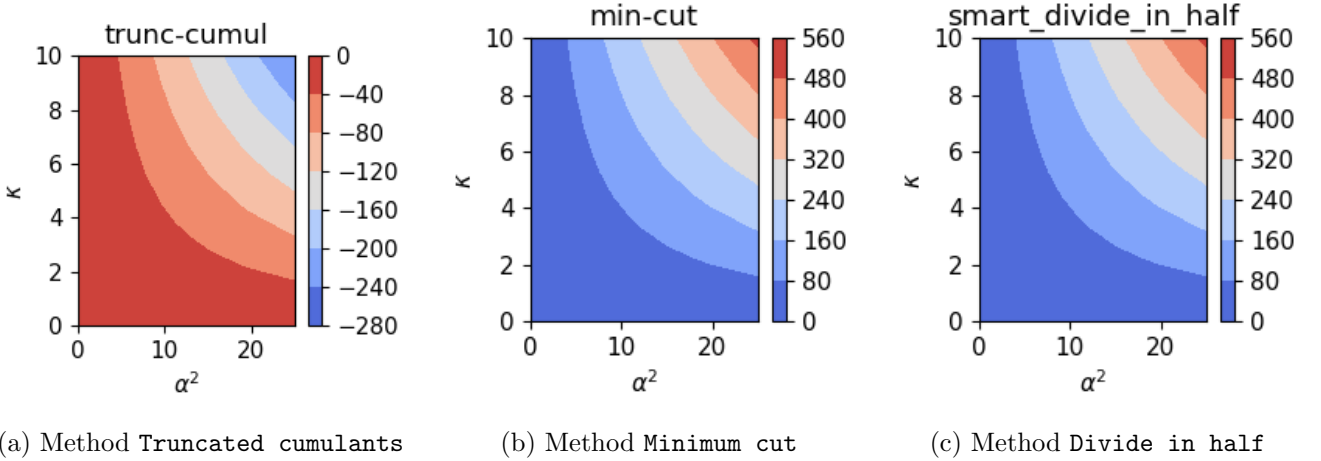


Figure 2.4: Maximal value for the real part of the eigenvalues of the stability matrix \mathcal{L} for quantum jump $\sqrt{\kappa}a^2$, coherent state $|\alpha\rangle$ and $p = 2$.

2.3 Time Evolution Approximation (TEA)

The hope of this method is to compute the time evolution in a symbolic manner, which can be done using `SymPy` [41]. The computed result is saved to solve the initial value problem for any initial value. The method allows to have changing parameters, which can be very useful for machine learning tasks [19–21].

The method corresponds to computing the expression $\sum_{n=0}^{\infty} \frac{1}{n!} \left(\frac{it}{\hbar}\right)^n \text{Comm}_p(H|O(0))$ in Equation 1.23 using symbolic computation [41] up to some cut-off p . One advantage of this approach comparatively to the mean field approximations is that it ensures that the solution is correct for short times (in a rigorous manner). Furthermore, the divergence of the method is well-understood and very intuitive (the neglected terms become important). Additionally, this method has an advantage over the Schrödinger representation since the commutation relations are canonical. Such canonical relations do

not exist with the density matrix. Finally, we access directly the correlations $\langle a^{\dagger j}(t)a^k(t) \rangle$, and not the moments $\langle a^{\dagger j}a^k \rangle(t)$.

Can We Include Quantum Jumps?

It turns out that we don't have an easy way to include quantum jumps for the TEA approximation. Nevertheless, we can do it in an **approximate** manner. For example, for one mode with ν -photon loss, the term that needs to be added to the equation of evolution is: $-\nu \frac{\kappa_\nu}{2} a^{\dagger(\nu-1)} a^\nu$. This can be represented **approximately** by adding the term $-i\hbar \frac{\kappa_\nu}{2} a^{\dagger\nu} a^\nu$ to the Hamiltonian.

In [section H.8](#), we show that the complexity of computing the commutators is given by

$$C(p) = O\left(\sum_{n=0}^{p-1} w_H^{n+1} (1 + m + n\tau_H)\right) \quad (2.10)$$

where w_H is the number of terms in H . Furthermore, it turns out (cf. [section H.9](#)) that the time of validity, i.e. the time where we expect the approximation to hold, grows at best in a linear fashion with p . Additionally, the proofs of [section H.9](#) allow us to extract the following pathological case.

Corollary 2.3.0.1. *We deduce from the proof that the Hamiltonians of the form $H = a^m + a^{\dagger m}$ for $m \geq 3$ are pathological in the sense that their validity time goes towards a constant. However, it turns out that TEA behaves better than **dynamiqs** [26] (cf. [Figure 2.5](#)).*

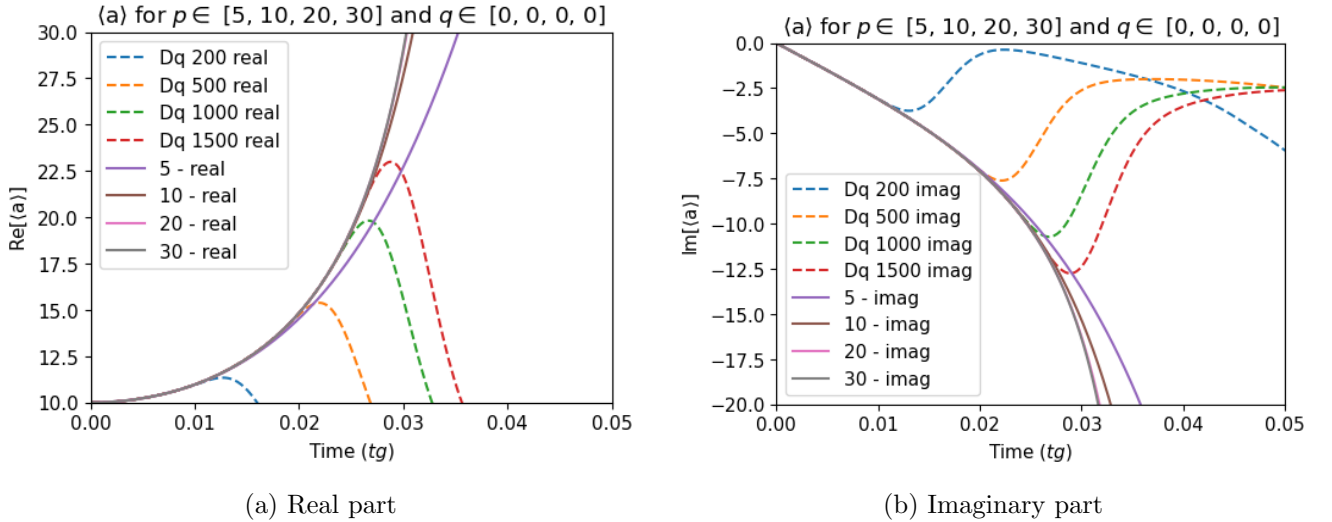


Figure 2.5: Evolution of $\langle a \rangle(t)$ for $H = a^{\dagger 3} + a^3$ comparing different cut-offs p and dimensions for **dynamiqs** [26]. Continuous line corresponds to the TEA for some cut-off while dashed line corresponds to **dynamiqs** for some dimension which corresponds to the value of p . $q = 0$ corresponds to not using the Padé approximate (cf. [section 2.3](#)).

Padé Approximate

The main takeaway of the previous part is that the time of validity of the TEA method increases at best linearly with the cut-off p while taking an exponential cost in time for the number of monomials $w_H \geq 2$ in the Hamiltonian H - in other words a little gain with a great cost. This prohibitive cost for improving accuracy can be partially tackled by using the Padé approximate [42, 43].

Let us consider a function approximated by a Taylor expansion: $f(t) = \sum_{n=0}^P a_p t^n + O(t^{P+1})$. We know that the Taylor expansion diverges for $t \rightarrow \infty$. This means that the approximation becomes very wrong for functions that are bounded. Padé approximate leverages this observation and proposes to approximate $f(t)$ by a rational function instead of a polynomial, i.e.

$$f(t) \approx \frac{\sum_{k=0}^p b_k t^k}{1 + \sum_{l=1}^q c_l t^l}. \quad (2.11)$$

We observe that the Padé approximant is at least as good as Taylor expansion if the optimal value of the coefficient is chosen ($q = 0$ corresponds to Taylor expansion). Nevertheless, the numerical system can be ill-conditioned and cause numerical problems. In order to obtain the values of the coefficients b_k and c_l , we solve the system

$$\sum_{n=0}^N a_p t^n = \frac{\sum_{k=0}^p b_k t^k}{1 + \sum_{l=1}^q c_l t^l}. \quad (2.12)$$

This can be done numerically using `scipy.interpolate.pade` [44], with p and q hyper-parameters that need to be tuned. The only requirement is that $p + q \leq P$ which ensures that the system has at least one solution. See Figure 2.6 for examples of how the Padé approximant improves the result.

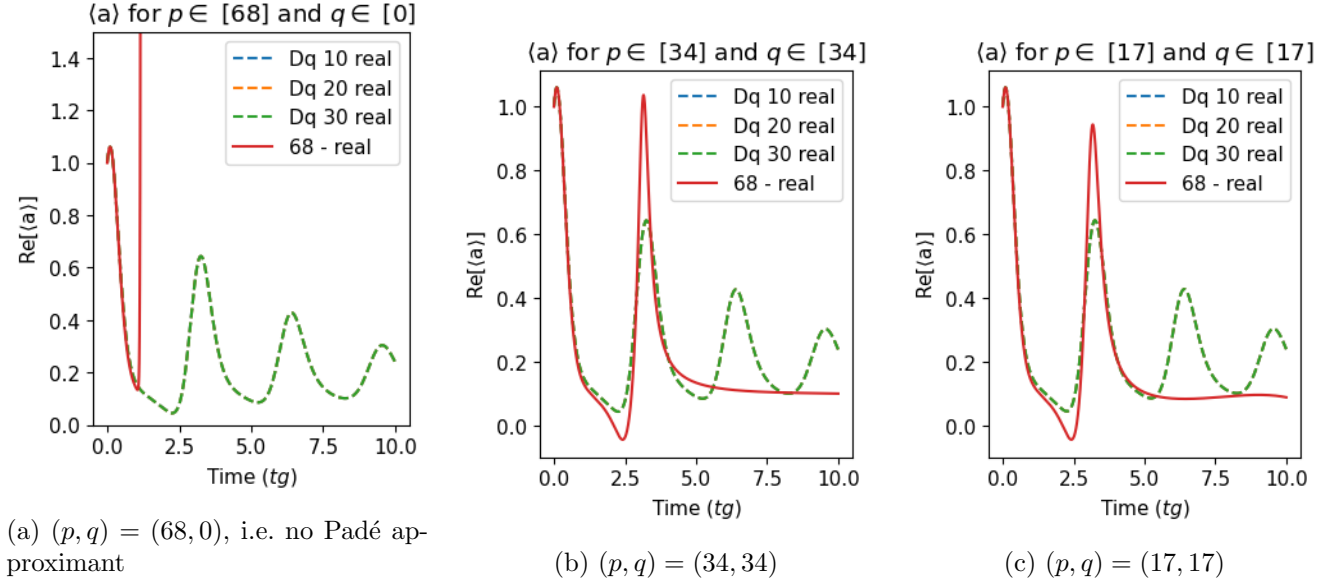


Figure 2.6: Evolution of $\text{Re}\{\langle a \rangle(t)\}$ using the TEA method improved using the Padé approximant for different values of p and q , for $H = a^\dagger b^\dagger b a$ and $L = \sqrt{0.1}a$. Continuous line corresponds to the TEA for some cut-off while dashed line corresponds to `dynamics` [26] for some dimension.

2.4 Complexity of the Methods

We compare the different methods by estimating their complexities in three different steps: writing the differential equations on scalar functions to solve, solving the differential system and evaluating the moments. We denote T the length of the time interval of interest. Solving the differential equation has a time and memory complexity proportional to T . As a reminder, N denotes the number of modes, p the cut-off, m the degree of the Hamiltonian, w_H the number of terms in the Hamiltonian, w_L the number of jump operators, $M_{\max,i}$ the maximal number of photons for the mode i , χ the number of terms for the sum on Gaussian states, B_p the p^{th} Bell number, cf. section A.2.

2.4.1 Density Matrix Method

We recall that the space dimension of the density matrix method is given by $\Theta\left(\prod_{i=1}^N M_{\max,i}\right)$, which is exponential in the number of modes N . The three steps require manipulating matrices of size $\Theta\left(\prod_{i=1}^N M_{\max,i}\right)$ via multiplication, addition or inversion. Thus, the time complexity is proportional to a polynomial of $\Theta\left(\prod_{i=1}^N M_{\max,i}\right)$.

2.4.2 Usual MF

This section refers to the methods `Divide in half` and `Minimum Cut`. The number of equations is $\sim \frac{1}{2} \sum_{q=1}^p \binom{2N+q-1}{q} = O((2N)^p)$. By using the bilinearity and product relation for the commuta-

Table 2.1: Comparison of the complexities of the methods (Part 1). For definition of notations, see [section 2.4](#)

Step / Method	Density Matrix	Usual MF
Writing equations (time)	$\Theta \left(\text{poly} \left(\prod_{i=1}^N M_{\max,i} \right) \right)$	$O((w_H + w_L)(p + m)(2N)^p)$
Writing equations (memory)	$\Theta \left(\prod_{i=1}^N M_{\max,i} \right)$	$O((2N)^p)$
Solving equations (time)	$\Theta \left(T \text{poly} \left(\prod_{i=1}^N M_{\max,i} \right) \right)$	$\Theta(\chi^2 T \text{poly}((2N)^p))$
Solving equations (memory)	$\Theta \left(T \prod_{i=1}^N M_{\max,i} \right)$	$\Theta(\chi^2 T \text{poly}((2N)^p))$
Retrieving a moment (time)	$\Theta \left(\text{poly} \left(\prod_{i=1}^N M_{\max,i} \right) \right)$	$O(\chi^2)$

Table 2.2: Comparison of the complexities of the methods (Part 2). For definition of notations, see [section 2.4](#)

Step / Method	Cumulant	TEA
Writing equations (time)	$O(B_p(w_H + w_L)(p + m)(2N)^p)$	$O(Npw_H^p(m + p\tau_H))$
Writing equations (memory)	$\sim \frac{1}{2}(2N)^p$	$\Theta(Np + Np^2\tau_H)$
Solving equations (time)	$\Theta(\chi^2 T \text{poly}((2N)^p))$	-
Solving equations (memory)	$\Theta(\chi^2 T \text{poly}((2N)^p))$	-
Retrieving a moment (time)	$\Theta(\chi^2 B_p)$	$O(\chi^2 \text{poly}(p, \tau_H))$

tor, we can show that each equation has a time complexity $O((w_H + w_L)(p + m))$, where w_H is the number of monomials in H and w_L is the number of jump operators. The memory complexity is $\sim \frac{1}{2} \sum_{q=1}^p \binom{2N+q-1}{q}$. The expressions can potentially be stored in an optimal manner. Solving the initial value problem requires using linear algebra polynomials, thus its time and memory complexities are given by $\Theta \left(T \text{poly} \left(\sum_{q=1}^p \binom{2N+q-1}{q} \right) \right)$. Retrieving the moments is straightforward since they are the values that are computed by solving the differential system. When the initial state is a sum over χ Gaussian states, we need to solve for each projector $\frac{|\alpha_\xi\rangle\langle\alpha_\zeta|}{\langle\alpha_\zeta|\alpha_\xi\rangle}$ independently, thus leading to a factor χ^2 .

2.4.3 Cumulant Method

The cumulant method is similar to the usual MF methods. One important difference is time needed to convert moments to cumulants and vice-versa. This time scales as B_p , i.e. the p^{th} Bell number, see [section A.2](#) for an introduction to Bell numbers. One important point is that B_p grows exponentially with p . Writing differential equations on cumulants is usually done by converting differential equations on moments [33]. Thus each term (a moment) needs to be converted into cumulants. For each equation, the number of terms is $O((w_H + w_L)(p + m))$. Furthermore, retrieving a moment requires converting back cumulants into moments, taking a time proportional to B_p .

2.4.4 Time Evolution Approximation

For the TEA, the state is represented by the evolution of the annihilators $a_i(t)$. These states can be represented, up to the time of validity which can be expanded using Padé approximate, by the coefficients which can be written symbolically. Thus, there is no need to solve a differential system, solving the problem of stability. Additionally, retrieving a moment requires multiplying symbolic representations, which requires computing χ^2 terms. The main limiting factor of this method is the time needed to compute the commutators.

The results of this part are summarized in [Table 2.1](#) and [Table 2.2](#). Complexities are over-estimated (with O) for the sake of making the comparison easier. See [section A.2](#) for the asymptotic behavior of Bell numbers.

Chapter 3

Conclusion

The conclusion does not belong
to the artist.

Emile Zola

This concluding chapter starts by providing a summary of the different subjects presented in the report. Afterwards, it directs the reader towards the open questions that might be the subject of subsequent research.

3.1 Summary of the Report

We have studied how to solve open bosonic systems when finding exact analytical solutions is challenging, cf. [Appendix E](#). After a brief overview of the literature (cf. [chapter 1](#)), we showed how to write the quantum Langevin equation for many photon loss (cf. [section 2.1](#) and [Appendix C](#)). Afterwards, we present our contribution to MF methods and introduced some tools to compare between them (cf. [subsection 2.2.3](#) and [section 2.4](#)) (cf. [Appendix I](#)). We can study dynamics from states that can be expressed as a sum over low-cumulant states. We also introduce the time evolution approximation (cf. [section 2.3](#)) which allows to approximate the finite series of $a_i(t)$. A great care has been taken in comparing quantitatively the different methods and in proving the different statements. Appendices give some clarifications and details that could not be put in the report.

In particular, a summarized comparison between the methods is provided in [Table F.1](#). The comparison highlights the strengths and weaknesses of the different methods. A key takeaway is that the choice of the method to apply depends on the particular needs of each case.

3.2 Open questions

Even though we had the opportunity to tackle many important and interesting questions during this project, many problems remain sadly unanswered. One such a question is the study of time-dependent inputs $a_{\text{in}}(t)$. The challenge arises from the difficulty of defining Green's functions for non-linear systems [\[39, 40\]](#). This question is important if we desire to engineer more complex pulses than piece-wise constant inputs, even though piece-wise constant inputs are easier to optimize [\[45\]](#). It is possible that the mean methods can be used to solve the problem numerically. Furthermore, other theoretical questions remain open as highlighted in [Table F.1](#). Even though, we have gained a greater understanding of the problem $(AB)_H \neq A_H B_H$ in [Appendix B](#), we do not have yet a satisfying answer. A clear answer to this question will allow us to know when TEA is exact for an open system, for example. It will also tell us when correlations and moments are equal.

Last but not least, these methods still need to be applied for experimental cases.

Bibliography

1. Mehra, J. The Birth of Quantum Mechanics. *CERN*. https://inis.iaea.org/collection/NCLCollectionStore/_Public/08/282/8282072.pdf?r=1 (1976).
2. *Webpage of the International Year of Quantum Science and Technology* [Online; accessed 27-May-2024]. <https://quantum2025.org/en/>.
3. Taddei, M. M. *et al.* Computational Advantage from the Quantum Superposition of Multiple Temporal Orders of Photonic Gates. *PRX Quantum* **2**, 010320. <https://link.aps.org/doi/10.1103/PRXQuantum.2.010320> (1 2021).
4. Schuld, M. & Killoran, N. Quantum Machine Learning in Feature Hilbert Spaces. *Phys. Rev. Lett.* **122**, 040504. <https://link.aps.org/doi/10.1103/PhysRevLett.122.040504> (4 2019).
5. Aspect, A., Dalibard, J. & Roger, G. Experimental test of Bell's inequalities using time-varying analyzers. *Physical Review Letters* **49**, 1804. <https://link.aps.org/doi/10.1103/PhysRevLett.49.1804> (1982).
6. Debnath, S. *et al.* Demonstration of a small programmable quantum computer with atomic qubits. *Nature* **536**, 63–66. <https://doi.org/10.1038/nature18648> (2016).
7. Pogorelov, I. *et al.* Compact ion-trap quantum computing demonstrator. *PRX Quantum* **2**, 020343. <https://doi.org/10.1103/PRXQuantum.2.020343> (2021).
8. Haroche, S. & Raimond, J.-M. *Exploring the Quantum: Atoms, Cavities, And Photons* ISBN: 0198509146 (Oxford Graduate Texts, 2013).
9. Lukacs, E. *Characteristic Functions* 2nd ed. ISBN: 0852641702 (Griffin, 1970).
10. Ebadi, S. *et al.* Quantum optimization of maximum independent set using Rydberg atom arrays. *Science* **376**, 1209–1215. <https://www.science.org/doi/abs/10.1126/science.abo6587> (2022).
11. Prawer, S. & Greentree, A. D. Diamond for quantum computing. *Science* **320**, 1601–1602. <https://www.science.org/doi/abs/10.1126/science.1158340> (2008).
12. Castelvechi, D. Quantum computers ready to leap out of the lab in 2017. *en. Nature* **541**, 9–10. <https://doi.org/10.1038/541009a> (2017).
13. Ryan, C. A., Johnson, B. R., Ristè, D., Donovan, B. & Ohki, T. A. Hardware for Dynamic Quantum Computing. arXiv: [1704.08314](https://arxiv.org/abs/1704.08314) [quant-ph] (2017).
14. Somaschi, N. *et al.* Near-optimal single-photon sources in the solid state. *Nature Photonics* **10**, 340–345. <https://doi.org/10.1038/nphoton.2016.23> (2016).
15. Mezher, R., Carvalho, A. F. & Mansfield, S. Solving graph problems with single photons and linear optics. *Phys. Rev. A* **108**, 032405. <https://link.aps.org/doi/10.1103/PhysRevA.108.032405> (3 2023).
16. Choe, S. *Quantum computing overview: discrete vs. continuous variable models* 2022. arXiv: [2206.07246](https://arxiv.org/abs/2206.07246) [quant-ph].
17. Gouzien, É., Ruiz, D., Le Régent, F.-M., Guillaud, J. & Sangouard, N. Performance Analysis of a Repetition Cat Code Architecture: Computing 256-bit Elliptic Curve Logarithm in 9 Hours with 126 133 Cat Qubits. *Phys. Rev. Lett.* **131**, 040602. <https://link.aps.org/doi/10.1103/PhysRevLett.131.040602> (4 2023).
18. Hey, A. J. G. in *Feynman and computation* 1st ed., 133–153 (CRC Press, 2018). ISBN: 9780429500459.

19. Stoyanova, A., Hammadia, T., Ricou, A. & Penkovsky, B. *Photonic Quantum Computing For Polymer Classification* 2022. arXiv: [2211.12207](https://arxiv.org/abs/2211.12207) [quant-ph].
20. Marković, D., Mizrahi, A., Querlioz, D. & Grollier, J. Physics for neuromorphic computing. *Nature Reviews Physics* **2**, 499–510. <https://doi.org/10.1038/s42254-020-0208-2> (2020).
21. Dudas, J. *et al.* Quantum reservoir computing implementation on coherently coupled quantum oscillators. *npj Quantum Inf.* **9**. <https://doi.org/10.1038/s41534-023-00734-4> (2023).
22. Wikipedia contributors. *Commutator* — *Wikipedia, The Free Encyclopedia* <https://en.wikipedia.org/wiki/Commutator>. [Online; accessed 27-May-2024]. 2024.
23. Quesada, N. & Sipe, J. E. Why you should not use the electric field to quantize in nonlinear optics. *Opt. Lett.* **42**, 3443–3446. <https://opg.optica.org/ol/abstract.cfm?URI=ol-42-17-3443> (2017).
24. Dirac, P. *The Principles of Quantum Mechanics* 3rd ed. <https://digbib.bibliothek.kit.edu/volltexte/wasbleibt/57355817/57355817.pdf> (Oxford University Press, 1947).
25. Johansson, J. R., Nation, P. D. & Nori, F. QuTiP: An open-source Python framework for the dynamics of open quantum systems. *Computer Physics Communications* **183**, 1760–1772. ISSN: 0010-4655. <http://dx.doi.org/10.1016/j.cpc.2012.02.021> (2012).
26. Guilmin, P., Gautier, R., Bocquet, A. & Genois, É. *dynamiqs: an open-source Python library for GPU-accelerated and differentiable simulation of quantum systems* 2024. <https://github.com/dynamiqs/dynamiqs>.
27. Nielsen, M. A. & Chuang, I. L. *Quantum Computation and Quantum Information: 10th Anniversary Edition* ISBN: 9781107002173 (Cambridge University Press, 2011).
28. Mitchison, M. *Is the Heisenberg picture of an open-system very different than that of a closed one?* [Online; accessed 4-June-2024]. <https://physics.stackexchange.com/questions/422851/is-the-heisenberg-picture-of-an-open-system-very-different-than-that-of-a-closed>.
29. Gouzien, É. *Optique quantique multimode pour le traitement de l'information quantique* PhD thesis (Institut de Physique de Nice (INPHYNI), CNRS, UMR 7 010, 2019). <https://theses.hal.science/tel-02885960/document>.
30. Bourassa, J. E. *et al.* Fast Simulation of Bosonic Qubits via Gaussian Functions in Phase Space. *PRX Quantum* **2**, 040315. <https://doi.org/10.1103/PRXQuantum.2.040315> (4 2021).
31. Walls, D. F. & Milburn, G. J. *Quantum Optics* ISBN: 978-3-540-28574-8. <https://link.springer.com/book/10.1007/978-3-540-28574-8> (Springer Berlin, Heidelberg, 2007).
32. Ginzburg, V. & Pitaevskii, L. On the theory of superfluidity. *Sov. Phys. JETP* **7**, 858–861. http://jetp.ras.ru/cgi-bin/dn/e_007_05_0858.pdf (1958).
33. Khan, S. A., Hu, F., Angelatos, G. & Türeci, H. E. *Physical reservoir computing using finitely-sampled quantum systems* 2021. arXiv: [2110.13849](https://arxiv.org/abs/2110.13849) [quant-ph].
34. Wikipedia contributors. *Quasiprobability distribution* — *Wikipedia, The Free Encyclopedia* [Online; accessed 7-June-2024]. 2024. https://en.wikipedia.org/wiki/Quasiprobability_distribution.
35. Wikipedia contributors. *Glauber–Sudarshan P representation* — *Wikipedia, The Free Encyclopedia* [Online; accessed 7-June-2024]. 2023. https://en.wikipedia.org/wiki/Glauber%E2%80%93Sudarshan_P_representation.
36. Arbogast, L. F. A. *Du calcul des dérivations* ISBN: 978-1140544760 (De Imprimerie Berger-Levrault, 2010).
37. Wikipedia contributors. *Faà di Bruno's formula* — *Wikipedia, The Free Encyclopedia* [Online; accessed 12-June-2024]. 2024. https://en.wikipedia.org/wiki/Fa%C3%A0_di_Bruno%27s_formula.
38. Plankensteiner, D., Hotter, C. & Ritsch, H. QuantumCumulants. jl: A Julia framework for generalized mean-field equations in open quantum systems. *Quantum* **6**, 617. ISSN: 2521-327X. <https://doi.org/10.22331/q-2022-01-04-617> (2022).

39. Frasca, M. & Khurshudyan, A. *General Representation of Nonlinear Green's Function for Second Order Differential Equations Nonlinear in the First Derivative* 2018. arXiv: [1806.00274v2 \[math-ph\]](#).
40. Frasca, M. & Khurshudyan, A. Green's functions for higher order nonlinear equations. *International Journal of Modern Physics C* **29**, 1850104. <https://doi.org/10.1142/S0129183118501048> (2018).
41. Meurer, A. *et al.* SymPy: symbolic computing in Python. *PeerJ Computer Science* **3**, e103. ISSN: 2376-5992. <https://doi.org/10.7717/peerj-cs.103> (2017).
42. Padé, H. Mémoire sur les développements en fractions continues de la fonction exponentielle, pouvant servir d'introduction à la théorie des fractions continues algébriques. fr. *Annales scientifiques de l'École Normale Supérieure* **3e série, 16**, 395–426. <http://archive.numdam.org/articles/10.24033/asens.470/> (1899).
43. Wikipedia contributors. *Padé approximant* — *Wikipedia, The Free Encyclopedia* [Online; accessed 27-May-2024]. 2024. https://en.wikipedia.org/wiki/Pad%C3%A9_approximant.
44. Virtanen, P. *et al.* SciPy 1. 0: Fundamental Algorithms for Scientific Computing in Python. *Nature Methods* **17**, 261–272 (2020).
45. Wright, E. & de Sousa, R. *Fast Quantum Gate Design with Deep Reinforcement Learning Using Real-Time Feedback on Readout Signals* in *2023 IEEE International Conference on Quantum Computing and Engineering (QCE)* **01** (2023), 1295–1303. <https://doi.org/10.1109/QCE57702.2023.00146>.
46. Knuth, D. E. *The Art of Computer Programming* ISBN: 978-0201038040 (Addison-Wesley, Upper Saddle River, NJ, 2011).
47. Wikipédia. *Comparaison asymptotique* — *Wikipédia, l'encyclopédie libre* [En ligne; Page disponible le 18-mars-2024]. 2024. https://fr.wikipedia.org/wiki/Comparaison_asymptotique.
48. OEIS. *A000110 as a graph* <https://oeis.org/A000110>. [Online; accessed 28-May-2024].
49. De Bruijn, N. G. *Asymptotic methods in analysis* ISBN: 9780486150796 (Dover, 1981).
50. OEIS. *A000110 as a graph* <https://oeis.org/A000110/graph>. [Online; accessed 12-April-2024].
51. Wikipedia contributors. *Pascal's triangle* — *Wikipedia, The Free Encyclopedia* [Online; accessed 17-June-2024]. 2024. https://en.wikipedia.org/wiki/Pascal%27s_triangle.
52. Purcell, E. Optical emission. *Phys Rev* **69**, 681. <https://doi.org/10.1103/PhysRev.69.674.2> (1946).
53. Linowski, T. & Rudnicki, L. Relating the Glauber-Sudarshan, Wigner, and Husimi quasiprobability distributions operationally through the quantum-limited amplifier and attenuator channels. *Physical Review A* **109**. ISSN: 2469-9934. <http://dx.doi.org/10.1103/PhysRevA.109.023715> (2024).
54. Wikipedia contributors. *Husimi Q representation* — *Wikipedia, The Free Encyclopedia* [Online; accessed 7-June-2024]. 2024. https://en.wikipedia.org/wiki/Husimi_Q_representation.
55. Wikipedia contributors. *Wigner quasiprobability distribution* — *Wikipedia, The Free Encyclopedia* [Online; accessed 7-June-2024]. 2024. https://en.wikipedia.org/wiki/Wigner_quasiprobability_distribution.
56. Wikipedia contributors. *Ordered exponential* — *Wikipedia, The Free Encyclopedia* [Online; accessed 3-June-2024]. 2024. https://en.wikipedia.org/wiki/Ordered_exponential.
57. Santa Cruz Institute for Particle Physics. *The time evolution operator as a time-ordered exponential* [Online; accessed 3-June-2024]. <http://scipp.ucsc.edu/~haber/ph215/TimeOrderedExp.pdf>.
58. Suzuki, M. Quantum analysis—Non-commutative differential and integral calculi. en. *Commun. Math. Phys.* **183**, 339–363. <https://doi.org/10.1007/BF02506410> (1997).
59. Harris, C. R. *et al.* Array programming with NumPy. *Nature* **585**, 357–362. <https://doi.org/10.1038/s41586-020-2649-2> (2020).

60. Hunter, J. D. Matplotlib: A 2D graphics environment. *Computing in Science & Engineering* **9**, 90–95 (2007).
61. dynamiqs’ team. *Python API: dq.squeeze* [Online; accessed 18-June-2024]. 2024. https://www.dynamiqs.org/python_api/utils/operators/squeeze.html.
62. Guillaud, J. & Mirrahimi, M. Repetition Cat Qubits for Fault-Tolerant Quantum Computation. *Phys. Rev. X* **9**, 041053. <https://link.aps.org/doi/10.1103/PhysRevX.9.041053> (4 2019).
63. Nieto, M. M. & Truax, D. R. Holstein-Primakoff/Bogoliubov Transformations and the Multiboson System. *Fortschritte der Physik/Progress of Physics* **45**, 145–156. ISSN: 1521-3979. <http://dx.doi.org/10.1002/prop.2190450204> (1997).
64. Agarwal, G. *Quantum Optics* ISBN: 978-1107006409 (Cambridge University Press, 2012).
65. dynamiqs’ team. *Python API: dq.displace* [Online; accessed 21-June-2024]. 2024. https://www.dynamiqs.org/python_api/utils/operators/displace.html.
66. Wikipedia contributors. *Squeezed coherent state* — *Wikipedia, The Free Encyclopedia* [Online; accessed 24-June-2024]. 2024. https://en.wikipedia.org/wiki/Squeezed_coherent_state.

Appendix A

Additional Definitions

A.1 Notions of Complexity

In this appendix, we introduce some notations for studying complexity. Since there are different notations [46, 47], we fix the one we will follow in this report.

A.1.1 Presentation of the Problem

When we are considering computational problems whose input size is given by N , we want to evaluate the needed resources for solving the problem using a given problem. For example, the computational time (in some time unit) or the memory size (in bits for example) might be of great importance.

Nevertheless, there is usually no need to know the exact value of the needed resources. Indeed, the exact value of the needed resources depends on the details of the machine. Thus, only the global evolution for N going to infinity matters. For example, does the computation time go polynomially with N ? Does the memory requirement go exponentially with N ?

A.1.2 Notation Conventions

We consider two functions $f(N)$ and $g(N)$ two functions. We want to compare their behavior at infinity. For this, we introduce the following definitions:

Definition A.1.1 (*o* Notation). *We say that $f(N) = o(g(N))$ when:*

$$\forall \epsilon > 0, \exists N_0 \in \mathbb{N}, \forall N \geq N_0, |f(N)| \leq \epsilon |g(N)| \quad (\text{A.1})$$

This means that $f(N)$ is negligible in front of $g(N)$.

Definition A.1.2 (*O* Notation). *We say that $f(N) = O(g(N))$ when:*

$$\exists M > 0, \exists N_0 \in \mathbb{N}, \forall N \geq N_0, |f(N)| \leq M |g(N)| \quad (\text{A.2})$$

Remark A.1.0.1. *It is quite important to understand that this notation does not mean that $f(N)$ and $g(N)$ become comparable when $N \rightarrow \infty$. For example, we can write: $N = O(e^N)$.*

If we want to say that $f(N)$ and $g(N)$ become comparable when $N \rightarrow \infty$, we use the Θ notation:

Definition A.1.3 (Θ notation). *We say that $f(N) = \Theta(g(N))$ when:*

$$\exists M_1, M_2 > 0, \exists N_0 \in \mathbb{N}, \forall N \geq N_0, M_1 |g(N)| \leq |f(N)| \leq M_2 |g(N)| \quad (\text{A.3})$$

In particular, we have:

Theorem A.1.1. *We have:*

1. $f(N) = \Theta(g(N)) \iff g(N) = \Theta(f(N))$
2. $f(N) = \Theta(g(N)) \implies f(N) = O(g(N))$

Definition A.1.4 (Equivalence). *We say that $f(N) \sim g(N)$ (f and g are equivalent) when:*

$$\lim_{N \rightarrow \infty} \frac{f(N)}{g(N)} = 1 \quad (\text{A.4})$$

In particular, we have:

Theorem A.1.2. *We have:*

1. $f(N) \sim g(N) \iff g(N) \sim f(N)$
2. $f(N) \sim g(N) \implies f(N) = \Theta(g(N))$

A.2 Bell Numbers

Bell numbers are a notion of combinatorics. It is **not** related to the famous Bell inequality in quantum physics. B_n counts the number of partitions in a set I of size n [46, 48], i.e. the number of sets of disjoint subsets of I whose union is I . For example, $\{\{1, 2\}, \{3\}\}$ and $\{\{1, 2, 3\}\}$ are partitions of $I = \{1, 2, 3\}$.

Bell numbers are given by [Theorem A.2.1](#) which is due to Yoshisuke Matsunaga from the Japanese Edo era [46].

Theorem A.2.1 (Yoshisuke Matsunaga).

$$B_{n+1} = \sum_{k=0}^n \binom{n}{k} B_k \quad (\text{A.5})$$

For the purpose of analysing the complexity of the **truncated cumulants**(cf. [1.2.3](#)), we need to estimate the asymptotic behavior of B_n . We use the result of de Bruijn [49].

Theorem A.2.2 (De Bruijn).

$$\frac{\ln B_n}{n} = \ln n - \ln \ln n - 1 + o(1) \quad (\text{A.6})$$

In a hand-waving approach, we could say that B_n "behaves" as n^n , which signifies an exponential growth. Indeed, this can be seen in the plot [Figure A.1](#) from [50].

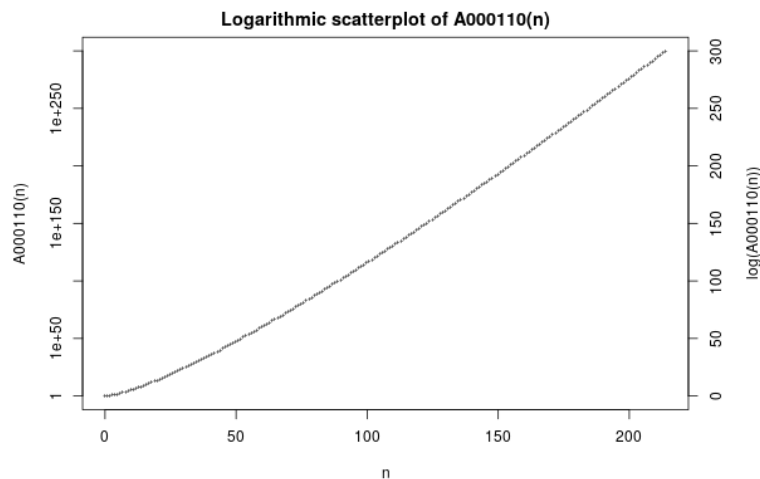


Figure A.1: Plot of Bell numbers from the OEIS [50] in \log_{10} scale

Appendix B

Sufficient Condition for Multiplicity of Heisenberg Representation

This result is motivated by the fact that being able to write $(AB)_H = A_H B_H$ allows to solve many problems. In particular, we could solve analytically (cf. [Appendix E](#)) many problems if it were the case.

”Multiplicity of the Heisenberg representation” refers to the fact that $(AB)_H = A_H B_H$. This appendix is presented in a way that mimics the reasoning that we followed. The appendix gives a good reason why the Heisenberg representation is non-multiplicative.

In this part, we find a sufficient condition for having $(AB)_H = A_H B_H$. To the best of our knowledge, this result is original. We limit ourselves to a time-independent Hamiltonian H_S and to quantum jumps $\{L_\mu\}_\mu$. Beforehand, we introduce the notation

$$\mathcal{L}_S(A) \equiv \frac{1}{i\hbar}[A, H_S] + \frac{1}{2} \sum_\mu \left(L_\mu^\dagger [A, L_\mu] - [A, L_\mu^\dagger] L_\mu \right) \quad (\text{B.1})$$

which corresponds to the right hand side of the equation in [Theorem 1.2.1](#) before taking the Heisenberg representation, i.e. $\frac{dA_H}{dt} = (\mathcal{L}_S(A))_H$.

We want to know whether $(AB)_H = A_H B_H$. Since at $t = 0$, $(AB)_H(t = 0) = AB = A_H(t = 0)B_H(t = 0)$, it suffices to show that $(AB)_H$ and $A_H B_H$ satisfy the same differential equation.

We start by writing the differential equations of $(AB)_H$ and of $A_H B_H$.

Theorem B.0.1. *We have:*

$$\frac{dA_H B_H}{dt} = A_H (\mathcal{L}_S(B))_H + (\mathcal{L}_S(A))_H B_H \quad (\text{B.2})$$

$$\frac{d(AB)_H}{dt} = (A\mathcal{L}_S(B))_H + (\mathcal{L}_S(A)B)_H + \sum_\mu \left([L_\mu^\dagger, A][B, L_\mu] \right)_H \quad (\text{B.3})$$

We strongly encourage the reader to read the following proof since it is very instructive and gives a very good reason why $(AB)_H \neq A_H B_H$ in general.

Proof. On the one hand, we have:

$$\frac{dA_H B_H}{dt} = A_H \frac{dB_H}{dt} + \frac{dA_H}{dt} B_H = A_H (\mathcal{L}_S(B))_H + (\mathcal{L}_S(A))_H B_H \quad (\text{B.4})$$

On the other hand, we have:

$$\begin{aligned} \frac{d(AB)_H}{dt} &= \left(\frac{1}{i\hbar}[AB, H_S] + \frac{1}{2} \sum_\mu \left(L_\mu^\dagger [AB, L_\mu] - [AB, L_\mu^\dagger] L_\mu \right) \right)_H \\ &= \left(\frac{1}{i\hbar}A[B, H_S] + \frac{1}{2} \sum_\mu \left(\textcolor{red}{L}_\mu^\dagger A[B, L_\mu] - A[B, L_\mu^\dagger] L_\mu \right) \right)_H \\ &\quad + \left(\frac{1}{i\hbar}[A, H_S]B + \frac{1}{2} \sum_\mu \left(L_\mu^\dagger [A, L_\mu]B - [A, L_\mu^\dagger] \textcolor{red}{B} L_\mu \right) \right)_H \end{aligned} \quad (\text{B.5})$$

Before continuing the computation, we see that obtaining a quantity in the form $A... + ...B$ that is expected from the product rule is prevented by the the presence of the jump operators on the right and on the left for A and B respectively. This confirms that the Heisenberg representation is non-multiplicative because of the jump operators. Let us try to put the product in the form $A... + ...B$:

$$\begin{aligned}\frac{d(AB)_H}{dt} &= (A\mathcal{L}_S(B))_H + (\mathcal{L}_S(A)B)_H + \frac{1}{2} \sum_{\mu} \left([L_{\mu}^{\dagger}, A][B, L_{\mu}] - [A, L_{\mu}^{\dagger}][B, L_{\mu}] \right)_H \\ &= (A\mathcal{L}_S(B))_H + (\mathcal{L}_S(A)B)_H + \sum_{\mu} \left([L_{\mu}^{\dagger}, A][B, L_{\mu}] \right)_H\end{aligned}\quad (\text{B.6})$$

□

From Equation B.2 and Equation B.3, we see that the difference between $(AB)_H$ and $A_H B_H$ is due to two facts. One the one hand, it is not guaranteed that $A_H (\mathcal{L}_S(B))_H + (\mathcal{L}_S(A))_H B_H = (A\mathcal{L}_S(B))_H + (\mathcal{L}_S(A)B)_H$. One the other hand, the quantum jumps lead to the additional term in the evolution of $(AB)_H$, namely $\sum_{\mu} \left([L_{\mu}^{\dagger}, A][B, L_{\mu}] \right)_H$.

One might be tempted to say that the sought condition is $\sum_{\mu} \left([L_{\mu}^{\dagger}, A][B, L_{\mu}] \right)_H = 0$. Indeed, the counter-example in subsection 1.2.2 does not satisfy this condition ($[a, a^{\dagger}][a^{\dagger}, a] \neq 0$). However, we still need to show that $A_H (\mathcal{L}_S(B))_H + (\mathcal{L}_S(A))_H B_H = (A\mathcal{L}_S(B))_H + (\mathcal{L}_S(A)B)_H$. We use the same strategy as before and write for eg.:

$$\frac{dA_H \mathcal{L}_S(B)}{dt} = A_H \left(\mathcal{L}_S^{(2)}(B) \right)_H + (\mathcal{L}_S(A))_H \mathcal{L}_S(B) \quad (\text{B.7})$$

$$\frac{d(A\mathcal{L}_S(B))_H}{dt} = \left(A\mathcal{L}_S^{(2)}(B) \right)_H + (\mathcal{L}_S(A) \mathcal{L}_S(B))_H + \sum_{\mu} \left([L_{\mu}^{\dagger}, A][\mathcal{L}_S(B), L_{\mu}] \right)_H \quad (\text{B.8})$$

with $f^{(n)}$ meaning the composition n times. Therefore, we find that a sufficient condition that we would like to have is that $\sum_{\mu} \left([L_{\mu}^{\dagger}, A][\mathcal{L}_S(B), L_{\mu}] \right)_H = 0$ and $A_H \left(\mathcal{L}_S^{(2)}(B) \right)_H + (\mathcal{L}_S(A))_H \mathcal{L}_S(B) = \left(A\mathcal{L}_S^{(2)}(B) \right)_H + (\mathcal{L}_S(A) \mathcal{L}_S(B))_H$. We start to see the inductive nature of the problem. Therefore, we introduce the following regularity condition:

Definition B.0.1 (Regularity condition). *We say that the pair of operators (A, B) is regular with respect to the quantum jumps $\{L_{\mu}\}_{\mu}$ when:*

$$\forall r, s \in \mathbb{N}, \sum_{\mu} \left([L_{\mu}^{\dagger}, \mathcal{L}_S^{(r)}(A)][\mathcal{L}_S^{(s)}(B), L_{\mu}] \right)_H = 0 \quad (\text{B.9})$$

Further, we introduce the sequence of propositions:

Definition B.0.2 (Sequence of propositions). *For $n \in \mathbb{N}$, we introduce the proposition $\mathcal{P}(n)$:*

$$\mathcal{P}(n) \equiv \left\{ \forall r, s \in \mathbb{N}, r + s = n \implies \left(\mathcal{L}_S^{(r)}(A) \mathcal{L}_S^{(s)}(B) \right)_H = \left(\mathcal{L}_S^{(r)}(A) \right)_H \left(\mathcal{L}_S^{(s)}(B) \right)_H \right\} \quad (\text{B.10})$$

We will show the following theorem:

Theorem B.0.2 (Sufficient condition if regularity). *Under the **regularity condition**, we have:*

$$\forall n \in \mathbb{N}, \mathcal{P}(n+1) \implies \mathcal{P}(n) \quad (\text{B.11})$$

Proof. Let $n \in \mathbb{N}$, let us suppose $\mathcal{P}(n+1)$. Let $r, s \in \mathbb{N}$, such that $r + s = n$, we have, using the regularity condition:

$$\frac{d \left(\mathcal{L}_S^{(r)}(A) \mathcal{L}_S^{(s)}(B) \right)_H}{dt} = \left(\mathcal{L}_S^{(r+1)}(A) \mathcal{L}_S^{(s)}(B) \right)_H + \left(\mathcal{L}_S^{(r)}(A) \mathcal{L}_S^{(s+1)}(B) \right)_H \quad (\text{B.12})$$

Since $(r + 1) + s = r + (s + 1) = n + 1$, applying the proposition $\mathcal{P}(n + 1)$, we can write:

$$\begin{aligned} \frac{d \left(\mathcal{L}_S^{(r)}(A) \mathcal{L}_S^{(s)}(B) \right)_H}{dt} &= \left(\mathcal{L}_S^{(r+1)}(A) \right)_H \left(\mathcal{L}_S^{(s)}(B) \right)_H + \left(\mathcal{L}_S^{(r)}(A) \right)_H \left(\mathcal{L}_S^{(s+1)}(B) \right)_H \\ &= \frac{d \left[\left(\mathcal{L}_S^{(r)}(A) \right)_H \left(\mathcal{L}_S^{(s)}(B) \right)_H \right]}{dt} \end{aligned} \quad (\text{B.13})$$

Therefore: $\left(\mathcal{L}_S^{(r)}(A) \mathcal{L}_S^{(s)}(B) \right)_H = \left(\mathcal{L}_S^{(r)}(A) \right)_H \left(\mathcal{L}_S^{(s)}(B) \right)_H$, which shows $\mathcal{P}(n)$. \square

We can represent the structure that we uncovered using a reverse Pascal triangle [51], cf. Figure B.1.

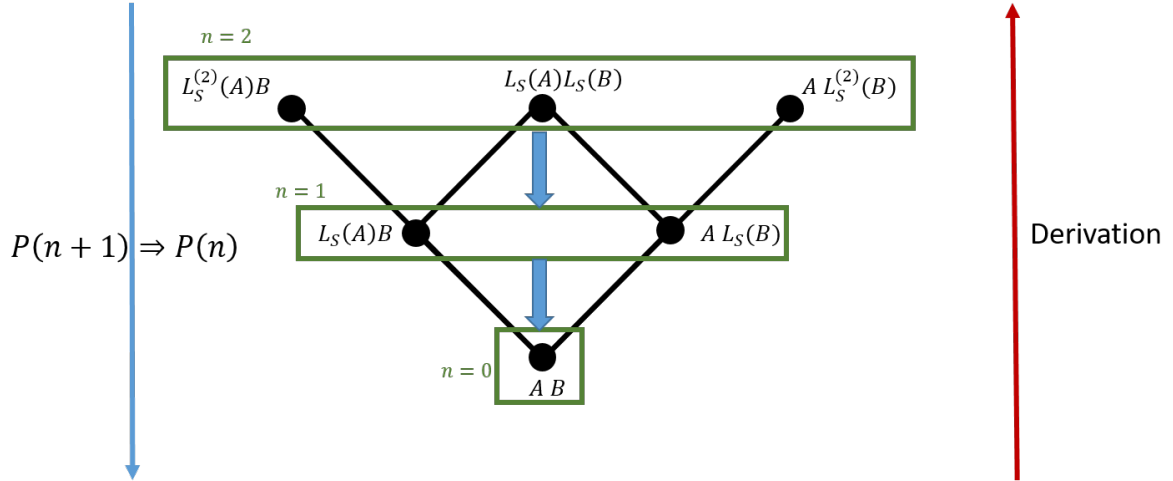


Figure B.1: Inverse Pascal triangle structure that appears under the regularity condition for the pair of operators (A, B) . Deriving corresponds to creating two upwards branches to the left (derive A) and to the right (derive B). The implication $\mathcal{P}(n + 1) \implies \mathcal{P}(n)$ goes downwards.

Appendix C

Derivation of Quantum Langevin Equation

In this appendix, we present two derivations of the quantum Langevin equation. The first is more general and allows to add many photon loss. The second is based on a more physical model which incorporates two-photon loss.

C.1 General Derivation

This derivation is inspired by the proof of the usual quantum Langevin equation given by Prof. Zaki Leghtas in the class Cavity and Circuit QED in the second semester of the ICFP - Quantum Physics Master 2. The following derivation generalizes the result for any number ν of photon loss and includes potential jump operators L_n that can affect the cavity from the inside (for eg. dephasing).

Presentation of the Problem

We consider a cavity of frequency Ω , whose Unitary evolution is given by H and which is coupled to free propagating modes b_q of frequencies ω_q . The Hamiltonian of the bath is $H_{\text{bath}} = \sum_q \omega_q b_q^\dagger b_q$. Since we consider many photon losses, the modes that matter are the ones such that $\omega_q \approx \nu\Omega$, $\nu \geq 1$. Therefore, we are justified in taking the continuous limit and introducing fictitious modes of negative frequencies. The Hamiltonian can be written in the following manner $H_{\text{bath}} = \int_{-\infty}^{\infty} d\omega \hbar\omega b_\omega^\dagger b_\omega$. The modes b_ω satisfy the commutation relations: $[b_\omega, b_{\omega'}^\dagger] = \delta(\omega - \omega')$. b_ω are propagating modes and have the dimension $T^{\frac{1}{2}}$.

Applying the rotating wave (i.e. only conserving the terms that conserve energy) and the Markov approximations (i.e. the coupling constant has no characteristic frequency), we can write the interaction Hamiltonian

$$H_{\text{int}} = \sum_{\nu=1}^{\infty} \frac{\hbar}{\sqrt{2\pi}} \int_{-\infty}^{\infty} d\omega \sqrt{\kappa_\nu} \left(a^\nu b_\omega^\dagger + a^\dagger{}^\nu b_\omega \right), \quad (\text{C.1})$$

such that the total Hamiltonian is finally given by: $H_{\text{tot}} = H + H_{\text{bath}} + H_{\text{int}}$.

Heisenberg-Langevin Equations

We write the Heisenberg-Langevin equations for $a(t)$ and $b_\omega(t)$:

$$\begin{aligned} \frac{da}{dt} &= \frac{1}{i\hbar} [a, H_{\text{tot}}] + \frac{1}{2} \sum_n \left(L_n^\dagger [a, L_n] - [a, L_n^\dagger] L_n \right) \\ &= \frac{1}{i\hbar} [a, H] + \frac{1}{2} \sum_n \left(L_n^\dagger [a, L_n] - [a, L_n^\dagger] L_n \right) + \sum_{\nu=1}^{\infty} \frac{-i}{\sqrt{2\pi}} \int_{-\infty}^{\infty} d\omega \sqrt{\kappa_\nu} \nu a^{\dagger(\nu-1)} b_\omega \\ \frac{db_\omega}{dt} &= -i\omega b_\omega + \sum_{\nu=1}^{\infty} \frac{-i}{\sqrt{2\pi}} \sqrt{\kappa_\nu} a^\nu \end{aligned} \quad (\text{C.2})$$

We take an initial time t_0 defined by the input $b_\omega(t_0)$ and solve the second differential equation:

$$b_\omega(t) = b_\omega(t_0)e^{-i\omega(t-t_0)} - i \sum_{\nu=1}^{\infty} \sqrt{\frac{\kappa_\nu}{2\pi}} \int_{t_0}^t dt' e^{-i\omega(t-t')} a^\nu(t') \quad (C.3)$$

We inject it in the differential equation of $a(t)$:

$$\begin{aligned} \frac{da}{dt} &= \frac{1}{i\hbar}[a, H] + \frac{1}{2} \sum_n \left(L_n^\dagger[a, L_n] - [a, L_n^\dagger] L_n \right) + \sum_{\nu=1}^{\infty} \frac{-i}{\sqrt{2\pi}} \int_{-\infty}^{\infty} d\omega \sqrt{\kappa_\nu} \nu a^{\dagger(\nu-1)} b_\omega(t_0) e^{-i\omega(t-t_0)} \\ &\quad - \sum_{\nu=1}^{\infty} \frac{\kappa_\nu}{2\pi} \nu \int_{-\infty}^{\infty} d\omega \int_{t_0}^t dt' e^{-i\omega(t-t')} a^{\dagger(\nu-1)}(t) a^\nu(t') \\ &= \frac{1}{i\hbar}[a, H] + \frac{1}{2} \sum_n \left(L_n^\dagger[a, L_n] - [a, L_n^\dagger] L_n \right) + \sum_{\nu=1}^{\infty} \frac{-i}{\sqrt{2\pi}} \int_{-\infty}^{\infty} d\omega \sqrt{\kappa_\nu} \nu a^{\dagger(\nu-1)} b_\omega(t_0) e^{-i\omega(t-t_0)} \\ &\quad - \sum_{\nu=1}^{\infty} \kappa_\nu \nu \int_{t_0}^t dt' a^{\dagger(\nu-1)}(t) a^\nu(t') \int_{-\infty}^{\infty} \frac{d\omega}{2\pi} e^{-i\omega(t-t')} \end{aligned} \quad (C.4)$$

To simplify the last term, we use the identities: $\int_{-\infty}^{\infty} \frac{d\omega}{2\pi} e^{-i\omega(t-t')} = \delta(t-t')$ and $\int_{t_0}^t dt' \delta(t-t') = \int_0^{t-t_0} d\tau \delta(\tau) = \int_0^\infty d\tau \delta(\tau) = \int_0^\infty \frac{1}{2} d\tau$. We get:

$$\begin{aligned} \frac{da}{dt} &= \frac{1}{i\hbar}[a, H] + \frac{1}{2} \sum_n \left(L_n^\dagger[a, L_n] - [a, L_n^\dagger] L_n \right) - \sum_{\nu=1}^{\infty} \nu \sqrt{\kappa_\nu} a^{\dagger(\nu-1)} \frac{i}{\sqrt{2\pi}} \int_{-\infty}^{\infty} d\omega b_\omega(t_0) e^{-i\omega(t-t_0)} \\ &\quad - \sum_{\nu=1}^{\infty} \frac{\nu \kappa_\nu}{2} a^{\dagger(\nu-1)} a^\nu \end{aligned} \quad (C.5)$$

We introduce $a_{\text{in}}(t) \equiv \frac{i}{\sqrt{2\pi}} \int_{-\infty}^{\infty} d\omega b_\omega(t_0) e^{-i\omega(t-t_0)}$ where $a_{\text{in}}(t)$ has the dimension $T^{-\frac{1}{2}}$. We finally get:

$$\frac{da}{dt} = \frac{1}{i\hbar}[a, H] + \frac{1}{2} \sum_n \left(L_n^\dagger[a, L_n] - [a, L_n^\dagger] L_n \right) - \sum_{\nu=1}^{\infty} \nu a^{\dagger(\nu-1)} \left(\sqrt{\kappa_\nu} a_{\text{in}}(t) + \frac{\kappa_\nu}{2} a^\nu \right) \quad (C.6)$$

C.2 Two-Cavity Model

We present a more realistic model based on the devices of Alice & Bob. We will try to find the necessary hypotheses to recover the equation [Equation 2.1](#) we found previously.

C.2.1 Model

Let us consider the model of two cavities corresponding to the annihilators a and b respectively. We consider that the first cavity is the cavity of interest (called the *memory*) whose Unitary evolution is given by the Hamiltonian H . The memory is supposed to be lossless. The second cavity is used to induce two photon loss (called the *buffer*). The second cavity corresponds to a free evolving mode $H_b = \hbar\omega b^\dagger b$ with one photon loss given by the rate κ . Further, we suppose that the second cavity is driven by the input field $b_{\text{in}}(t)$. To obtain two-photon loss, we consider the interaction Hamiltonian $H_{\text{int}} = \hbar g (a^{\dagger 2} b + a^2 b^\dagger)$.

C.2.2 Heisenberg-Langevin Equations

We write the standard quantum Langevin equations:

$$\frac{da}{dt} = \frac{1}{i\hbar}[a, H] - 2iga^\dagger b \quad (C.7)$$

$$\frac{db}{dt} = -i\omega b - iga^2 - \frac{\kappa}{2}b - \sqrt{\kappa}b_{\text{in}} \quad (C.8)$$

The second equation is an unhomogeneous linear equation and can be solved directly:

$$b(t) = e^{-(i\omega + \frac{\kappa}{2})(t-t_0)} b(t_0) - ig \int_{t_0}^t dt' e^{-(i\omega + \frac{\kappa}{2})(t-t')} a^2(t') - \sqrt{\kappa} \int_{t_0}^t dt' e^{-(i\omega + \frac{\kappa}{2})(t-t')} b_{\text{in}}(t') \quad (\text{C.9})$$

We take the **long time limit**: $\kappa(t - t_0) \gg 1$, allowing us to drop the first term:

$$b(t) \approx -ig \int_{t_0}^t dt' e^{-(i\omega + \frac{\kappa}{2})(t-t')} a^2(t') - \sqrt{\kappa} \int_{t_0}^t dt' e^{-(i\omega + \frac{\kappa}{2})(t-t')} b_{\text{in}}(t') \quad (\text{C.10})$$

Further, we consider the **slow evolution approximation** which stipulates that $a(t')$ evolves on time scales much larger than $\frac{1}{\kappa}$. This allows us to write:

$$\int_{t_0}^t dt' e^{-(i\omega + \frac{\kappa}{2})(t-t')} a^2(t') \approx a^2(t) \int_{t_0}^t dt' e^{-(i\omega + \frac{\kappa}{2})(t-t')} \approx \frac{2}{\kappa} a^2(t) \quad (\text{C.11})$$

Additionally, we introduce:

$$a_{\text{in}}(t) \equiv -i \frac{\kappa}{2} \int_{t_0}^t dt' e^{-(i\omega + \frac{\kappa}{2})(t-t')} b_{\text{in}}(t') \quad (\text{C.12})$$

We finally get the equation:

$$\frac{da}{dt} = \frac{1}{i\hbar} [a, H] - \frac{4g^2}{\kappa} a^\dagger a^2 - 2 \frac{2g}{\sqrt{\kappa}} a^\dagger a_{\text{in}}(t) \quad (\text{C.13})$$

We thus recover the previous equation. Further, we see that the decay rate is given by the ratio $\eta \equiv \frac{4g^2}{\kappa}$, which looks like the Purcell effect constant [52].

Appendix D

Expression of Some Quantities as a Function of Moments

The goal of this appendix is to show how to express different quantities that are used to characterize the state. These quantities will not be introduced here for the sake of brevity. A good introduction to quasi-probabilities can be found in [8, 31, 35, 53–55]. For the sake of simplicity, we limit ourselves to one-mode states. All the computations of this part are done in the **Schrödinger picture**. The final result does not depend on the representation.

D.1 Quasi-Probabilities

The goal of this part is to express the P -distribution, Wigner function and Q Husimi function as a function of the moments. We limit ourselves to one mode where the quasi-probabilities are usually used. We will prove the following result:

Theorem D.1.1 (Expression of the Quasi-Probabilities in Function of Moments). *The P -distribution can be written as:*

$$P(\beta, \beta^*) = \sum_{j=0}^{\infty} \sum_{k=0}^{\infty} \frac{\langle a^{\dagger j} a^k \rangle}{j!k!} (-1)^{j+k} \frac{\partial^{j+k}}{\partial \beta^{*j} \partial \beta^k} \delta(\beta, \beta^*) \quad (\text{D.1})$$

The Wigner function can be expressed as:

$$W(\alpha, \alpha^*) = \frac{2e^{-2|\alpha|^2}}{\pi} \sum_{j=0}^{\infty} \sum_{k=0}^{\infty} \frac{\langle a^{\dagger j} a^k \rangle}{j!k!} 2^{k+j} \sum_{r=0}^{\min(j,k)} \binom{j}{r} \frac{k!}{(k-r)!} (-1)^r \frac{\alpha^{*(k-r)} \alpha^{j-r}}{2^r} \quad (\text{D.2})$$

Finally, the Husimi function is given by:

$$Q(\alpha, \alpha^*) = \frac{e^{-|\alpha|^2}}{\pi} \sum_{j=0}^{\infty} \sum_{k=0}^{\infty} \sum_{r=0}^{\min(j,k)} (-1)^r \frac{\langle a^{\dagger j} a^k \rangle}{j!k!} \binom{j}{r} \frac{k!}{(k-r)!} \alpha^{*(k-r)} \alpha^{j-r} \quad (\text{D.3})$$

Proof. To prove this theorem, we recall the expression of the P -distribution [33]:

$$P(\beta, \beta^*) = \int \frac{d^2 z}{\pi^2} M(z, z^*) e^{-i\beta z} e^{-i\beta^* z^*} \quad (\text{D.4})$$

with $M(z, z^*) = \langle e^{iz^* a^\dagger} e^{iza} \rangle = \sum_{j=0}^{\infty} \sum_{k=0}^{\infty} \frac{(iz^*)^j (iz)^k}{j!k!} \langle a^{\dagger j} a^k \rangle$. Thus:

$$P(\beta, \beta^*) = \sum_{j=0}^{\infty} \sum_{k=0}^{\infty} \frac{\langle a^{\dagger j} a^k \rangle}{j!k!} \int \frac{d^2 z}{\pi^2} (iz^*)^j (iz)^k e^{-i\beta z} e^{-i\beta^* z^*} \quad (\text{D.5})$$

We introduce the integral:

$$I_{jk}(\beta, \beta^*) = \int \frac{d^2 z}{\pi^2} (iz^*)^j (iz)^k e^{-i\beta z} e^{-i\beta^* z^*} = (-1)^{j+k} \frac{\partial^{j+k}}{\partial \beta^{*j} \partial \beta^k} \int \frac{d^2 z}{\pi^2} e^{-i\beta z} e^{-i\beta^* z^*} \quad (\text{D.6})$$

where: $\int \frac{d^2z}{\pi^2} e^{-i\beta z} e^{-i\beta^* z^*} = \delta(\beta, \beta^*)$. Thus:

$$P(\beta, \beta^*) = \sum_{j=0}^{\infty} \sum_{k=0}^{\infty} \frac{\langle a^{\dagger j} a^k \rangle}{j!k!} (-1)^{j+k} \frac{\partial^{j+k}}{\partial \beta^{*j} \partial \beta^k} \delta(\beta, \beta^*) \quad (\text{D.7})$$

Since we know that a state is fully characterized by its P -distribution, we conclude that a state is fully characterized by its moments. We can relate the Wigner function to the P -distribution using the Weiestrass transform or called Gaussian smoothing [53]:

$$\begin{aligned} W(\alpha, \alpha^*) &= 2 \int \frac{d^2\beta}{\pi} P(\beta, \beta^*) e^{-2(\beta-\alpha)(\beta^*-\alpha^*)} \\ &= 2 \sum_{j=0}^{\infty} \sum_{k=0}^{\infty} \frac{\langle a^{\dagger j} a^k \rangle}{j!k!} (-1)^{j+k} \int \frac{d^2\beta}{\pi} e^{-2(\beta-\alpha)(\beta^*-\alpha^*)} \frac{\partial^{j+k}}{\partial \beta^{*j} \partial \beta^k} \delta(\beta, \beta^*) \\ &= 2 \sum_{j=0}^{\infty} \sum_{k=0}^{\infty} \frac{\langle a^{\dagger j} a^k \rangle}{j!k!} \left[\frac{\partial^{j+k}}{\partial \beta^{*j} \partial \beta^k} e^{-2(\beta-\alpha)(\beta^*-\alpha^*)} \right]_{\beta=0, \beta^*=0} \\ &= \frac{2}{\pi} \sum_{j=0}^{\infty} \sum_{k=0}^{\infty} \frac{\langle a^{\dagger j} a^k \rangle}{j!k!} \left[\frac{\partial^j}{\partial \beta^{*j}} (-2)^k (\beta^* - \alpha^*)^k e^{-2(\beta-\alpha)(\beta^*-\alpha^*)} \right]_{\beta=0, \beta^*=0} \end{aligned} \quad (\text{D.8})$$

Using Bernoulli's identity for the derivative of a product, we find:

$$\begin{aligned} W(\alpha, \alpha^*) &= \frac{2}{\pi} \sum_{j=0}^{\infty} \sum_{k=0}^{\infty} \frac{\langle a^{\dagger j} a^k \rangle}{j!k!} (-2)^k \\ &\times \sum_{r=0}^{\min(j,k)} \binom{j}{r} \left[\frac{\partial^r}{\partial \beta^{*r}} (\beta^* - \alpha^*)^k \right]_{\beta=\beta^*=0} \left[\frac{\partial^{j-r}}{\partial \beta^{*(j-r)}} e^{-2(\beta-\alpha)(\beta^*-\alpha^*)} \right]_{\beta=\beta^*=0} \\ &= \frac{2}{\pi} \sum_{j=0}^{\infty} \sum_{k=0}^{\infty} \frac{\langle a^{\dagger j} a^k \rangle}{j!k!} (-2)^k \\ &\times \sum_{r=0}^{\min(j,k)} \binom{j}{r} \left[\frac{k!}{(k-r)!} (\beta^* - \alpha^*)^{k-r} \right]_{\beta=\beta^*=0} \left[(-2)^{j-r} (\beta - \alpha)^{j-r} e^{-2(\beta-\alpha)(\beta^*-\alpha^*)} \right]_{\beta=\beta^*=0} \\ &= \frac{2}{\pi} \sum_{j=0}^{\infty} \sum_{k=0}^{\infty} \frac{\langle a^{\dagger j} a^k \rangle}{j!k!} (-2)^k \sum_{r=0}^{\min(j,k)} \binom{j}{r} \frac{k!}{(k-r)!} (-\alpha^*)^{k-r} (-2)^{j-r} (-\alpha)^{j-r} e^{-2|\alpha|^2} \\ &= \frac{2e^{-2|\alpha|^2}}{\pi} \sum_{j=0}^{\infty} \sum_{k=0}^{\infty} \frac{\langle a^{\dagger j} a^k \rangle}{j!k!} 2^{k+j} \sum_{r=0}^{\min(j,k)} \binom{j}{r} \frac{k!}{(k-r)!} (-1)^r \frac{\alpha^{*(k-r)} \alpha^{j-r}}{2^r} \end{aligned} \quad (\text{D.9})$$

We finally find:

$$W(\alpha, \alpha^*) = \frac{2e^{-2|\alpha|^2}}{\pi} \sum_{j=0}^{\infty} \sum_{k=0}^{\infty} \frac{\langle a^{\dagger j} a^k \rangle}{j!k!} 2^{k+j} \sum_{r=0}^{\min(j,k)} \binom{j}{r} \frac{k!}{(k-r)!} (-1)^r \frac{\alpha^{*(k-r)} \alpha^{j-r}}{2^r} \quad (\text{D.10})$$

Similarly, the Husimi Q -distribution is related to the P -distribution by the Gaussian smoothing [53]:

$$Q(\alpha, \alpha^*) = \int \frac{d^2\beta}{\pi} P(\beta, \beta^*) e^{-|\alpha - \beta|^2} \quad (\text{D.11})$$

$$\begin{aligned} &= \sum_{j=0}^{\infty} \sum_{k=0}^{\infty} \frac{\langle a^{\dagger j} a^k \rangle}{j!k!} (-1)^{j+k} \int \frac{d^2\beta}{\pi} e^{-(\beta - \alpha)(\beta^* - \alpha^*)} \frac{\partial^{j+k}}{\partial \beta^{*j} \partial \beta^k} \delta(\beta, \beta^*) \\ &= \frac{1}{\pi} \sum_{j=0}^{\infty} \sum_{k=0}^{\infty} \frac{\langle a^{\dagger j} a^k \rangle}{j!k!} (-1)^{j+k} \left[\frac{\partial^{j+k}}{\partial \beta^{*j} \partial \beta^k} e^{(\beta - \alpha)(\beta^* - \alpha^*)} \right]_{\beta=0, \beta^*=0} \\ &= \frac{1}{\pi} \sum_{j=0}^{\infty} \sum_{k=0}^{\infty} \frac{\langle a^{\dagger j} a^k \rangle}{j!k!} \left[\frac{\partial^j}{\partial \beta^{*j}} (-1)^k (\beta^* - \alpha^*)^k e^{-(\beta - \alpha)(\beta^* - \alpha^*)} \right]_{\beta=0, \beta^*=0} \end{aligned} \quad (\text{D.12})$$

Using Bernoulli's identity for the derivative of a product and evaluating at $(0, 0)$, we find:

$$Q(\alpha, \alpha^*) = \frac{e^{-|\alpha|^2}}{\pi} \sum_{j=0}^{\infty} \sum_{k=0}^{\infty} \sum_{r=0}^{\min(j,k)} (-1)^r \frac{\langle a^{\dagger j} a^k \rangle}{j!k!} \binom{j}{r} \frac{k!}{(k-r)!} \alpha^{*(k-r)} \alpha^{j-r} \quad (\text{D.13})$$

□

D.1.1 Sanity Check: Coherent State

In this part, we verify the relations Equation D.1 and Equation D.2 for a one-mode coherent state $|\gamma\rangle$.

P -distribution

For the state $|\gamma\rangle$, we know that the P -distribution is given by $P(\beta, \beta^*) = \delta(\beta - \gamma, \beta^* - \gamma^*)$. Further, let $\phi(\beta, \beta^*)$ be a function that admits a Taylor power series expansion (recall that the P -distribution is a distribution, not a function). We have:

$$\begin{aligned} \int d^2\beta P(\beta, \beta^*) \phi(\beta, \beta^*) &= \phi(\gamma, \gamma^*) \\ &= \sum_{j=0}^{\infty} \sum_{k=0}^{\infty} \frac{\gamma^{*j} \gamma^k}{j!k!} \frac{\partial^{j+k} \phi}{\partial \beta^{*j} \partial \beta^k} (0, 0) \\ &= \sum_{j=0}^{\infty} \sum_{k=0}^{\infty} \frac{\gamma^{*j} \gamma^k}{j!k!} (-1)^{j+k} \int d^2\beta \phi(\beta, \beta^*) \frac{\partial^{j+k} \delta}{\partial \beta^{*j} \partial \beta^k} (\beta, \beta^*) \end{aligned} \quad (\text{D.14})$$

Since this equality is true for any $\phi(\beta, \beta^*)$, we deduce that:

$$P(\beta, \beta^*) = \sum_{j=0}^{\infty} \sum_{k=0}^{\infty} \frac{\gamma^{*j} \gamma^k}{j!k!} (-1)^{j+k} \frac{\partial^{j+k}}{\partial \beta^{*j} \partial \beta^k} \delta(\beta, \beta^*) \quad (\text{D.15})$$

which is Equation D.1 for the coherent state $|\gamma\rangle$.

Wigner Function and Husimi Function

For the state $|\gamma\rangle$, we know that the Wigner function is given by $W(\alpha, \alpha^*) = \frac{2}{\pi} e^{-2(\gamma - \alpha)(\gamma^* - \alpha^*)}$ (this can be seen from Equation D.8). $W(\alpha, \alpha^*)$ can be given by the Taylor expansion:

$$W(\alpha, \alpha^*) = \frac{2}{\pi} \sum_{j=0}^{\infty} \sum_{k=0}^{\infty} \frac{\gamma^{*j} \gamma^k}{j!k!} \left[\frac{\partial^{j+k}}{\partial \gamma^{*j} \partial \gamma^k} e^{-2(\gamma - \alpha)(\gamma^* - \alpha^*)} \right]_{\gamma=\gamma^*=0} \quad (\text{D.16})$$

Expanding the derivatives and evaluating them at $(0, 0)$ corresponds to Equation D.2 for the state $|\gamma\rangle$. We obtain a similar result for Equation D.3 with $Q(\alpha, \alpha^*) = \frac{1}{\pi} e^{-(\gamma - \alpha)(\gamma^* - \alpha^*)}$

D.2 Probability of Number Occupation

In this part, we evaluate $\text{Pr}[n]$, the probability of being occupied by n photons. The goal is to prove the following result:

Theorem D.2.1 (Expression of the Probability of Occupation in Function of Moments). *$\text{Pr}[n]$ is given by:*

$$\text{Pr}[n] = \frac{1}{n!} \sum_{k=0}^{\infty} (-1)^k \frac{\langle a^{\dagger(k+n)} a^{k+n} \rangle}{k!} \quad (\text{D.17})$$

Proof. We introduce the P -distribution:

$$\text{Pr}[n] = \langle n | \rho | n \rangle = \int d^2\alpha P(\alpha, \alpha^*) \langle n | \alpha \rangle \langle \alpha | n \rangle = \int d^2\alpha P(\alpha, \alpha^*) \frac{|\alpha|^{2n}}{n!} e^{-|\alpha|^2} = \int d^2\alpha P(\alpha, \alpha^*) \frac{\alpha^{*n} \alpha^n}{n!} e^{-\alpha^* \alpha} \quad (\text{D.18})$$

Using Equation D.1, we have:

$$\begin{aligned} \text{Pr}[n] &= \sum_{j=0}^{\infty} \sum_{k=0}^{\infty} \frac{\langle a^{\dagger j} a^k \rangle}{j! k!} (-1)^{j+k} \int d^2\alpha \frac{\alpha^{*n} \alpha^n}{n!} e^{-\alpha^* \alpha} \frac{\partial^{j+k}}{\partial \alpha^{*j} \partial \alpha^k} \delta(\alpha, \alpha^*) \\ &= \sum_{j=0}^{\infty} \sum_{k=0}^{\infty} \frac{\langle a^{\dagger j} a^k \rangle}{j! k! n!} \left[\frac{\partial^{j+k}}{\partial \alpha^{*j} \partial \alpha^k} \alpha^{*n} \alpha^n e^{-\alpha^* \alpha} \right]_{\alpha=\alpha^*=0} \end{aligned}$$

Using Bernoulli's identity twice, we get:

$$\begin{aligned} \frac{\partial^{j+k}}{\partial \alpha^{*j} \partial \alpha^k} \alpha^{*n} \alpha^n e^{-\alpha^* \alpha} &= \frac{\partial^j}{\partial \alpha^{*j}} \left\{ \alpha^{*n} \sum_{r=0}^k \binom{k}{r} \left(\frac{\partial^r}{\partial \alpha^r} \alpha^n \right) \left(\frac{\partial^{k-r}}{\partial \alpha^{k-r}} e^{-\alpha^* \alpha} \right) \right\} \\ &= \frac{\partial^j}{\partial \alpha^{*j}} \left\{ \alpha^{*n} \sum_{r=0}^{\min(k,n)} \binom{k}{r} \frac{n!}{(n-r)!} \alpha^{n-r} (-\alpha^*)^{k-r} e^{-\alpha^* \alpha} \right\} \\ &= \sum_{r=0}^{\min(k,n)} \binom{k}{r} \frac{n!}{(n-r)!} (-1)^{k-r} \alpha^{n-r} \frac{\partial^j}{\partial \alpha^{*j}} \left(\alpha^{*(n+k-r)} e^{-\alpha^* \alpha} \right) \\ &= \sum_{r=0}^{\min(k,n)} \binom{k}{r} \frac{n!}{(n-r)!} (-1)^{k-r} \alpha^{n-r} \sum_{s=0}^j \binom{j}{s} \left(\frac{\partial^s}{\partial \alpha^s} \alpha^{n+k-r} \right) \left(\frac{\partial^{j-s}}{\partial \alpha^{j-s}} e^{-\alpha^* \alpha} \right) \\ &= \sum_{r=0}^{\min(k,n)} \sum_{s=0}^{\min(j, n+k-r)} \binom{k}{r} \binom{j}{s} \frac{n!(n+k-r)!}{(n-r)!(n+k-r-s)!} \\ &\quad \times (-1)^{k+j-r-s} \alpha^{n+j-r-s} \alpha^{*(n+k-r-s)} e^{-\alpha^* \alpha} \quad (\text{D.19}) \end{aligned}$$

Evaluating at $\alpha = 0$, finding the nonzero term corresponds to solving the system:

$$n + j = r + s \quad (\text{D.20})$$

$$n + k = r + s \quad (\text{D.21})$$

$$0 \leq s \leq \min(j, n + k - r) \quad (\text{D.22})$$

$$0 \leq r \leq \min(k, n) \quad (\text{D.23})$$

Equation D.20 and Equation D.21 imply that $j = k$. Further, Equation D.23 implies that $r \leq n$, Equation D.22 becomes $0 \leq s \leq k$. Therefore, satisfying Equation D.21 imposes that $s = k$ and $r = n$, which implies that $n \leq k$. Thus, we have the simple expression:

$$\text{Pr}[n] = \frac{1}{n!} \sum_{k=0}^{\infty} (-1)^k \frac{\langle a^{\dagger(k+n)} a^{k+n} \rangle}{k!} \quad (\text{D.24})$$

□

Corollary D.2.1.1. *Pr[n] depends only on the averages $\langle a^{\dagger q} a^q \rangle$ for $q \geq n$.*

D.2.1 Sanity Checks

We test the validity of the formula [Equation D.17](#) by taking the case of a coherent state and a Fock state.

Coherent State $|\alpha\rangle$

We know that: $\langle a^{\dagger(k+n)} a^{k+n} \rangle = |\alpha|^{2(k+n)}$, thus:

$$\frac{1}{n!} \sum_{k=0}^{\infty} (-1)^k \frac{\langle a^{\dagger(k+n)} a^{k+n} \rangle}{k!} = \frac{1}{n!} \sum_{k=0}^{\infty} (-1)^k \frac{|\alpha|^{2(k+n)}}{k!} = \frac{|\alpha|^{2n}}{n!} \sum_{k=0}^{\infty} (-1)^k \frac{|\alpha|^{2k}}{k!} = \frac{|\alpha|^{2n}}{n!} e^{-|\alpha|^2} \quad (\text{D.25})$$

which is the correct value

Fock State $|\nu\rangle$

We have $\langle \nu | a^{\dagger(k+n)} a^{k+n} | \nu \rangle = \|a^{k+n} |\nu\rangle\|^2$, thus:

$$\langle \nu | a^{\dagger(k+n)} a^{k+n} | \nu \rangle = \frac{\nu!}{(\nu - k - n)!}, \quad k \leq \nu - n \quad (\text{D.26})$$

$$\langle \nu | a^{\dagger(k+n)} a^{k+n} | \nu \rangle = 0, \quad k > \nu - n \quad (\text{D.27})$$

Thus, if $n > \nu$, $\frac{1}{n!} \sum_{k=0}^{\infty} (-1)^k \frac{\langle a^{\dagger(k+n)} a^{k+n} \rangle}{k!} = 0$. Otherwise:

$$\frac{1}{n!} \sum_{k=0}^{\infty} (-1)^k \frac{\langle a^{\dagger(k+n)} a^{k+n} \rangle}{k!} = \sum_{k=0}^{\nu-n} (-1)^k \frac{\nu!}{(\nu - k - n)!} = \frac{\nu!}{(\nu - n)!} \sum_{k=0}^{\nu-n} (-1)^k \frac{(\nu - n)!}{(\nu - k - n)!} = \frac{\nu!}{(\nu - n)!} (1-1)^{\nu-n} \quad (\text{D.28})$$

Therefore: $\frac{1}{n!} \sum_{k=0}^{\infty} (-1)^k \frac{\langle a^{\dagger(k+n)} a^{k+n} \rangle}{k!} = \delta_{\nu,n}$, which is the exact value.

Appendix E

Analytical Expressions for Some Hamiltonians

In this part, we solve exactly some Hamiltonians and give examples where our methods for analytical resolution fail. The analytical expressions given here were not found in the literature.

E.1 Results and Techniques

In this section, we present the time-ordered exponential and show how we can use it for solving some differential systems.

E.1.1 Time-Ordered Exponential

Definition

The time-ordered exponential is defined as the solution of the initial value problem [56, 57]:

$$\frac{d\mathcal{T} \exp\left\{\int_0^t dt' A(t')\right\}}{dt} = A(t)\mathcal{T} \exp\left\{\int_0^t dt' A(t')\right\} \quad (\text{E.1})$$

$$\mathcal{T} \exp\left\{\int_0^t dt' A(t')\right\}(t=0) = \mathbb{1} \quad (\text{E.2})$$

$\mathcal{T} \exp\left\{\int_0^t dt' A(t')\right\}$ can be expressed as the following series [57]:

$$\mathcal{T} \exp\left\{\int_0^t dt' A(t')\right\} = \mathbb{1} + \sum_{n=1}^{\infty} \int_0^t dt_1 \int_0^{t_1} dt_2 \dots \int_0^{t_{n-1}} dt_n A(t_1) \dots A(t_n) \quad (\text{E.3})$$

It turns out the time ordered exponential is different from the usual exponential when the operators $\{A(t')\}_{t'}$ do not commute. Indeed, time ordering refers to putting the operators in an increasing value of time from the right to the left. This ensures that they are applied in a chronological order.

Technique

Let us consider the evolution of the operator $O(t)$. The following theorem gives the expression of $O(t)$ in a particular case:

Theorem E.1.1 (Resolution with Time-Ordered Exponential). *Supposes that: $\frac{dO}{dt} = \mathbb{F}(t)O$, then:*

$$O(t) = \mathcal{T} \exp\left\{\int_0^t dt' \mathbb{F}(t')\right\} O(0) \quad (\text{E.4})$$

Proof. We have: $\mathcal{T} \exp \left\{ \int_0^t dt' \mathbb{F}(t') \right\} (t=0) O(0) = O(0)$ and

$$\frac{d \mathcal{T} \exp \left\{ \int_0^t dt' \mathbb{F}(t') \right\} O(0)}{dt} = \mathbb{F}(t) \mathcal{T} \exp \left\{ \int_0^t dt' \mathbb{F}(t') \right\} O(0).$$

Since $O(t)$ and $\mathcal{T} \exp \left\{ \int_0^t dt' \mathbb{F}(t') \right\} O(0)$ satisfy the same differential equation with the same initial condition, we deduce that they are equal. \square

Thus, if we know how to express $\mathbb{F}(t)$, we fully know the evolution of $O(t)$. In [subsection E.2.1](#), [subsection E.2.2](#) and [subsection E.2.3](#), we present examples where this is the case.

E.1.2 Derivation with Respect to Operators

Many techniques for solving differential equations where the unknown function takes complex values use the identification of an expression as the derivative relative to the complex function. A usual example is the method of separation of variables. Generalizing this approach requires defining derivatives with respect to operators. This is challenging since two operators do not commute in general. This is particularly important when we want to integrate with respect to an operator, which imposes putting the differential on the right or on the left. Nevertheless, this can be done properly [58]. This required introducing commutators. We invite the interested reader to look into the paper [58] where derivatives of powers, exponentials and logarithms, amongst others, are derived. Here, we limit ourselves to an example to illustrate the need for commutators.

Let us consider the differential equation on the operator X : $\frac{dX}{dt} = \frac{1}{X}$ (in this example, we do not bother whether the equation is well-defined). We might attempt to use the separation of variables and write: $X dX = dt$. Formally, the expression is correct. The next step is to integrate the two expressions from 0 to t . However, this required from us to know the primitive of $X \mapsto X$. Sadly, it is not $X \mapsto \frac{X^2}{2}$. Indeed:

$$\begin{aligned} \lim_{h \rightarrow 0} \frac{(X + h dX)^2 - X^2}{h} &= \lim_{h \rightarrow 0} \frac{X^2 + h X dX + h dX X + h^2 dX^2 - X^2}{h} = X dX + dX X \\ &= 2X dX + [dX, X] = (2X + [., X]) dX \end{aligned} \quad (\text{E.5})$$

Thus, it is not straightforward to find the primitive of $X \mapsto X$. The method of separation of variables cannot be used directly on operators.

E.2 Examples

In this section, we present some examples where an analytical expression is found and others where we did not manage to do so. We present an explanation for the failure.

E.2.1 One-Mode Kerr Hamiltonian

The self-Kerr Hamiltonian is given by $H = \hbar g a^\dagger^2 a^2$.

The annihilator a satisfies the differential equation:

$$\frac{da}{dt} = -2i g a^\dagger a^2 = (-2i g a^\dagger a) a \quad (\text{E.6})$$

We have:

$$\frac{da^\dagger a}{dt} = \frac{da^\dagger}{dt} a(t) + a^\dagger(t) \frac{da}{dt} = 0 \quad (\text{E.7})$$

Thus, $a^\dagger(t) a(t) = a^\dagger(0) a(0)$. The differential equation is in the form of [Theorem E.1.1](#) and thus:

$$a(t) = \mathcal{T} \exp \left\{ -2i g t a^\dagger(0) a(0) \right\} a(0) = e^{-2i g t a^\dagger(0) a(0)} a(0) \quad (\text{E.8})$$

Expression of the moments

We can use the expression $a(t) = e^{-2igta^\dagger(0)a(0)}a(0)$ to find the time evolution of the moments $\langle \alpha | a^{\dagger j}(t) a^k(t) | \alpha \rangle$ for example.

To do this, we write $a(t) | \alpha \rangle$:

$$a(t) | \alpha \rangle = e^{-2igta^\dagger(0)a(0)} a(0) | \alpha \rangle = \alpha e^{-2igta^\dagger(0)a(0)} | \alpha \rangle = \alpha e^{-\frac{|\alpha|^2}{2}} \sum_{n=0}^{\infty} \frac{\alpha^n}{\sqrt{n!}} e^{-2igtn} | n \rangle = \alpha | \alpha e^{-2igt} \rangle \quad (\text{E.9})$$

with: $|\beta(t)\rangle \equiv e^{-\frac{|\beta(t)|^2}{2}} \sum_{n=0}^{\infty} \frac{\beta(t)^n}{\sqrt{n!}} | n \rangle$. Thus, by induction, we have: $a^k(t) | \alpha \rangle = \left(\prod_{l=0}^{k-1} \alpha e^{-2ilgt} \right) | \alpha e^{-2ikgt} \rangle = \alpha^k e^{-2igtk(k-1)} | \alpha e^{-2ikgt} \rangle$. Therefore, $\langle \alpha | a^{\dagger j}(t) a^k(t) | \alpha \rangle = \alpha^{*j} \alpha^k e^{-2igt[k(k-1)-j(j-1)]} \langle \alpha e^{-2ijgt} | \alpha e^{-2ikgt} \rangle$, with:

$$\langle \alpha e^{-2ijgt} | \alpha e^{-2ikgt} \rangle = e^{-|\alpha|^2} \sum_{n=0}^{\infty} \frac{|\alpha|^{2n} e^{-2i(k-j)ngt}}{n!} = e^{-|\alpha|^2} e^{|\alpha|^2 e^{-2i(k-j)gt}}.$$

Thus:

$$\langle \alpha | a^{\dagger j}(t) a^k(t) | \alpha \rangle = \alpha^{*j} \alpha^k e^{-|\alpha|^2} e^{|\alpha|^2 e^{-2i(k-j)gt}} \exp\{-2ig(k-j)(k+j-1)t\} \quad (\text{E.10})$$

E.2.2 Cross-Kerr Hamiltonian

Let us consider two bosonic modes represented by their annihilators a and b . The cross-Kerr Hamiltonian is given by $H = \hbar g a^\dagger b^\dagger b a$. $a(t)$ and $b(t)$ satisfy the equations of evolution:

$$\frac{da}{dt} = -igb^\dagger b a \quad (\text{E.11})$$

$$\frac{db}{dt} = -iga^\dagger a b \quad (\text{E.12})$$

We have:

$$\frac{da^\dagger a}{dt} = 0 \quad (\text{E.13})$$

$$\frac{db^\dagger b}{dt} = 0 \quad (\text{E.14})$$

Again, the differential system is in the form [Theorem E.1.1](#), thus:

$$a(t) = \exp\{-igtb^\dagger(0)b(0)\} a(0) \quad (\text{E.15})$$

$$b(t) = \exp\{-igta^\dagger(0)a(0)\} b(0) \quad (\text{E.16})$$

E.2.3 Partial Generalization

The examples above can be solved without any greater effort if *diagonal quadratic* terms are added to the Hamiltonian. This observation is more general in fact. The same method used in [subsection E.2.1](#) and [subsection E.2.2](#) can be used for any Hamiltonian in the form: $H = H(a_1^\dagger a_1, \dots, a_N^\dagger a_N)$ (i.e. each term has the same number of creators and annihilators for each mode). Indeed, in this case, the equation of evolution of the annihilators is of the form of [Theorem E.1.1](#) and $\mathbb{F} = \mathbb{F}(a_1^\dagger a_1, \dots, a_N^\dagger a_N)$.

Let us show this more rigorously:

Proof. $H = H(a_1^\dagger a_1, \dots, a_N^\dagger a_N)$, thus we can write for the mode i , by writing H in normal order for the mode i for example:

$$H = \sum_{q=0}^{\infty} h_q^{(i)} \left(\{a_j^\dagger a_j\}_{j \neq i} \right) a_i^{\dagger q} a_i^q \quad (\text{E.17})$$

Therefore, the equation of evolution of a_i is:

$$\frac{da_i}{dt} = \frac{1}{i\hbar} \sum_{q=0}^{\infty} h_q^{(i)} \left(\{a_j^\dagger a_j\}_{j \neq i} \right) q a_i^{\dagger(q-1)} a_i^q = \left[\frac{1}{i\hbar} \sum_{q=0}^{\infty} h_q^{(i)} \left(\{a_j^\dagger a_j\}_{j \neq i} \right) q a_i^{\dagger(q-1)} a_i^{q-1} \right] a_i \quad (\text{E.18})$$

Further, using that $\mathbb{F}^\dagger = \mathbb{F}$, we have $\frac{da_j^\dagger a_j}{dt} = 0$, thus this equation is of the form of [Theorem E.1.1](#), its corresponding $\mathbb{F} = \mathbb{F}(a_1^\dagger a_1, \dots, a_N^\dagger a_N)$, implying that $\mathbb{F}^\dagger = \mathbb{F}$. \square

Appendix F

Summary of the Methods

In this appendix, we present a brief summary of a variety of aspects of the different methods. In [Table F.1](#), we present a summary of the different methods that were explored in this report. In [Table F.2](#), we present the summary of the stability of the methods. In [Table F.3](#), we present many stability plots for the mean field methods.

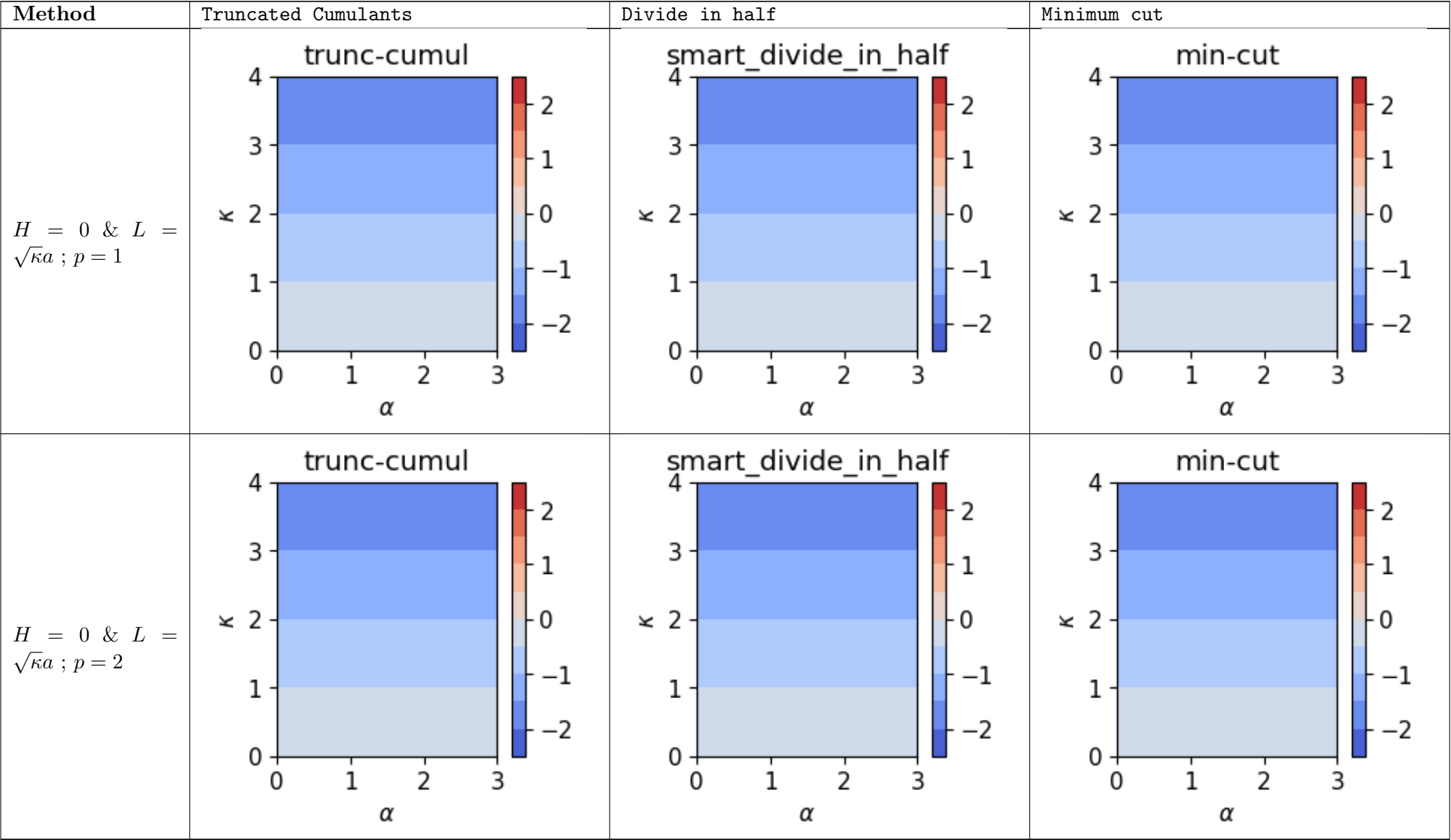
Method	dynamiqs [26]	Usual MF	Truncated Cumulants	TEA	Analytical Expression
Followed Quantity	Density matrix	Moments	Cumulants	Operator $a_i(t)$ in symbolic representation	Exact analytical expression
Cut-off	Number of photons (cut-off in the Fock basis)	Degree of the moment, impose some closure relation linking moments of higher degree to moments of lower degrees	Degree of the cumulant, set cumulants to zero beyond some p	Compute the infinite series of operators up to some p	-
Generality / Validity	Very general if small number of modes / photons	Limited by how well MF describes the state	Initial sum over Gaussian states	In theory for closed systems, works for open systems in some cases	Requires being able to find the solution
Advantages	Can be optimised using linear algebra tools	Fast, accurate for short times. Can be improved with no relative cost using Padé approximate.	Very accurate at short times. More stable than usual MF methods	Can solve for any initial condition. Can compute symbolically for a set of parameters (can be useful for machine learning).	Computing exact analytical expressions numerically is much better than estimating the value numerically (in terms of accuracy, stability, time...)
Problems / Open Questions	Many modes with a significant number of photons (for eg. 4 modes with a cut-off of ~ 20 photons per mode)	If non-Gaussian interaction, instability. How to describe non-Gaussian states in general?	Slow, needs to precompute equations if machine learning applications. If non-Gaussian interaction, instability. How to describe non-Gaussian states in general?	Small improvement at large time expense. Gives correlations instead of moments. How to deal with open systems properly?	Integrals and differential of operators are tricky. $(AB)_H \neq A_H B_H$ for open systems. Green's function for non-linear systems?

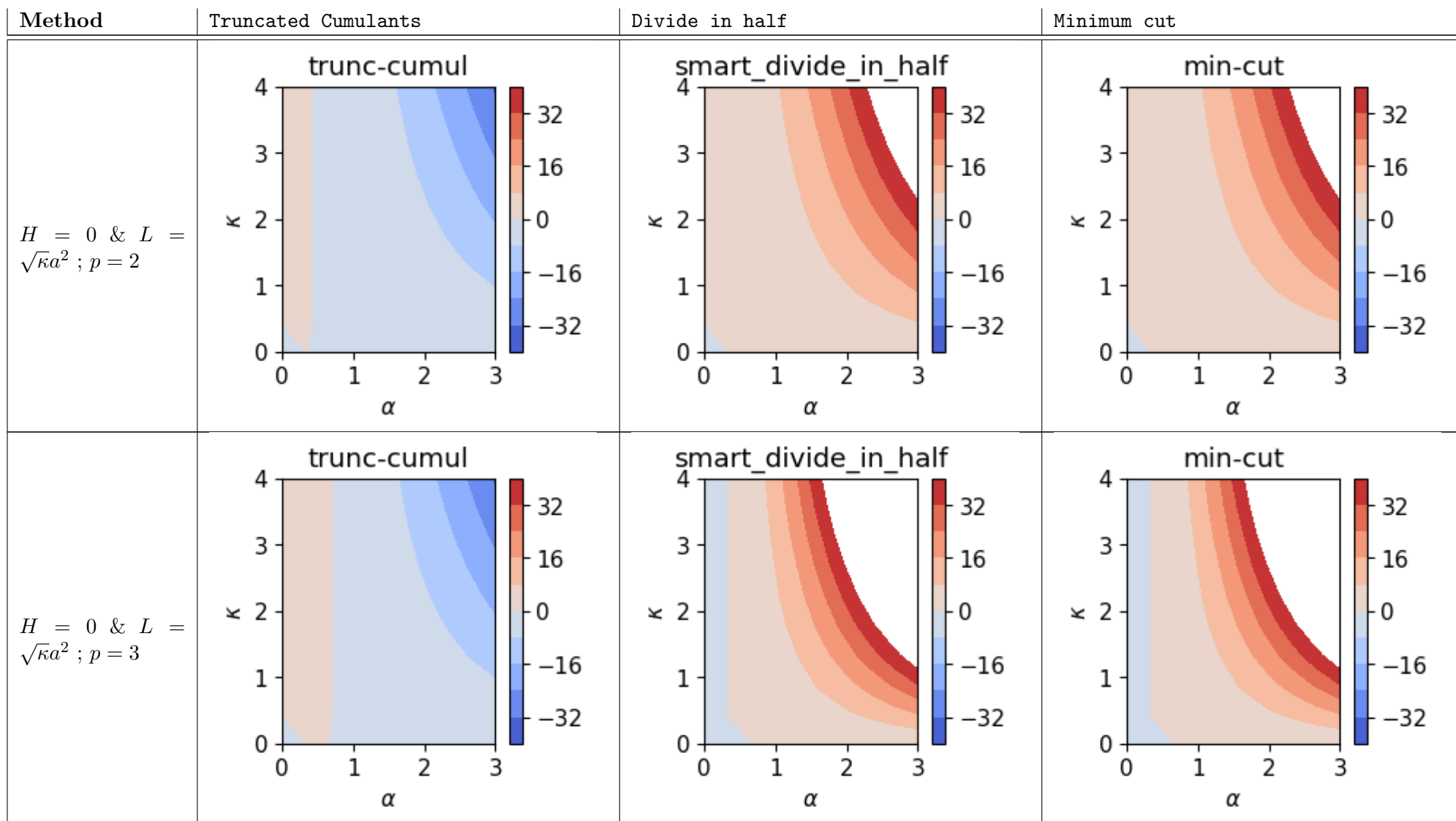
Table F.1: Summary of the methods

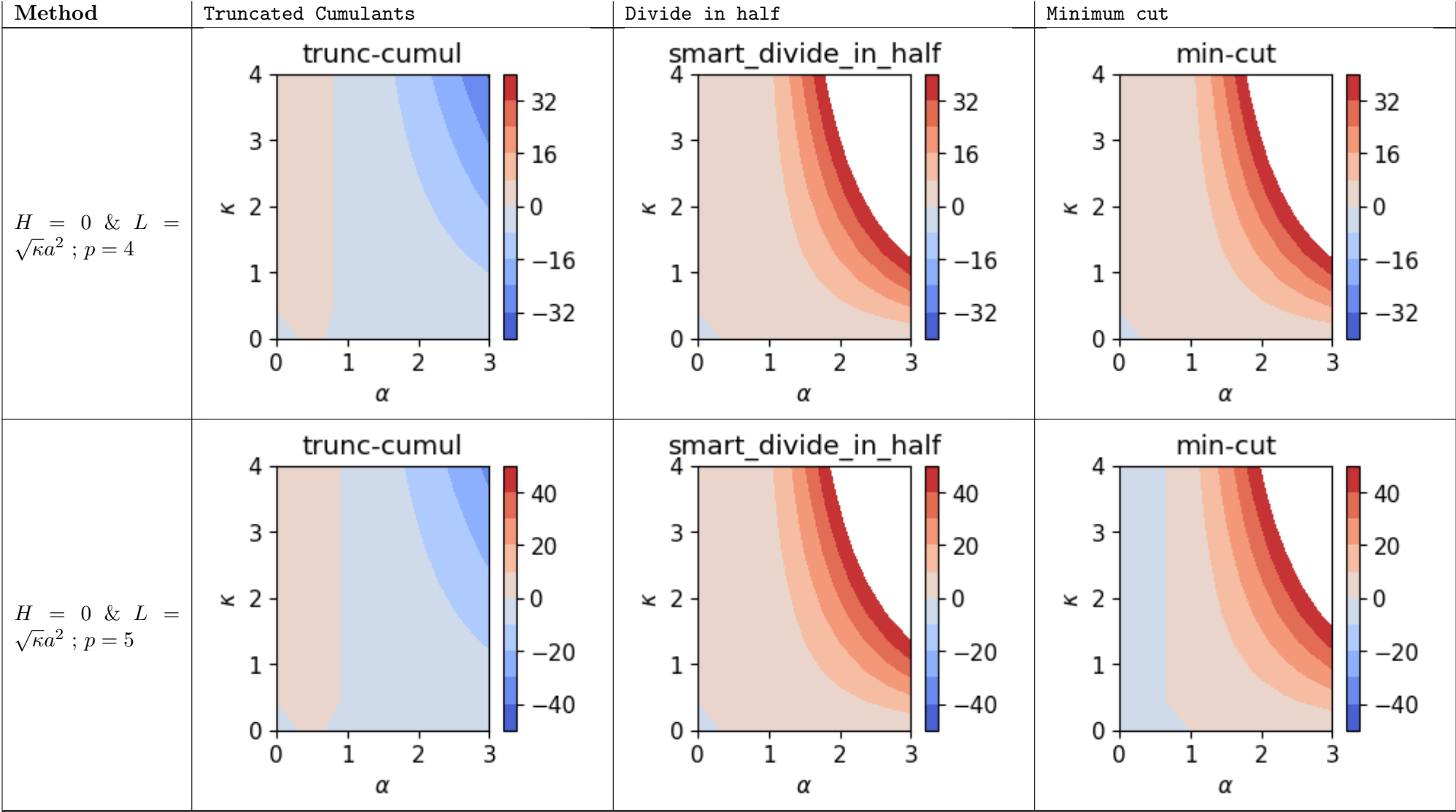
Method	dynamiqs [26]	Usual MF	Truncated Cumulants	TEA	Analytical Expression
General description	Very stable if cut-off large enough	Becomes unstable once non-linearity kicks in	Becomes unstable once non-linearity kicks in	Can be made stable using Padé approximate (with no relative cost)	-
One Photon-Loss	-	Stabilized	Stabilized	-	-
Two Photon-Loss	-	Destabilized	Stabilized	-	-
Dephasing	-	Neutral	Neutral	-	-
$H = a^{\dagger 2} + a^2$ and $L = \sqrt{\kappa}a^2$	-	Very unstable	Stable if α and κ and large enough	-	-

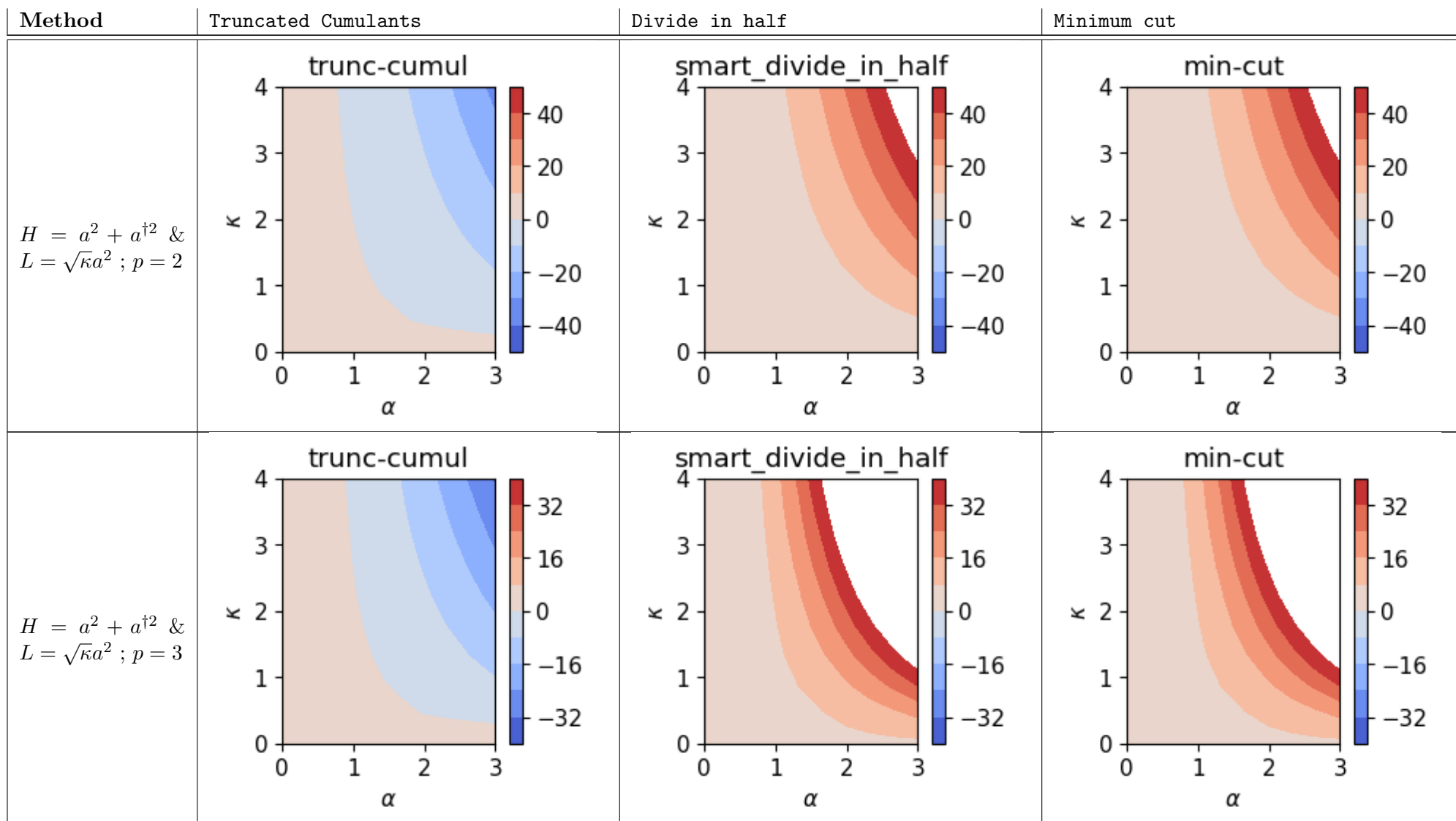
Table F.2: Stability of the Methods - Verbal description

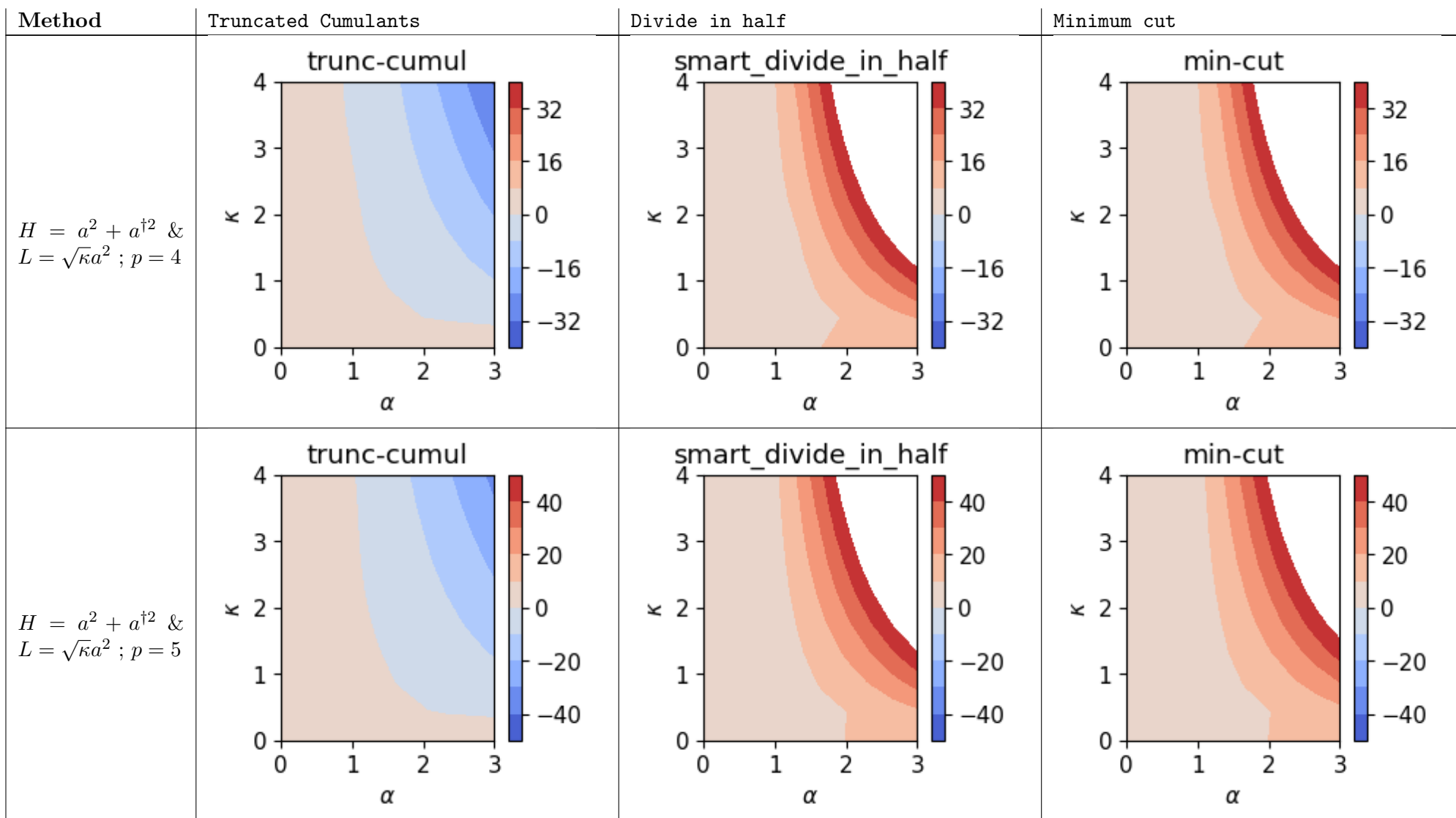
In general, having higher p is better if stable.

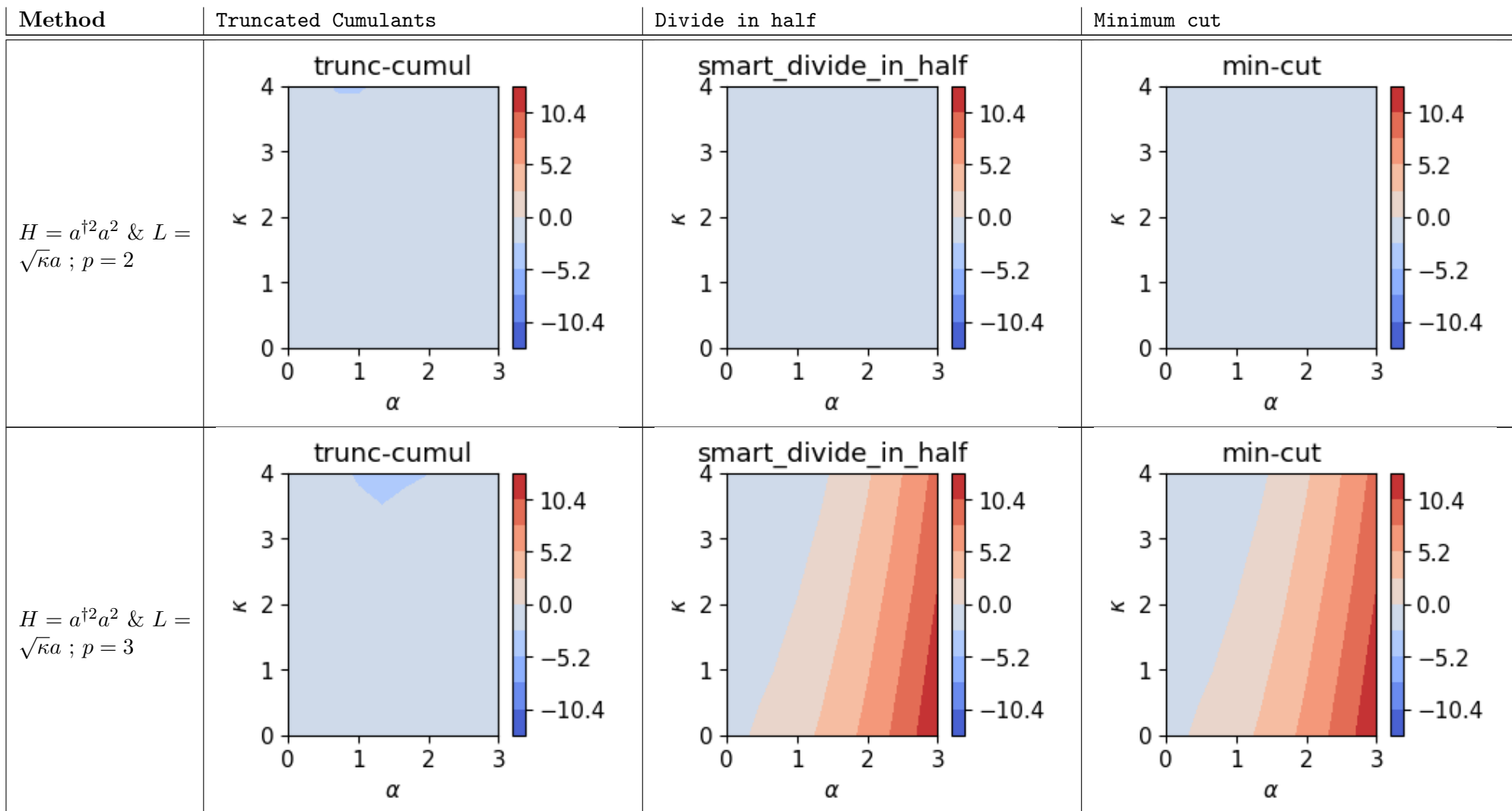


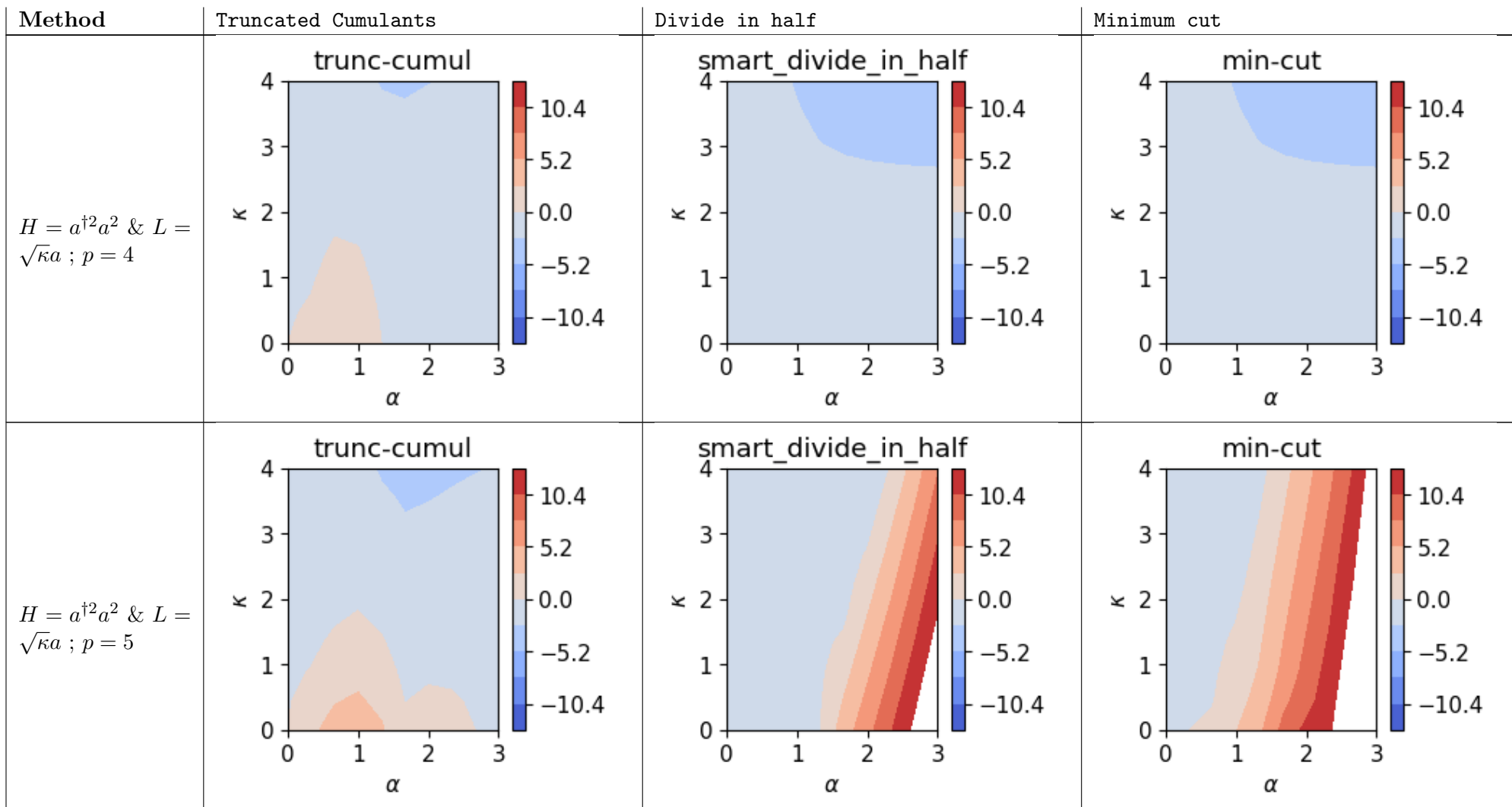












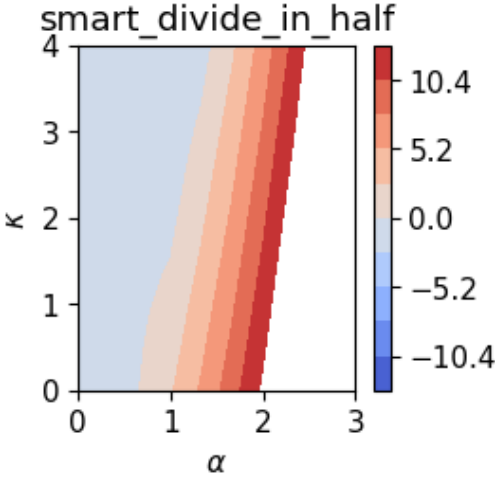
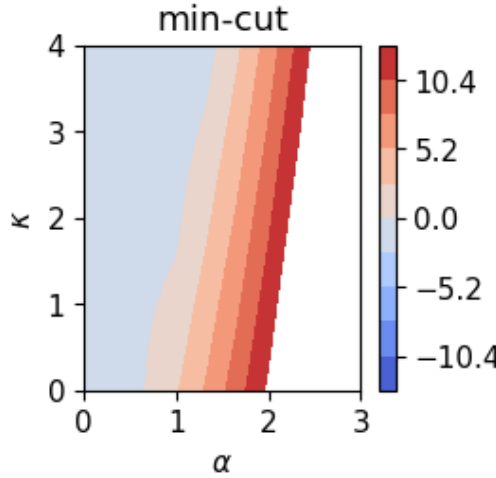
Method	Truncated Cumulants	Divide in half	Minimum cut
$H = a^{\dagger 2} a^2$ & $L = -\sqrt{\kappa} a$; $p = 6$	-		

Table F.3: Stability of the MF Methods - Plots. The red corresponds to positive values while blue corresponds to negative values of the maximum real value of the eigenvalues of the stability matrix for an initial coherent state $|\alpha\rangle$. The same color-bar is used for the same physical system which are separated by a double line.

Appendix G

Other Numerical Results

We will express times in units of $\frac{1}{g}$ where g is a characteristic frequency. The rate constants κ are expressed in units of g . Any other energy scale will be expressed in units of $\hbar g$. The plots were plotted using the Python modules NumPy [59], SciPy [44], SymPy [41], matplotlib [60] and dynamiqs [26]. dynamiqs represents the states by matrices in the Fock basis.

Numerical resolution for MF methods: `scipy.solve_ivp` with options `method="DOP853"` and `dense_output=True`.

G.1 General Considerations

In Figure G.1, we plot $\langle a^\dagger a \rangle(t)$ and $\langle a^\dagger(t) a(t) \rangle$ for the Hamiltonian $H = \hbar a^\dagger a$ and quantum jumps a , $\frac{1}{2}a^\dagger$.

In Figure G.2, we plot the cumulants and moments for the the squeezed state $S[0.5] |1.5\rangle$ with $S[z] \equiv \exp\{\frac{1}{2}(z^* a^2 - z a^{\dagger 2})\}$ [61].

From Figure G.4 and Figure G.5, we see that the the stability does *not* depend on the sign of the coupling constant for self-Kerr.

Figure G.6 shows that the divergence and instabilities start to appear in a time proportional to the inverse of the coupling constant. Adding one-photon loss stabilizes the system (cf. Figure G.7).

G.2 Test of X-gate

In this section, we test how to implement the X-gate for the encoding where the states $|0\rangle$ and $|1\rangle$ correspond to the coherent states $|\alpha\rangle$ and $|\alpha\rangle$ respectively. These states are stabilized by applying the quantum jump $a^2 - \alpha^2$ [62]. As explained in [62], the X-gate corresponds to the rotation of the lobe $|\pm\alpha\rangle$ to the lobe $|\mp\alpha\rangle$ in the phase space. Even though applying $H = -\frac{\pi}{T} a^\dagger a$ during T suffices theoretically, small perturbations can lead to undesired dynamics, for example a bit flip where the lobe "jumps" to the other position. Therefore, this process can be stabilized by applying the time-dependent quantum jump $a^2 - \alpha^2 e^{\frac{2i\pi t}{T}}$, which stabilizes the states $|\pm\alpha e^{\frac{i\pi t}{T}}\rangle$ at any time $t \in (0, T)$. At the end of the process, the quadrature $\langle x \rangle(T)$ is measured. Note that our mean-field methods can be implemented for *time-dependent Hamiltonians and quantum jumps*.

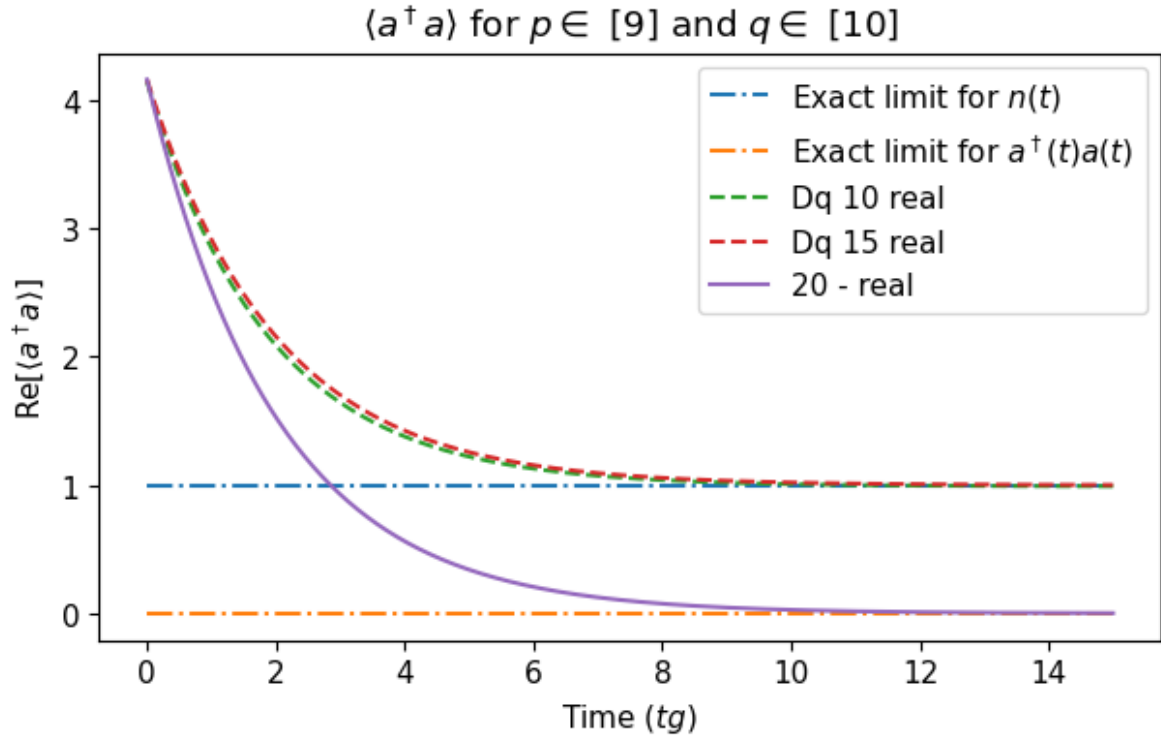


Figure G.1: Plot of $\langle a^\dagger a \rangle(t)$ using `dynamiqs` [26] in dashed lines. Plot of $\langle a^\dagger(t)a(t) \rangle$ using TEA using Padé approximate (cf. section 2.3) in continuous line. The dashed-dotted lines correspond to the limits for $\langle a^\dagger a \rangle(t)$ (1) and for $\langle a^\dagger(t)a(t) \rangle$ (0).

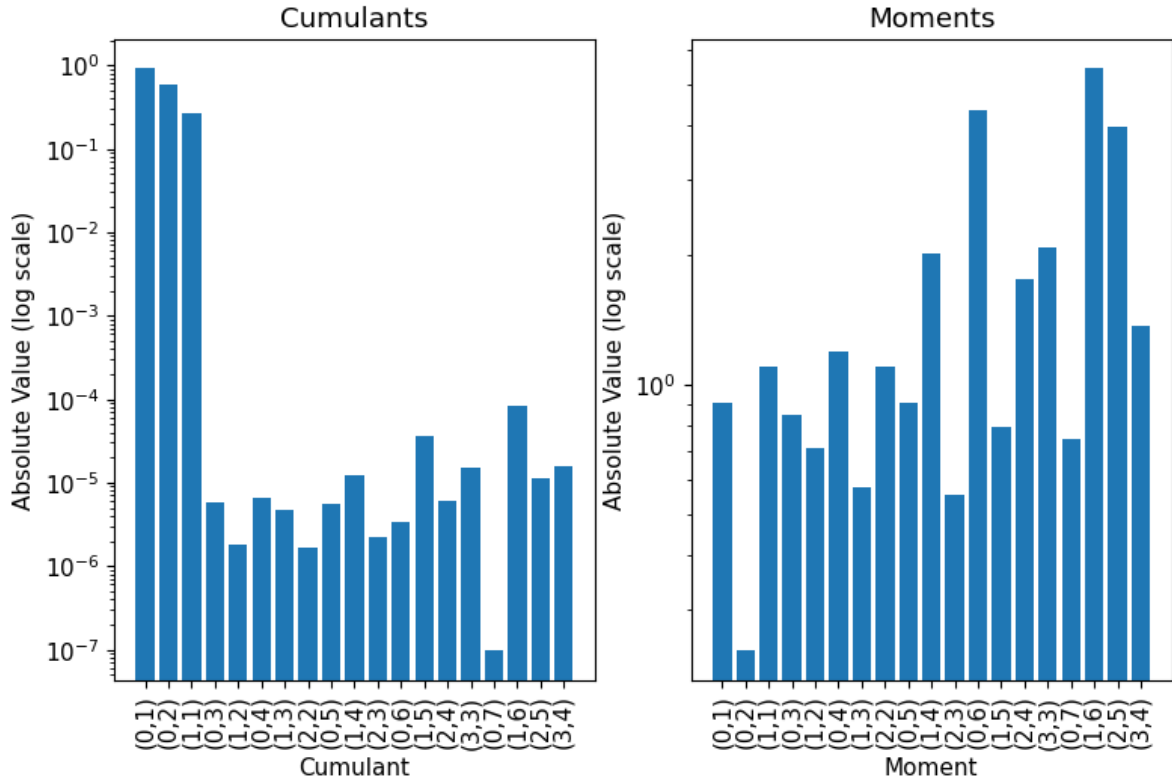


Figure G.2: Cumulants and moments for the projector $S[0.5] |1.5\rangle$ with $S[z] \equiv \exp\{\frac{1}{2}(z^*a^2 - za^{\dagger 2})\}$ [61] using `dynamiqs` [26] for the space dimension 500. The index (j, k) corresponds to $\langle a^{\dagger j} a^k \rangle$. $\langle a^{\dagger k} a^j \rangle$ and $\langle a^{\dagger j} a^k \rangle$ are complex-conjugate, thus we limit ourselves to $j \leq k$. The indices are ranked in an increasing order of $j + k$. For each subset of fixed $j + k$, the lexicographic order is imposed.

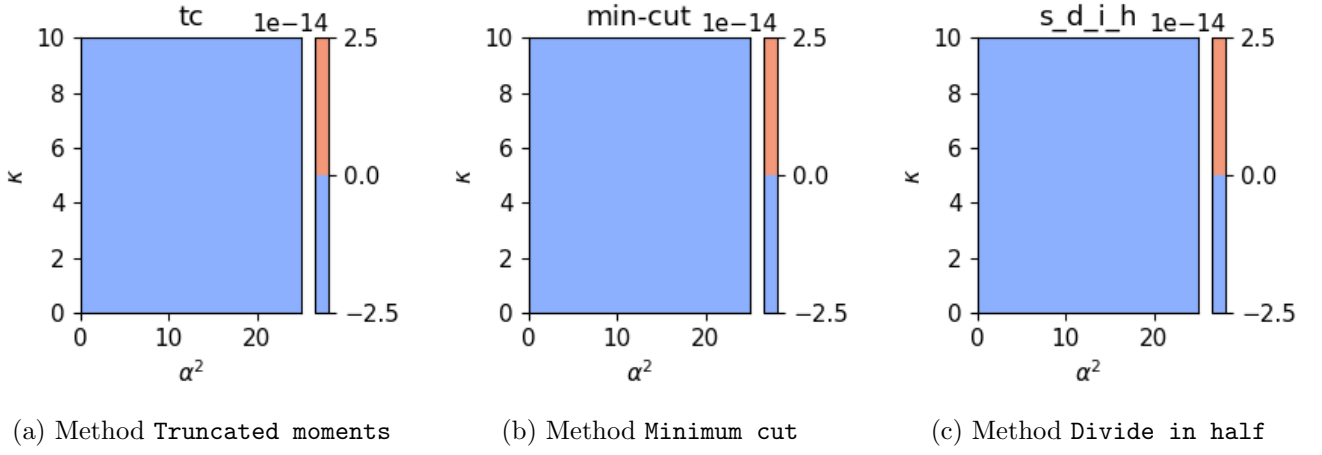


Figure G.3: Maximal value for the real part of the eigenvalues of the stability matrix \mathcal{L} for quantum jump $\sqrt{\kappa}a^\dagger a$, coherent state $|\alpha\rangle$ and $p = 2$.

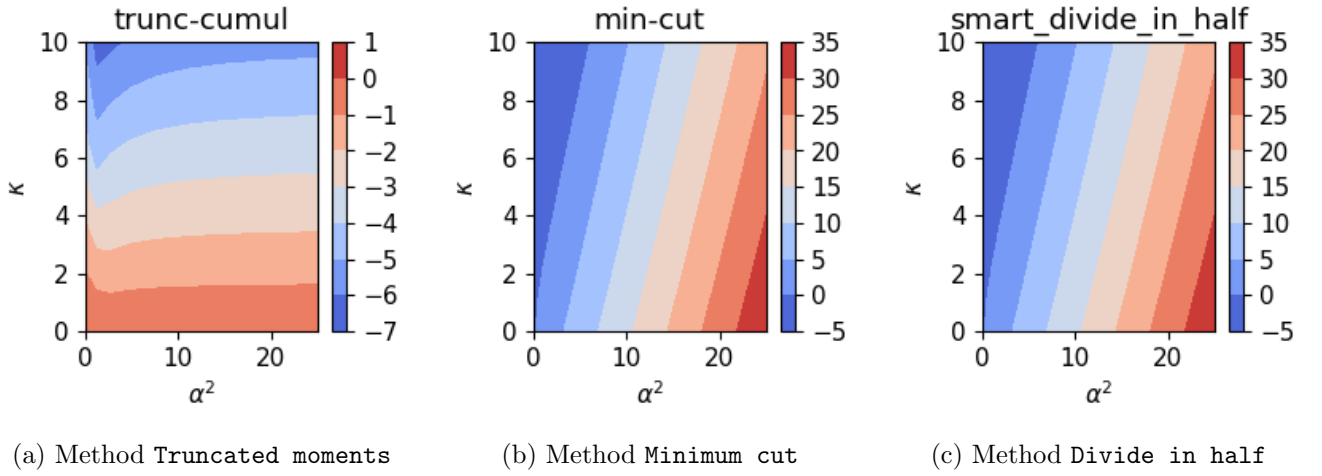


Figure G.4: Maximal value for the real part of the eigenvalues of the stability matrix \mathcal{L} for Hamiltonian $H = a^{\dagger 2} a^2$, quantum jump $\sqrt{\kappa}a$ and coherent state $|\alpha\rangle$ and $p = 3$. `khan` refers to `cumulant method`, `min-cut` refers to the method `Minimum cut` and `smart_divide_in_half` refers to the method `Divide in half`.

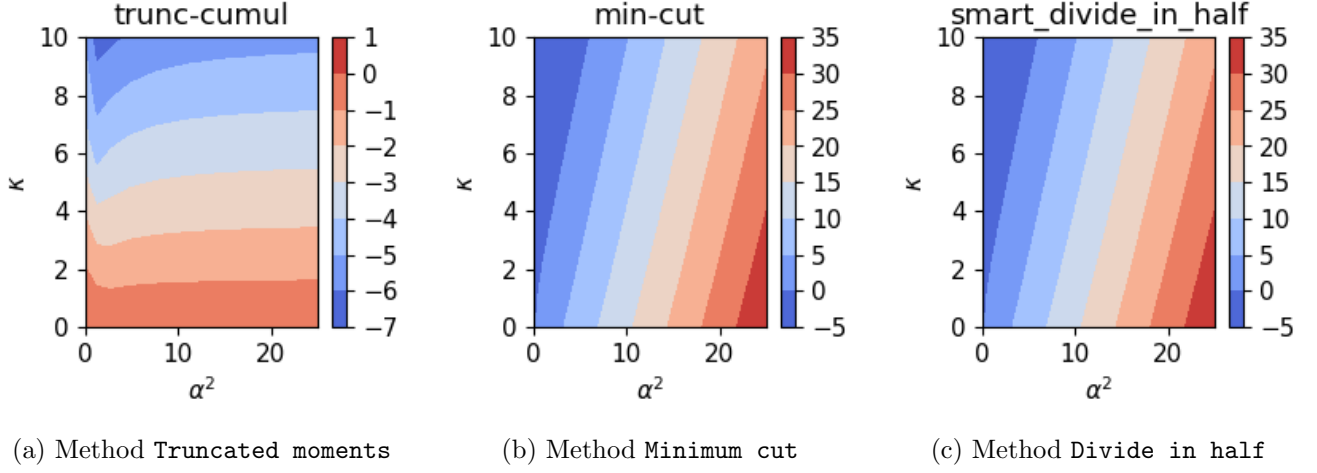


Figure G.5: Maximal value for the real part of the eigenvalues of the stability matrix \mathcal{L} for Hamiltonian $H = -a^{\dagger 2}a^2$, quantum jump $\sqrt{\kappa}a$ and coherent state $|\alpha\rangle$ and $p = 3$. `khan` refers to `cumulant method`, `min-cut` refers to the method `Minimum cut` and `smart_divide_in_half` refers to the method `Divide in half`.

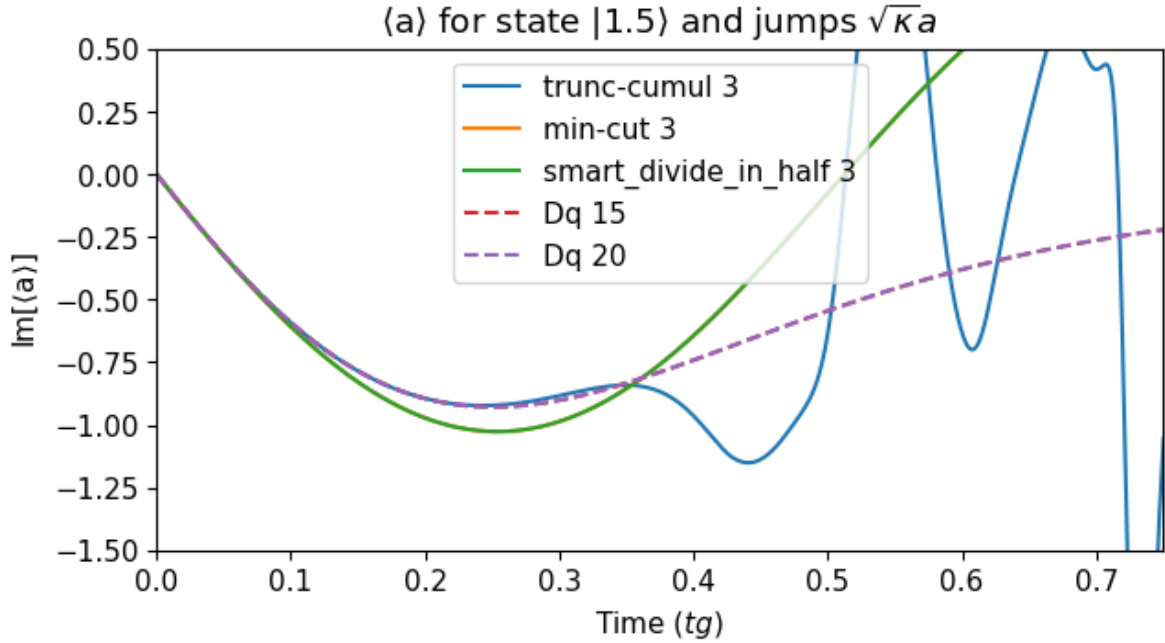


Figure G.6: $\text{Im}\{\langle a \rangle(t)\}$ for the Hamiltonian $H = a^{\dagger 2}a^2$, initial state $|\alpha = 1.5\rangle$, and jump operator $\sqrt{0.5}a$. Continuous line corresponds to MF methods for $p = 3$. Dashed lines correspond to `dynamics` [26].

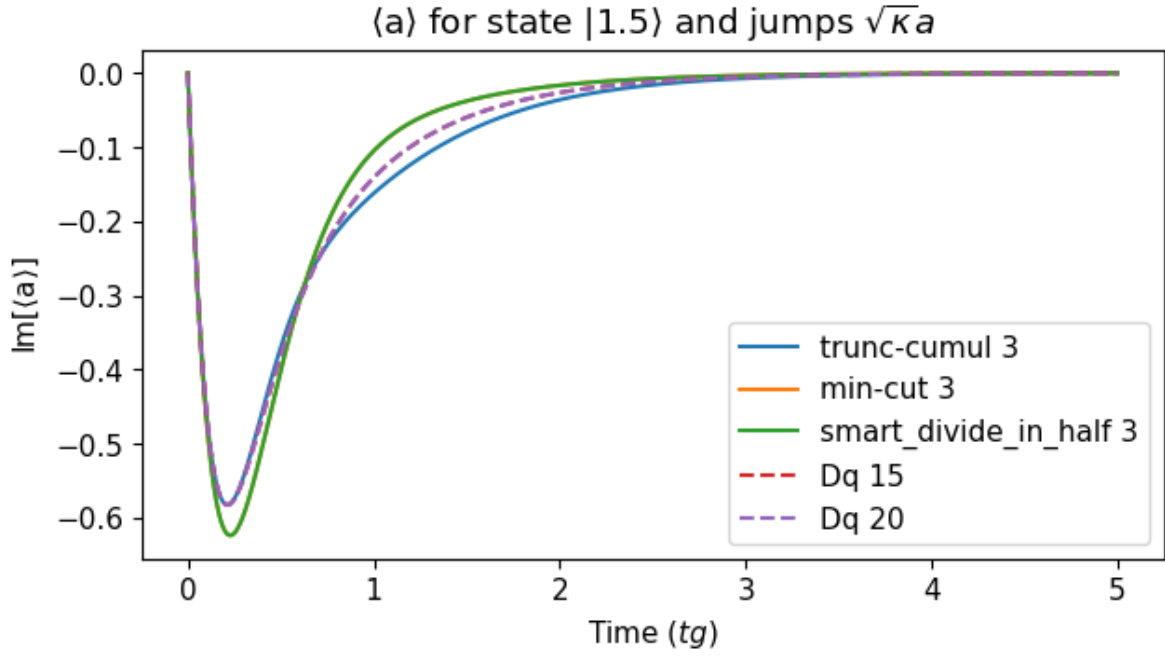


Figure G.7: $\text{Im}\{\langle a \rangle(t)\}$ for the Hamiltonian $H = a^{\dagger 2}a^2$, initial state $|\alpha = 1.5\rangle$, and jump operator $\sqrt{3.25}a$. Continuous line corresponds to MF methods for $p = 3$. Dashed lines correspond to `dynamiqs` [26].

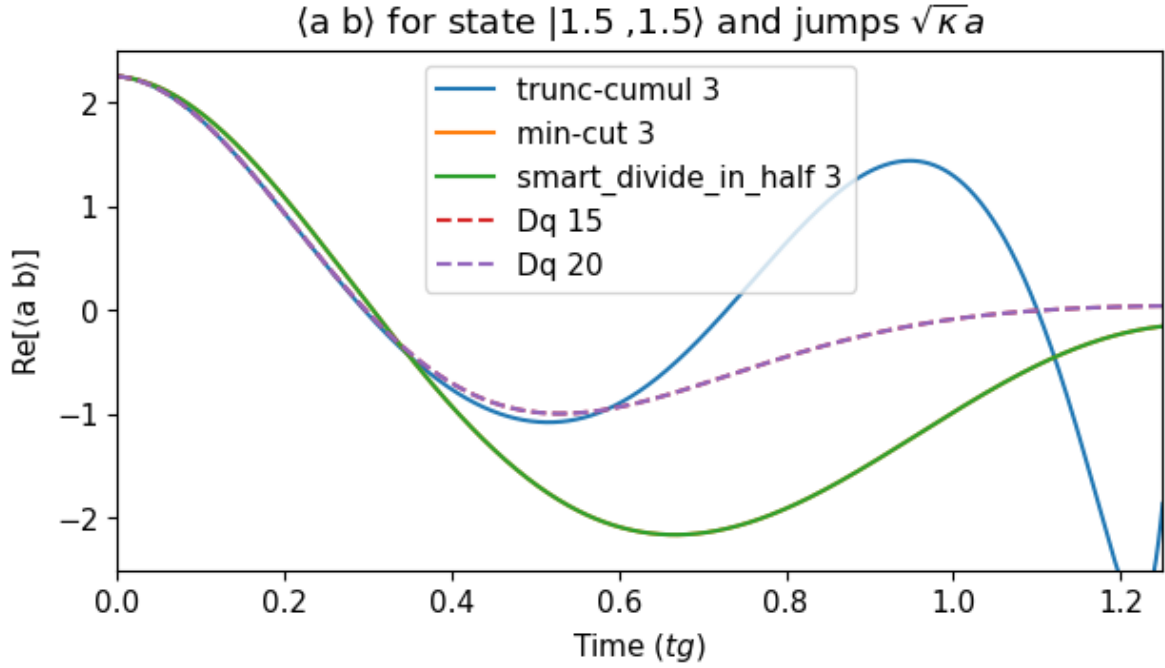


Figure G.8: $\text{Re}\{\langle ab \rangle(t)\}$ for the Hamiltonian $H = a^{\dagger}b^{\dagger}ba$, initial state $|\alpha = 1.5, \beta = 1.5\rangle$, and jump operator $\sqrt{0.5}a$. Continuous line corresponds to MF methods for $p = 3$. Dashed lines correspond to `dynamiqs` [26].

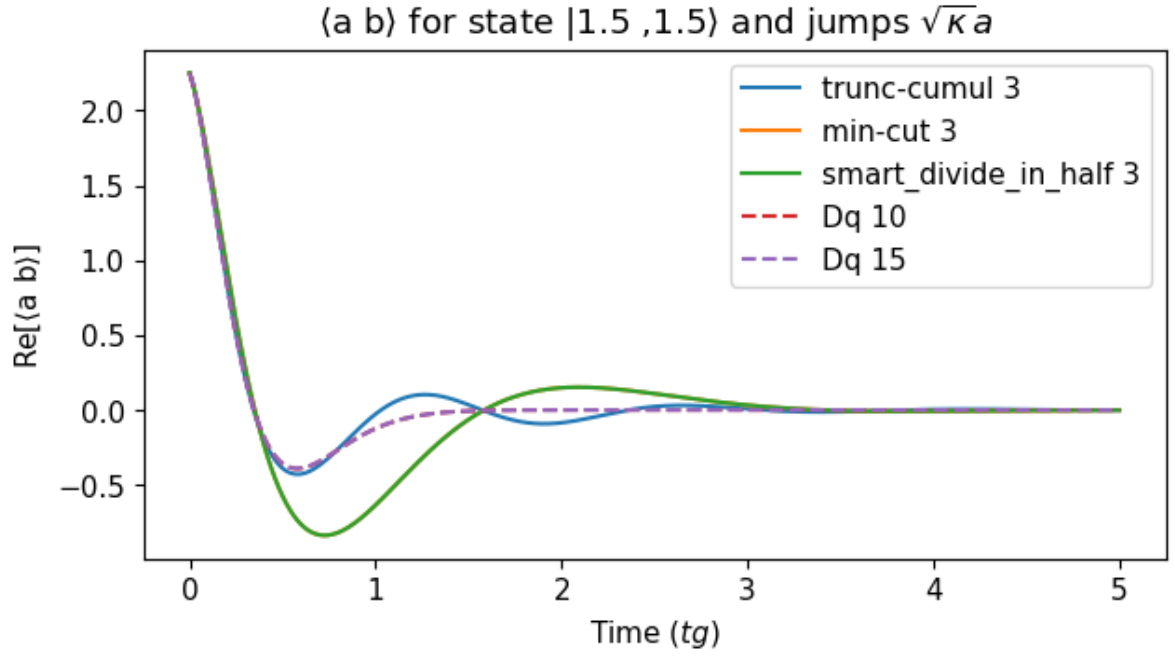


Figure G.9: $\text{Re}\{\langle ab \rangle(t)\}$ for the Hamiltonian $H = a^\dagger b^\dagger b a$, initial state $|\alpha = 1.5, \beta = 1.5\rangle$, and jump operator $\sqrt{3.25}a$. Continuous line corresponds to MF methods for $p = 3$. Dashed lines correspond to dynamiqs [26].

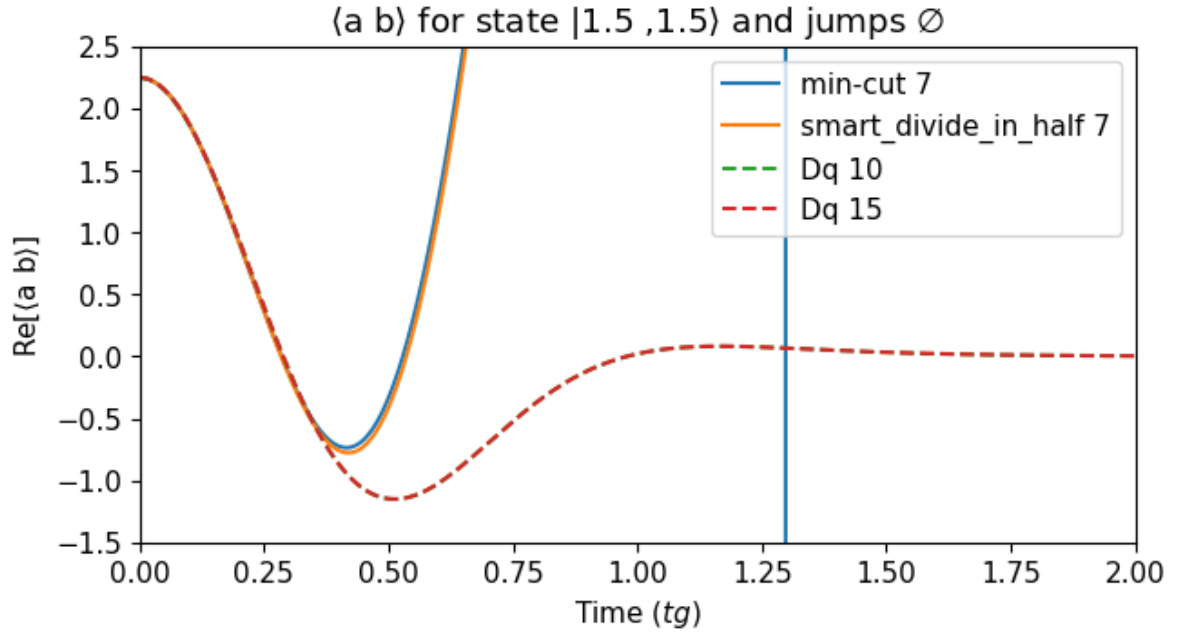


Figure G.10: $\text{Re}\{\langle ab \rangle(t)\}$ for the Hamiltonian $H = a^\dagger b^\dagger b a$, initial state $|\alpha = 1.5, \beta = 1.5\rangle$, without jump operators (i.e. very instable). Continuous line corresponds to MF methods for $p = 7$. Dashed lines correspond to dynamiqs [26].

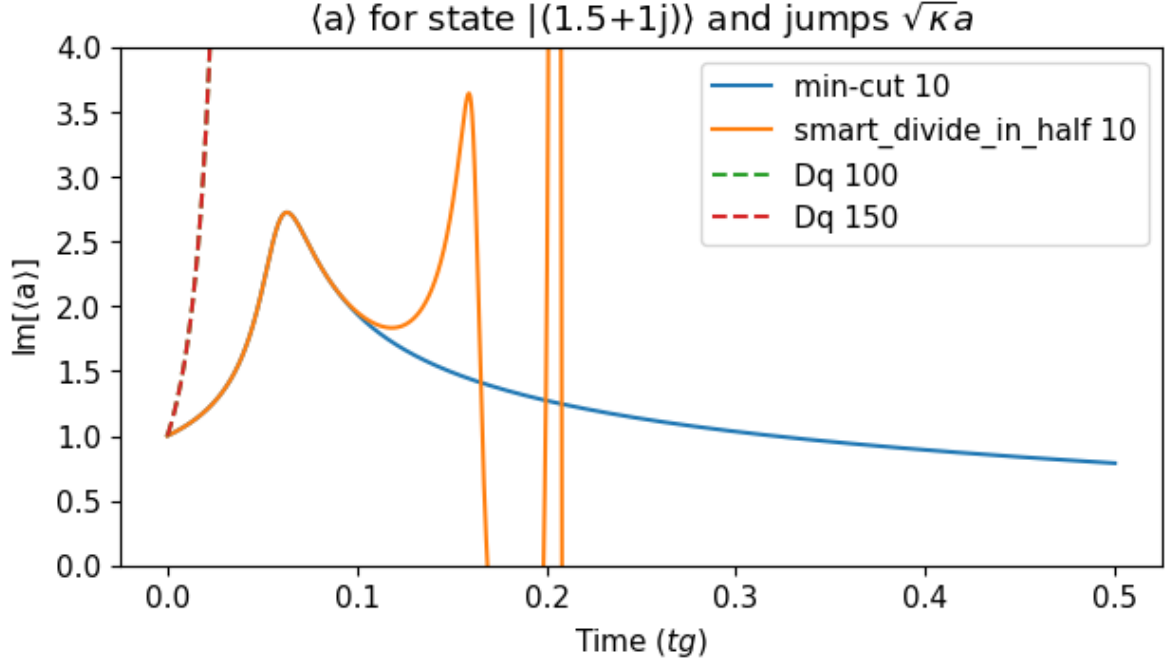


Figure G.11: $\text{Im}\{\langle a \rangle(t)\}$ for the non-Hermitian Hamiltonian $H = a^\dagger a^4$, initial state $|\alpha = 1.5 + i\rangle$, without jump operator a . Continuous line corresponds to MF methods for $p = 10$. Dashed lines correspond to dynamiqs [26].

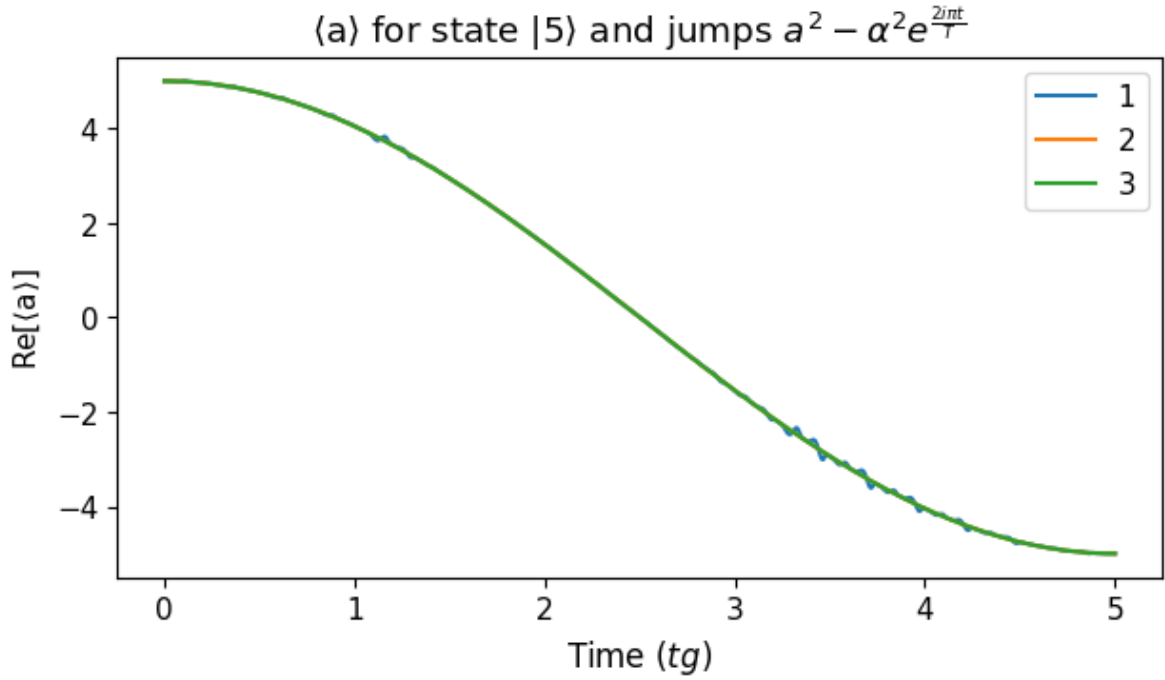


Figure G.12: Dynamics of a stabilized X-gate that transfers the state $|0\rangle$ to the state $|1\rangle$ during T , [62]. Plot obtained using the `cumulant method` for different values of p . $\langle x \rangle(t)$ goes from $+5$ at $t = 0$ to -5 at $t = T$.

Appendix H

Miscellaneous

In this appendix, we put all the small remarks that cannot find a place in any other appendix. The different sections are fully independent from each other.

H.1 Proof of Theorem 1.1.1

Theorem H.1.1. *The commutator $[\cdot, \cdot]$ satisfies the following properties:*

1. $[\cdot, \cdot]$ is anti-symmetric under exchange of the arguments.
2. $[\cdot, \cdot]$ is bilinear (i.e. linear in each variable).
3. $\forall A, B, C, [A, BC] = [A, B]C + B[A, C]$ and $[BC, A] = [B, A]C + B[C, A]$

Proof. 1. Let A and B be two operators, we have: $[A, B] = AB - BA = -(BA - AB) = -[B, A]$.

2. Since $[\cdot, \cdot]$ is anti-symmetric, we only need to show the result for one variable. Let A, B and C be three operators, $\lambda \in \mathbb{C}$, we have: $[A, B + \lambda C] = A(B + \lambda C) - (B + \lambda C)A = AB + \lambda AC - BA - \lambda CA = [A, B] + \lambda[A, C]$.

3. Here again, since $[\cdot, \cdot]$ is anti-symmetric, we only need to show the result for one variable. Let A, B and C be three operators, we have: $[A, BC] = ABC - BCA = ABC - BAC + BAC - BCA = [A, B]C + B[A, C]$. □

The last result has an interesting corollary if we consider a bosonic annihilator a :

Corollary H.1.1.1. *Let a be a bosonic annihilator, for each $n \in \mathbb{N}$, $[a, a^{\dagger n}] = na^{\dagger(n-1)}$ and $[a^n, a^{\dagger}] = na^{(n-1)}$*

Proof. For $n = 0$, the result is straightforward. Let $n \in \mathbb{N}$, suppose the result to be true for n and let us show it for $n + 1$. We have: $[a, a^{\dagger(n+1)}] = [a, a^{\dagger n} a^{\dagger}] = [a, a^{\dagger n}] a^{\dagger} + a^{\dagger n} [a, a^{\dagger}] = na^{\dagger n} + a^{\dagger n} = (n + 1)a^{\dagger n}$. Similarly, $[a^{n+1}, a^{\dagger}] = (n + 1)a^n$. □

H.2 Proof of Theorem 1.1.2

Theorem H.2.1. *Let $p, m \in \mathbb{N}$, we have:*

$$\left[\text{poly}_p(a_1, \dots, a_N; a_1^{\dagger}, \dots, a_N^{\dagger}), \text{poly}_m(a_1, \dots, a_N; a_1^{\dagger}, \dots, a_N^{\dagger}) \right] = \text{poly}_{p+m-2}(a_1, \dots, a_N; a_1^{\dagger}, \dots, a_N^{\dagger}) \quad (\text{H.1})$$

where $\text{poly}_q(a_1, \dots, a_N; a_1^{\dagger}, \dots, a_N^{\dagger})$ designates any polynomial of degree q .

The proof starts by observing that we only need to prove the result for monomial (a polynomial with one term) since the commutator is bilinear. In order to complete the proof, we need to show the following lemma, which is actually a corollary of 1.1.1.

Lemma H.2.1.1. Let A, B_1, \dots, B_n be operators, we have:

$$\left[A, \prod_{i=1}^n B_i \right] = \sum_{i=1}^n \left(\prod_{j=1}^{i-1} B_j \right) [A, B_i] \left(\prod_{j=i+1}^n B_j \right) \quad (\text{H.2})$$

where \prod_i is ordered from the left to the right in an increasing order of i .

Proof. For $n = 1$, the result is straightforward. Let us suppose the result to be true for n and let us show it for $n + 1$.

Let A, B_1, \dots, B_{n+1} be operators, we have:

$$\left[A, \prod_{i=1}^{n+1} B_i \right] = \left[A, \prod_{i=1}^n C_i \right] \quad (\text{H.3})$$

where $C_i \equiv B_i$ for $i < n$ and $C_n \equiv B_n B_{n+1}$. Using the result for n , we get:

$$\begin{aligned} \left[A, \prod_{i=1}^{n+1} B_i \right] &= \sum_{i=1}^n \left(\prod_{j=1}^{i-1} C_j \right) [A, C_i] \left(\prod_{j=i+1}^n C_j \right) \\ &= \sum_{i=1}^{n-1} \left(\prod_{j=1}^{i-1} B_j \right) [A, B_i] \left(\prod_{j=i+1}^{n-1} B_j \right) B_n B_{n+1} \\ &\quad + \left(\prod_{j=1}^{n-1} B_j \right) [A, B_n B_{n+1}] \end{aligned} \quad (\text{H.4})$$

In order to compute $[A, B_n B_{n+1}]$, we use the third result in [Theorem 1.1.1](#): $[A, B_n B_{n+1}] = [A, B_n] B_{n+1} + B_n [A, B_{n+1}]$. We finally get:

$$\left[A, \prod_{i=1}^{n+1} B_i \right] = \sum_{i=1}^{n+1} \left(\prod_{j=1}^{i-1} B_j \right) [A, B_i] \left(\prod_{j=i+1}^{n+1} B_j \right) \quad (\text{H.5})$$

□

With this lemma, we can look at the monomes $\prod_{i=1}^q o_i, \prod_{i=1}^n \tilde{o}_i$ with o_i and \tilde{o}_i being annihilators or creators. We have:

$$\left[\prod_{i=1}^q o_i, \prod_{j=1}^n \tilde{o}_j \right] = \sum_{j=1}^n \left(\prod_{k=1}^{j-1} \tilde{o}_k \right) \left[\prod_{i=1}^q o_i, \tilde{o}_j \right] \left(\prod_{j=j+1}^n \tilde{o}_j \right) \quad (\text{H.6})$$

Since $[\cdot, \cdot]$ is anti-symmetric, we can develop the commutators on the right hand side:

$$\left[\prod_{i=1}^q o_i, \prod_{j=1}^n \tilde{o}_j \right] = \sum_{j=1}^n \sum_{i=1}^q \left(\prod_{k=1}^{j-1} \tilde{o}_k \right) \left(\prod_{l=1}^{i-1} o_l \right) [o_i, \tilde{o}_j] \left(\prod_{l=i+1}^q o_l \right) \left(\prod_{j=j+1}^n \tilde{o}_j \right) \quad (\text{H.7})$$

Since the commutators on the right hand side are scalars, the right hand side is a polynomial of the annihilators and creators whose degree is less or equal to $q + n - 2$, which shows [Theorem 1.1.2](#).

H.3 Solving Quadratic Hamiltonian with One Photon Loss

We consider the Hamiltonian $H \equiv \hbar \omega a^\dagger a$ with the quantum jump $L \equiv \sqrt{\kappa} a$. The Heisenberg equation for the operator a is given by

$$\frac{da}{dt} = -i\omega a - \frac{\kappa}{2} a. \quad (\text{H.8})$$

Thus: $a(t) = e^{(-i\omega - \frac{\kappa}{2})t} a(0)$. Therefore,

$$\left[a(t), a^\dagger(t) \right] = \left[e^{(-i\omega - \frac{\kappa}{2})t} a(0), e^{(i\omega - \frac{\kappa}{2})t} a^\dagger(0) \right] = e^{(-i\omega - \frac{\kappa}{2})t} e^{(i\omega - \frac{\kappa}{2})t} \left[a(0), a^\dagger(0) \right] = e^{-\kappa t}. \quad (\text{H.9})$$

H.4 Number of Equations - MF Equations

We prove the following theorem:

Theorem H.4.1. *We have:*

$$\frac{1}{2} \sum_{q=1}^p \binom{2N+q-1}{q} = O(p^{2N}), \text{ for } N \text{ constant and } p \rightarrow \infty \quad (\text{H.10})$$

$$\frac{1}{2} \sum_{q=1}^p \binom{2N+q-1}{q} \sim \frac{(2N)^p}{2p!}, \text{ for } p \text{ constant and } N \rightarrow \infty \quad (\text{H.11})$$

Proof. Let us take N constant and $p \rightarrow \infty$, we have:

$$\begin{aligned} \frac{1}{2} \sum_{q=1}^p \binom{2N+q-1}{q} &= \frac{1}{2(2N-1)!} \sum_{q=1}^p \frac{(q+2N-1)!}{q!} = \frac{1}{2(2N-1)!} \sum_{q=1}^p \prod_{k=q+1}^{q+2N-1} k \\ &\leq \frac{1}{2(2N-1)!} p(p+2N-1)^{2N-1} = O(p^{2N}) \end{aligned} \quad (\text{H.12})$$

Similarly, let us take p constant and $N \rightarrow \infty$, we have:

$$\begin{aligned} \frac{1}{2} \sum_{q=1}^p \binom{2N+q-1}{q} &= \frac{1}{2} \sum_{q=1}^p \frac{(q+2N-1)!}{(2N-1)!q!} = \frac{1}{2} \sum_{q=1}^p \frac{1}{q!} \prod_{k=2N}^{q+2N-1} k \\ &\sim \frac{1}{2} \sum_{q=1}^p \frac{1}{q!} (2N)^q \sim \frac{(2N)^p}{2p!} \end{aligned} \quad (\text{H.13})$$

□

H.5 Proofs and Corollaries - Initial States ([Theorem 2.2.1](#))

Theorem H.5.1 (Initial Value of Moments). *Let us consider the states $\{|\phi[\xi]\rangle\}_\xi$. We denote $a|\phi[\xi]\rangle = \lambda[\xi]|\phi^{(1)}[\xi]\rangle$, with $|\phi^{(1)}[\xi]\rangle$ is another state obtained after applying a once on $|\phi[\xi]\rangle$. Let $|\psi\rangle = \sum_{\xi=1}^\chi c_\xi \bigotimes_{i=1}^N |\phi_i[\xi]\rangle$. We have*

$$\langle\psi| \left(\prod_{l=1}^N a_l^{\dagger j_l} \right) \left(\prod_{l=1}^N a_l^{k_l} \right) |\psi\rangle = \sum_{\xi=1}^\chi \sum_{\zeta=1}^\chi c_\xi^* c_\zeta \prod_{l=1}^N \left(\prod_{\gamma=0}^{j_l-1} \lambda_l^{(\gamma)*}[\xi] \right) \left(\prod_{\kappa=0}^{k_l-1} \lambda_l^{(\kappa)}[\zeta] \right) \langle\phi_l^{(j_l)}[\xi] | \phi_l^{(k_l)}[\zeta]\rangle \quad (\text{H.14})$$

where $|\phi^{(k)}[\xi]\rangle$ is the resulting state after applying k times a on $|\phi[\xi]\rangle$.

Proof.

$$\begin{aligned} \langle\psi| \left(\prod_{l=1}^N a_l^{\dagger j_l} \right) \left(\prod_{l=1}^N a_l^{k_l} \right) |\psi\rangle &= \sum_{\xi=1}^\chi \sum_{\zeta=1}^\chi c_\xi^* c_\zeta \bigotimes_{i=1}^N \langle\phi_i[\xi]| \left(\prod_{l=1}^N a_l^{\dagger j_l} \right) \left(\prod_{l=1}^N a_l^{k_l} \right) \bigotimes_{i'=1}^N |\phi_{i'}[\zeta]\rangle \\ &= \sum_{\xi=1}^\chi \sum_{\zeta=1}^\chi c_\xi^* c_\zeta \prod_{l=1}^N \langle\phi_l[\xi] | a_l^{\dagger j_l} a_l^{k_l} | \phi_l[\zeta]\rangle \\ &= \sum_{\xi=1}^\chi \sum_{\zeta=1}^\chi c_\xi^* c_\zeta \prod_{l=1}^N \left(\prod_{\gamma=0}^{j_l-1} \lambda_l^{(\gamma)*}[\xi] \right) \left(\prod_{\kappa=0}^{k_l-1} \lambda_l^{(\kappa)}[\zeta] \right) \langle\phi_l^{(j_l)}[\xi] | \phi_l^{(k_l)}[\zeta]\rangle \end{aligned}$$

□

We give the expression for a sum of Fock states and for a sum of coherent states:

Corollary H.5.1.1 (Initial Sum of Fock States). *Let $|\psi\rangle = \sum_{\xi=1}^{\chi} c_{\xi} \bigotimes_{i=1}^N |n_i[\xi]\rangle$ a finite sum over the multi-mode Fock states $\bigotimes_{i=1}^N |n_i[\xi]\rangle$. We have:*

$$\langle\psi|\left(\prod_{l=1}^N a_l^{\dagger j_l}\right)\left(\prod_{l=1}^N a_l^{k_l}\right)|\psi\rangle = \sum_{\xi=1}^{\chi} \sum_{\zeta=1}^{\chi} c_{\xi}^* c_{\zeta} \prod_{l=1}^N \delta_{n_l[\xi]-j_l, n_l[\zeta]-k_l} \left(\prod_{\gamma=0}^{j_l-1} \sqrt{n_l[\xi]-\gamma}\right) \left(\prod_{\kappa=0}^{k_l-1} \sqrt{n_l[\zeta]-\kappa}\right) \quad (\text{H.15})$$

Proof. We have: $a|n\rangle = \sqrt{n}|n-1\rangle$ and $\langle n|m\rangle = \delta_{nm}$. Thus, for $|\psi\rangle = \sum_{\xi=1}^{\chi} c_{\xi} \bigotimes_{i=1}^N |n_i[\xi]\rangle$, we find:

$$\begin{aligned} \langle\psi|\left(\prod_{l=1}^N a_l^{\dagger j_l}\right)\left(\prod_{l=1}^N a_l^{k_l}\right)|\psi\rangle &= \sum_{\xi=1}^{\chi} \sum_{\zeta=1}^{\chi} c_{\xi}^* c_{\zeta} \prod_{l=1}^N \left(\prod_{\gamma=0}^{j_l-1} \sqrt{n_l[\xi]-\gamma}\right) \left(\prod_{\kappa=0}^{k_l-1} \sqrt{n_l[\zeta]-\kappa}\right) \langle n_l[\xi]-j_l | n_l[\zeta]-k_l \rangle \\ &= \sum_{\xi=1}^{\chi} \sum_{\zeta=1}^{\chi} c_{\xi}^* c_{\zeta} \prod_{l=1}^N \delta_{n_l[\xi]-j_l, n_l[\zeta]-k_l} \left(\prod_{\gamma=0}^{j_l-1} \sqrt{n_l[\xi]-\gamma}\right) \left(\prod_{\kappa=0}^{k_l-1} \sqrt{n_l[\zeta]-\kappa}\right) \end{aligned}$$

□

Corollary H.5.1.2 (Initial Sum of Coherent States). *Let $|\psi\rangle = \sum_{\xi=1}^{\chi} c_{\xi} \bigotimes_{i=1}^N |\alpha_i[\xi]\rangle$ a finite sum over the multi-mode coherent states $\bigotimes_{i=1}^N |\alpha_i[\xi]\rangle$. We have:*

$$\langle\psi|\left(\prod_{l=1}^N a_l^{\dagger j_l}\right)\left(\prod_{l=1}^N a_l^{k_l}\right)|\psi\rangle = \sum_{\xi=1}^{\chi} \sum_{\zeta=1}^{\chi} c_{\xi}^* c_{\zeta} \prod_{l=1}^N \alpha_l^{*j_l}[\xi] \alpha_l^{k_l}[\zeta] e^{-\frac{|\alpha_l[\xi]-\alpha_l[\zeta]|^2}{2}} e^{\frac{\alpha_l^*[\xi]\alpha_l[\zeta]-\alpha_l^*[\zeta]\alpha_l[\xi]}{2}} \quad (\text{H.16})$$

Proof. We have: $a|\alpha\rangle = \alpha|\alpha\rangle$ and $\langle\alpha|\beta\rangle = e^{-\frac{1}{2}|\alpha-\beta|^2} e^{\frac{1}{2}(\alpha^*\beta-\beta^*\alpha)}$ [8]. Thus, we have:

$$\begin{aligned} \langle\psi|\left(\prod_{l=1}^N a_l^{\dagger j_l}\right)\left(\prod_{l=1}^N a_l^{k_l}\right)|\psi\rangle &= \sum_{\xi=1}^{\chi} \sum_{\zeta=1}^{\chi} c_{\xi}^* c_{\zeta} \prod_{l=1}^N \alpha_l^{*j_l}[\xi] \alpha_l^{k_l}[\zeta] \langle\alpha_l[\xi]|\alpha_l[\zeta]\rangle \\ &= \sum_{\xi=1}^{\chi} \sum_{\zeta=1}^{\chi} c_{\xi}^* c_{\zeta} \prod_{l=1}^N \alpha_l^{*j_l}[\xi] \alpha_l^{k_l}[\zeta] e^{-\frac{|\alpha_l[\xi]-\alpha_l[\zeta]|^2}{2}} e^{\frac{\alpha_l^*[\xi]\alpha_l[\zeta]-\alpha_l^*[\zeta]\alpha_l[\xi]}{2}} \end{aligned}$$

□

Corollary H.5.1.3 (Initial Mixed State). *If the initial state is a mixed state ρ instead of a pure state, then we can diagonalize the density matrix and write $\rho = \sum_{\mu=1}^{\Xi} p_{\mu} |\psi_{\mu}\rangle \langle\psi_{\mu}|$ where $\langle O \rangle = \sum_{\mu=1}^{\Xi} p_{\mu} \langle\psi_{\mu}|O|\psi_{\mu}\rangle$. Thus, we can estimate the moments if the states $|\psi_{\mu}\rangle$ satisfy the condition of [Theorem 2.2.1](#).*

H.6 Proof of Independent Resolution on Projectors

In this section, we prove that

Theorem H.6.1. *If the initial state can be written as $|\psi\rangle = \sum_{\xi=1}^{\chi} c_{\xi} |\phi_{\xi}\rangle$, then we can obtain the evolution of the averages of the operators $\{O_i\}_{i \in I}$ by solving the differential system for each projector $\frac{|\phi_{\xi}\rangle \langle\phi_{\xi}|}{\langle\phi_{\xi}|\phi_{\xi}\rangle}$ independently, provided the values of $\langle\phi_{\zeta}|\phi_{\xi}\rangle$ and $\langle\phi_{\zeta}|O_i(0)|\phi_{\xi}\rangle$ are known.*

Proof. Let $i \in I$

$$\langle O_i \rangle(t) = \sum_{\xi=1}^{\chi} \sum_{\zeta=1}^{\chi} c_{\xi}^* c_{\zeta} \langle\phi_{\zeta}|O_i(t)|\phi_{\xi}\rangle = \sum_{\xi=1}^{\chi} \sum_{\zeta=1}^{\chi} c_{\xi}^* c_{\zeta} \frac{\langle\phi_{\zeta}|O_i(t)|\phi_{\xi}\rangle}{\langle\phi_{\zeta}|\phi_{\xi}\rangle} \langle\phi_{\zeta}|\phi_{\xi}\rangle \quad (\text{H.17})$$

Thus, if $\langle\phi_{\zeta}|\phi_{\xi}\rangle$ are known, we only need to know $\frac{\langle\phi_{\zeta}|O_i(t)|\phi_{\xi}\rangle}{\langle\phi_{\zeta}|\phi_{\xi}\rangle}$. Since the initial condition is known, we focus on the differential system. We write the Langevin equation:

$$\frac{dO_i}{dt} = \mathbb{f}_i(\{O_j\}_{j \in I}) \quad (\text{H.18})$$

By taking the average for the projector $\frac{|\phi_\xi\rangle\langle\phi_\zeta|}{\langle\phi_\zeta|\phi_\xi\rangle}$, we find

$$\frac{d \operatorname{Tr} \left\{ \frac{|\phi_\xi\rangle\langle\phi_\zeta|}{\langle\phi_\zeta|\phi_\xi\rangle} O_i \right\}}{dt} = \operatorname{Tr} \left\{ \frac{|\phi_\xi\rangle\langle\phi_\zeta|}{\langle\phi_\zeta|\phi_\xi\rangle} \mathbb{F}_i(\{O_j\}_{j \in I}) \right\} \quad (\text{H.19})$$

i.e.

$$\frac{d \frac{\langle\phi_\zeta|O_i(t)|\phi_\xi\rangle}{\langle\phi_\zeta|\phi_\xi\rangle}}{dt} = \frac{\langle\phi_\zeta|\mathbb{F}_i(\{O_j\}_{j \in I})(t)|\phi_\xi\rangle}{\langle\phi_\zeta|\phi_\xi\rangle} \quad (\text{H.20})$$

Thus, we can solve for each projector independently. \square

H.7 Properties of Stability Matrix

We study some properties of the stability matrix. This matrix is close to symplectic matrices that were studied in chapters 7 and 8 of [29].

Real initial condition with no quantum jump One special case of interest is when the initial condition is real (i.e. a coherent state with $\alpha \in \mathbb{R}$) and without quantum jump. In this case, \mathcal{L} can be written in the form:

$$\mathcal{L} = -i \begin{pmatrix} X & Y \\ -Y & -X \end{pmatrix} \quad (\text{H.21})$$

with X and Y real matrices. In this case, we have the following result:

Theorem H.7.1. *Let \mathcal{L} be a matrix in the form Equation H.21. If λ is an eigenvalue of \mathcal{L} , then $-\lambda$ is also an eigenvalue of \mathcal{L} .*

Proof. Let $\mathbb{X} \equiv \begin{pmatrix} 0 & \mathbb{1} \\ \mathbb{1} & 0 \end{pmatrix}$, such that $\mathbb{X}^{-1} = \mathbb{X}^2$. We have: $\mathbb{X}\mathcal{L}\mathbb{X} = -\mathcal{L}$. Thus, if $\mathcal{L}\vec{x} = \lambda\vec{x}$, $\vec{x} \neq \vec{0}$, then $\mathcal{L}\mathbb{X}\vec{x} = -\lambda\mathbb{X}\vec{x}$, where $\mathbb{X}\vec{x} \neq \vec{0}$. \square

Corollary H.7.1.1. *In particular, this case is at best neutral.*

General Case

In the general case, we only have the following result that is not very enlightening concerning the stability problem:

Theorem H.7.2. *Let \mathcal{L} be a matrix in the form Equation 2.9. If λ is an eigenvalue of \mathcal{L} , then λ^* is also an eigenvalue of \mathcal{L} .*

Proof. We have $\mathbb{X}\mathcal{L}\mathbb{X} = \mathcal{L}^*$. Thus, if $\mathcal{L}\vec{x} = \lambda\vec{x}$, $\vec{x} \neq \vec{0}$, then $\mathcal{L}\mathbb{X}\vec{x}^* = \mathbb{X}\mathcal{L}^*\vec{x}^* = \lambda^*\mathbb{X}\vec{x}^*$, with $\mathbb{X}\vec{x}^* \neq \vec{0}$. \square

H.8 Complexity of TEA - Computation of the Commutators

Theorem H.8.1 (Time Complexity). *The time complexity for computing $a_i(t)$ up to the cut-off p is given by:*

$$C(p) = O \left(\sum_{n=0}^{p-1} w_H^{n+1} (1 + m + n\tau_H) \right) \quad (\text{H.22})$$

Proof. To compute the time complexity of this method, we introduce the notation w_A , representing the number of terms in the operator A . Further, the complexity for computing the complexity of monomes of degrees p and m is $O(p + m)$ since the rule $[AB, C] = [A, C]B + A[B, C]$.

If H is a polynomial of degree m , then using the bilinearity of the commutation relations, the complexity of computing $[H, a_i]$ is $O(w_H(1 + m))$.

Equipped with this result, we can estimate the complexity of computing $\text{Comm}_{n+1}(H|a_i) = [H, \text{Comm}_n(H|a_i)]$. Using the previous result, it is:

$$O(w_H w_{\text{Comm}_n(H|a_i)}(1 + m + n\tau_H))$$

We need to estimate $w_{\text{Comm}_n(H|a_i)}$. To this, we observe that: $w_{\text{Comm}_{n+1}(H|a_i)} = w_H w_{\text{Comm}_n(H|a_i)}$ (number of terms in an expansion of two factors) and $w_{\text{Comm}_0(H|a_i)} = w_{a_i}$. Therefore: $w_{\text{Comm}_n(H|a_i)} = w_{a_i} w_H^n$.

Thus: the total complexity is:

$$C(p) = O\left(\sum_{n=0}^{p-1} w_H^{n+1}(1 + m + n\tau_H)\right) \quad (\text{H.23})$$

□

Remark H.8.1.1. *We can make the following observations:*

1. For $p \rightarrow \infty$, $\ln C(p) \sim p \ln w_H$ for $w_H \geq 2$. This confirms that the time complexity is mainly controlled by the number of terms in the Hamiltonian.
2. For $w_H = 1$, the cost is polynomial.
3. We see that there is an advantage in going into a rotating frame that can allow to drop some terms of the Hamiltonian.
4. The time to compute the $(n+1)^{\text{st}}$ term is roughly w_H times longer than the time to compute the n^{th} term if $w_H \geq 2$.

H.9 Proofs for Times of Validity - TEA

For this part, time is expressed of units of g and we focus on the one mode case. In this part, we try to estimate the time validity of the approximation for a coherent state $|\alpha\rangle$. This time will be denoted $t_p[\alpha]$. We shall consider two limit cases which will allow us to restrict the time of validity.

Theorem H.9.1 (Overestimate of Time of Validity). *The time of validity can be overestimated by:*

$$t_N[\alpha] = O\left(\frac{p}{|\alpha|^{\tau_H}}\right) \quad (\text{H.24})$$

Proof. To estimate the time of validity, we can compare the last term taken into account which is of the order $\frac{t^p}{p!}|\alpha|^{1+p\tau_H}$ with the next one: $\frac{t^{p+1}}{(p+1)!}|\alpha|^{1+(p+1)\tau_H}$. The ratio is of the order of 1 when:

$$t_N[\alpha] = O\left(\frac{Np}{|\alpha|^{\tau_H}}\right) \quad (\text{H.25})$$

This result gives an *overestimation* of the time of validity. □

Theorem H.9.2 (Underestimate of Time of Validity). *The time of validity can be underestimate by a constant:*

$$t_p[\alpha] = \Omega(1) \quad (\text{H.26})$$

Proof. The highest coefficient for the term $n+1$ is due to the powers m of the Hamiltonian and $1 + n\tau_H$ of the previous term. Thus, by recursion, the coefficient of order n is given by:

$$\frac{1}{n!} t^n m^n |\alpha|^{1+n\tau_H} \prod_{k=0}^{n-1} (1 + k\tau_H)$$

Comparing the terms p and $p+1$, we see that:

$$t_p[\alpha] \sim \frac{1}{(2 + \tau_H)|\alpha|^{\tau_H}} \quad (\text{H.27})$$

which is a well-defined constant for $\tau_H \geq 1$. □

Appendix I

Sum of Gaussian States (UNFINISHED)

In this appendix, we study how to handle the sum of Gaussian states. We start by studying one-mode Gaussian states, which can be generalized to tensor product of one-mode Gaussian states.

I.1 One-Mode Gaussian State

A one-mode Gaussian state is generated using the displacement operator and one-mode squeeze operator.

I.1.1 One-Mode Squeeze Operator

We use the convention of [61, 63] and define the one-mode squeeze operator.

Definition I.1.1 (One-mode squeeze operator). *We define*

$$S(z) \equiv \exp\left\{\frac{1}{2}\left(z^* a^2 - z a^{\dagger 2}\right)\right\}. \quad (\text{I.1})$$

From [63] (equation (14)), we have the following theorem. Note that [63] uses the opposite convention ($z \mapsto -z$).

Theorem I.1.1 (Squeeze operator in normal order (equation (14) from [63])). *We have for $z \equiv r e^{i\theta}$,*

$$S(z) = \exp\left\{-\frac{e^{i\theta}}{2} \tanh(r) a^{\dagger 2}\right\} \frac{1}{\sqrt{\cosh r}} \left\{\sum_{n=0}^{\infty} \frac{(\operatorname{sech} r - 1)^n}{n!} a^{\dagger n} a^n\right\} \exp\left\{\frac{e^{-i\theta}}{2} \tanh(r) a^2\right\} \quad (\text{I.2})$$

We deduce the following corollary.

Corollary I.1.1.1. *Let $|\alpha\rangle$ and $|\beta\rangle$ be two coherent states, we have for $z \equiv r e^{i\theta}$*

$$\langle\alpha|S(z)|\beta\rangle = \exp\left\{-\frac{e^{i\theta}}{2} \tanh(r) \alpha^{*2}\right\} \frac{\langle\alpha|\beta\rangle}{\sqrt{\cosh r}} \exp\{\alpha^* \beta (\operatorname{sech} r - 1)\} \exp\left\{\frac{e^{-i\theta}}{2} \tanh(r) \beta^2\right\} \quad (\text{I.3})$$

I.1.2 Scalar Product of One-Mode Gaussian States

For $z \equiv r e^{i\theta} \in \mathbb{C}$, we define $t \equiv e^{i\theta} \tanh r$. Let $z_1, z_2 \in \mathbb{C}$, the following theorem [64] gives the value of $S(z_1)S(z_2)$.

Theorem I.1.2 (Exercise 3.8 from [64]). *We define $t_3 \equiv \frac{t_1+t_2}{1+t_1^* t_2}$, $\xi \equiv \frac{1}{2} \ln \frac{1+t_1 t_2^*}{1+t_1^* t_2}$. We have*

$$S(z_1)S(z_2) = S(z_3) \exp\left\{\xi \left(a^{\dagger} a + \frac{1}{2}\right)\right\}. \quad (\text{I.4})$$

We can now compute the value of $\langle\alpha|S(z_1)S(z_2)|\beta\rangle$.

Theorem I.1.3. *We have*

$$\langle \alpha | S(z_1) S(z_2) | \beta \rangle = e^{\frac{\xi}{2}} e^{-\frac{|\beta|^2}{2}(1-|\xi|^2)} \langle \alpha | S(z_3) | \beta \rangle \quad (\text{I.5})$$

$$= e^{\frac{\xi}{2}} e^{-\frac{|\beta|^2}{2}(1-|\xi|^2)} \exp\left\{-\frac{e^{i\theta_3}}{2} \tanh(r_3) \alpha^{*2}\right\} \frac{\langle \alpha | \beta \rangle}{\sqrt{\cosh r_3}} \\ \times \exp\{\alpha^* \beta (\text{sech } r_3 - 1)\} \exp\left\{\frac{e^{-i\theta_3}}{2} \tanh(r_3) \beta^2\right\}. \quad (\text{I.6})$$

where z_3 and ξ are defined in [Theorem I.1.2](#).

I.1.3 Squeeze and Displacement Operators

We use the convention in [\[63, 65\]](#).

Definition I.1.2 (Displacement operator). *We define*

$$D(\alpha) \equiv \exp\{\alpha a^\dagger - \alpha^* a\} \quad (\text{I.7})$$

$D(\alpha)$ creates the coherent state $|\alpha\rangle$ from vacuum.

We can thus define a squeezed coherent state and a displaced squeezed state.

Definition I.1.3 (Squeezed coherent state vs. Displaced squeezed state). *A squeezed coherent state is obtained from vacuum by applying the operators in the order $S D$ (i.e. squeeze a coherent state).*

A displaced squeezed state is obtained by from vacuum by applying the operators in the order $D S$ (i.e. displace a squeezed vacuum).

The following theorem corresponds to equation (15) from [\[63\]](#).

Theorem I.1.4 (Exchanging squeeze and displacement operators). *Let $\alpha, z \in \mathbb{C}$, with $z \equiv r e^{i\theta}$ we have*

$$D(\alpha) S(z) = S(z) D(\gamma) \quad (\text{I.8})$$

with $\gamma \equiv \alpha \cosh r + \alpha^* e^{i\theta} \sinh r$.

Corollary I.1.4.1. [Theorem I.1.4](#) implies that the two notions of squeezed coherent state and of displaced squeezed state are equivalent if the parameter of the displacement operator is updated correctly. In particular, we can limit ourselves to **squeezed coherent states**. In this case, the overlaps are written in the form [Equation I.5](#).

I.1.4 Cumulants of One-Mode Gaussian States

A one-mode Gaussian state can be written as $S(z) D(\alpha) |\emptyset\rangle$, with $|\emptyset\rangle$ being vacuum. We introduce $z \equiv r e^{i\theta}$. From [\[66\]](#), we have the following cumulants

$$C_a = \alpha \cosh r - \alpha^* e^{i\theta} \sinh r \quad (\text{I.9})$$

$$C_{a^2} = -e^{i\theta} \cosh r \sinh r \quad (\text{I.10})$$

$$C_{a^\dagger a} = \sinh^2(r) \quad (\text{I.11})$$

$$\forall j, k \in \mathbb{N}, j + k > 2 \implies C_{a^\dagger j a^k} = 0 \quad (\text{I.12})$$

Additionally, we prove the following result for a **tensor product of one-mode states**.

Theorem I.1.5 (Moments and cumulants for tensor product). *Let the state $|\psi\rangle \equiv \bigotimes_{l=1}^N |\phi_l\rangle$, with $|\phi_l\rangle$ a state on the mode l . Let us consider $\left(\prod_{l=1}^N a_l^{\dagger j_l}\right) \left(\prod_{l=1}^N a_l^{k_l}\right)$. We have*

$$\left\langle \left(\prod_{l=1}^N a_l^{\dagger j_l}\right) \left(\prod_{l=1}^N a_l^{k_l}\right) \right\rangle = \prod_{l=1}^N \langle a_l^{\dagger j_l} a_l^{k_l} \rangle \quad (\text{I.13})$$

Additionally, if there are $l_1 \neq l_2$ such that $j_{l_1} + k_{l_1} > 0$ and $j_{l_2} + k_{l_2} > 0$, then

$$C_{\left(\prod_{l=1}^N a_l^{\dagger j_l}\right) \left(\prod_{l=1}^N a_l^{k_l}\right)} = 0 \quad (\text{I.14})$$

Proof. Since $|\psi\rangle = \bigotimes_{l=1}^N |\phi_l\rangle$, $M(\vec{z}, \vec{z}^*) = \prod_{l=1}^N M_l(z_l, z_l^*)$ (the notations $M(\vec{z}, \vec{z}^*)$ and $K(\vec{z}, \vec{z}^*)$ are introduced in [section 1.2.3](#)), with $M_l(z_l, z_l^*) \equiv \langle \phi_l | e^{iz_l^* a_l^\dagger} e^{iz_l a_l} | \phi_l \rangle$. Thus,

$$\left\langle \left(\prod_{l=1}^N a_l^{\dagger j_l} \right) \left(\prod_{l=1}^N a_l^{k_l} \right) \right\rangle = \left[\prod_{l=1}^N \frac{\partial^{j_l+k_l}}{\partial (iz^*)^{j_l} \partial (iz)^{k_l}} \right] M(\vec{0}, \vec{0}) = \prod_{l=1}^N \frac{\partial^{j_l+k_l} M_l}{\partial (iz^*)^{j_l} \partial (iz)^{k_l}}(0, 0) = \prod_{l=1}^N \langle a_l^{\dagger j_l} a_l^{k_l} \rangle \quad (\text{I.15})$$

Futhermore, we have $K(\vec{z}, \vec{z}^*) = \sum_{l=1}^N K_l(z_l, z_l^*)$, where $K_l(z_l, z_l^*) \equiv \ln M_l(z_l, z_l^*)$. If there are $l_1 \neq l_2$ such that $j_{l_1} + k_{l_1} > 0$ and $j_{l_2} + k_{l_2} > 0$, then

$$C_{\left(\prod_{l=1}^N a_l^{\dagger j_l}\right) \left(\prod_{l=1}^N a_l^{k_l}\right)} = \left[\prod_{l=1}^N \frac{\partial^{j_l+k_l}}{\partial (iz^*)^{j_l} \partial (iz)^{k_l}} \right] K(\vec{0}, \vec{0}) = \sum_{l=1}^N \frac{\partial^{j_l+k_l} K_l}{\partial (iz^*)^{j_l} \partial (iz)^{k_l}}(0, 0) = 0 \quad (\text{I.16})$$

□

I.1.5 Cumulants of One-Mode Gaussian *Projectors*

UNFINISHED